Chemical Constituents from the Natural Fruiting Bodies of *Serpula dendrocalami* C. L. Zhao

Chiraphat Takpho

A Thesis Submitted in Partial Fulfillment of Requirements for
degree of Master of Science in Chemistry
April 2025

สารองค์ประกอบทางเคมีจากดอกเห็ดธรรมชาติ *Serpula dendrocalami* C. L. Zhao

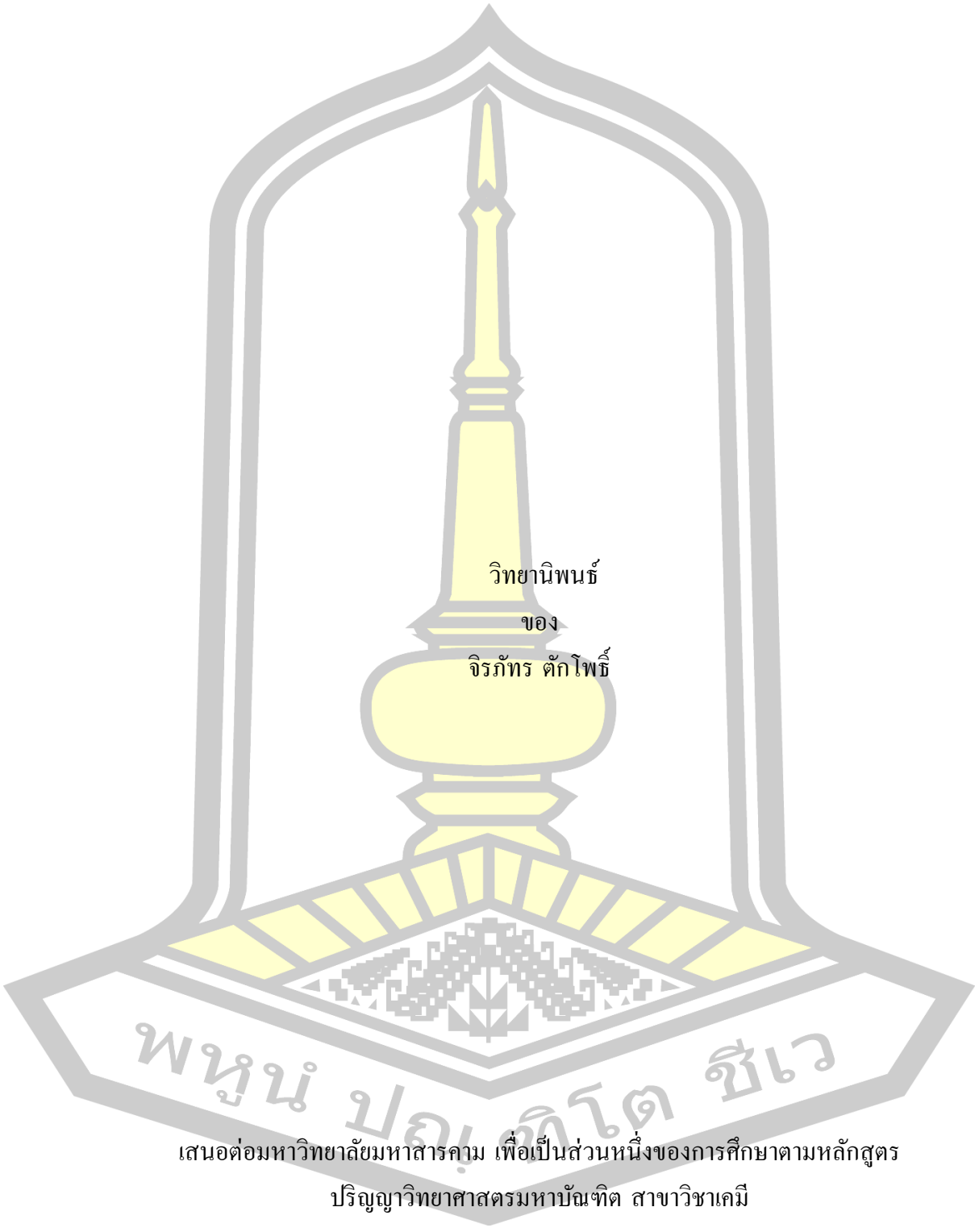

วิทยานิพนธ์

ของ

จิรภัทร ตักโพธิ์

เสนอต่อมหาวิทยาลัยมหาสารคาม เพื่อเป็นส่วนหนึ่งของการศึกษาตามหลักสูตร

ปริญญาวิทยาศาสตรมหาบัณฑิต สาขาวิชาเคมี

เมษายน 2568

Chemical Constituents from the Natural Fruiting Bodies of *Serpula dendrocalami* C. L. Zhao

Chiraphat Takpho

A Thesis Submitted in Partial Fulfillment of Requirements

for Master of Science (Chemistry)

April 2025

The examining committee has unanimously approved this Thesis, submitted by Mr. Chiraphat Takpho , as a partial fulfillment of the requirements for the Master of Science Chemistry at Mahasarakham University

Examining Committee

.....Chairman
(Assoc. Prof. Panawan Moosophon , Ph.D.)

.....Advisor
(Assoc. Prof. Prapairat Seephonkai , Ph.D.)

.....Co-advisor
(Assoc. Prof. Aphidech Sangdee , Ph.D.)

.....Committee
(Assoc. Prof. Chatthai Kaewtong , Ph.D.)

.....Committee
(Asst. Prof. Pakin Noppawan , Ph.D.)

Mahasarakham University has granted approval to accept this Thesis as a partial fulfillment of the requirements for the Master of Science Chemistry

.....
(Prof. Pairot Pramual , Ph.D.)
Dean of The Faculty of Science

.....
(Prof. Anongrit Kangrang , Ph.D.)
Acting Dean of Graduate School

TITLE Chemical Constituents from the Natural Fruiting Bodies of *Serpula dendrocalami* C. L. Zhao

AUTHOR Chiraphat Takpho

ADVISORS Associate Professor Prapairat Seephonkai , Ph.D.

Associate Professor Aphidech Sangdee , Ph.D.

DEGREE Master of Science **MAJOR** Chemistry

UNIVERSITY Mahasarakham University **YEAR** 2025

ABSTRACT

The natural fruiting bodies of *Serpula dendrocalami* C. L. Zhao have been chemically investigated for its bioactive compounds. In this research, the natural fruiting bodies of *Serpula dendrocalami* were collected from Nakhon Phanom Province, Northeastern Thailand. The living culture was isolated, grown on PDA, and preserved at the Department of Biology, Faculty of Science, Mahasarakham University (MSUCC032). This fungus was identified as *Serpula dendrocalami* on the basis of the ITS rDNA gene sequencing data. Biological activity and chemical study of this species have never been reported. The extract from dichloromethane was subjected to purify by silica gel and Sephadex LH-20 column chromatography. Chemical investigation led to the isolation of three undescribed *O*-prenyl-tyrosine oxime derivatives serpulanines D−F (8−10) together with five known compounds, serpulanine C (3), valencic acid (11), 4-prenyloxyphenylacetic acid (12), ergosterol (13), and ergosterol endoperoxide (14). The structures were elucidated on the basis of NMR spectroscopic and mass spectrometry data. The *E*-configuration of oxime group was proposed based on their spectroscopic data compared with serpulanine C from previous report. The undescribed compounds 8−10 have been evaluated for their antibacterial activities against Gram-positive pathogenic bacteria, methicillin-resistant *Staphylococcus aureus* (MRSA), methicillin-sensitive *Staphylococcus aureus* (MSSA), and *Bacillus cereus* and cytotoxicity against A549 cell lines. These compounds were inactive in antibacterial and cytotoxic activities assays.

Keyword : Serpulaceae, Serpula dendrocalami, Serpulanines, Oxime, Tyrosine oxime

ACKNOWLEDGEMENTS

I would like to express their heartfelt gratitude to the Center of Excellence for Innovation in Chemistry (PERCH-CIC) for their invaluable support, which significantly contributed to the success of this research. The National Research Council of Thailand (NRCT) and the Department of Chemistry, Faculty of Science, Mahasarakham University are gratefully acknowledged.

I am grateful to thank my advisor, Assoc. Prof. Dr. Prapairat Seephonkai, for accepting me to be your supervisee since I was an undergraduate student. Thak you for your invaluable guidance, support, encouragement, and unforgettable experiences throughout this research. Your expertise, patience, and insightful feedback have been instrumental in shaping the course of my work. I am truly grateful for the opportunity to learn from you and for your unweaving belief in my abilities. I would like to thank Assoc. Prof. Dr. Aphidech Sangdee, my co-advisor, for your constant support, thoughtful advice, and constructive suggestions. Your dedication and insights have been a source of inspiration and I deeply appreciate the time and effort you have invested in my growth and success.

Finally, I would like to thank to my family and friends for their unconditional love and encouragement that have made this study possible. Your belief in me has been my anchor, and your unwavering support has been my greatest source of strength.

Chiraphat Takpho

TABLE OF CONTENTS

Page

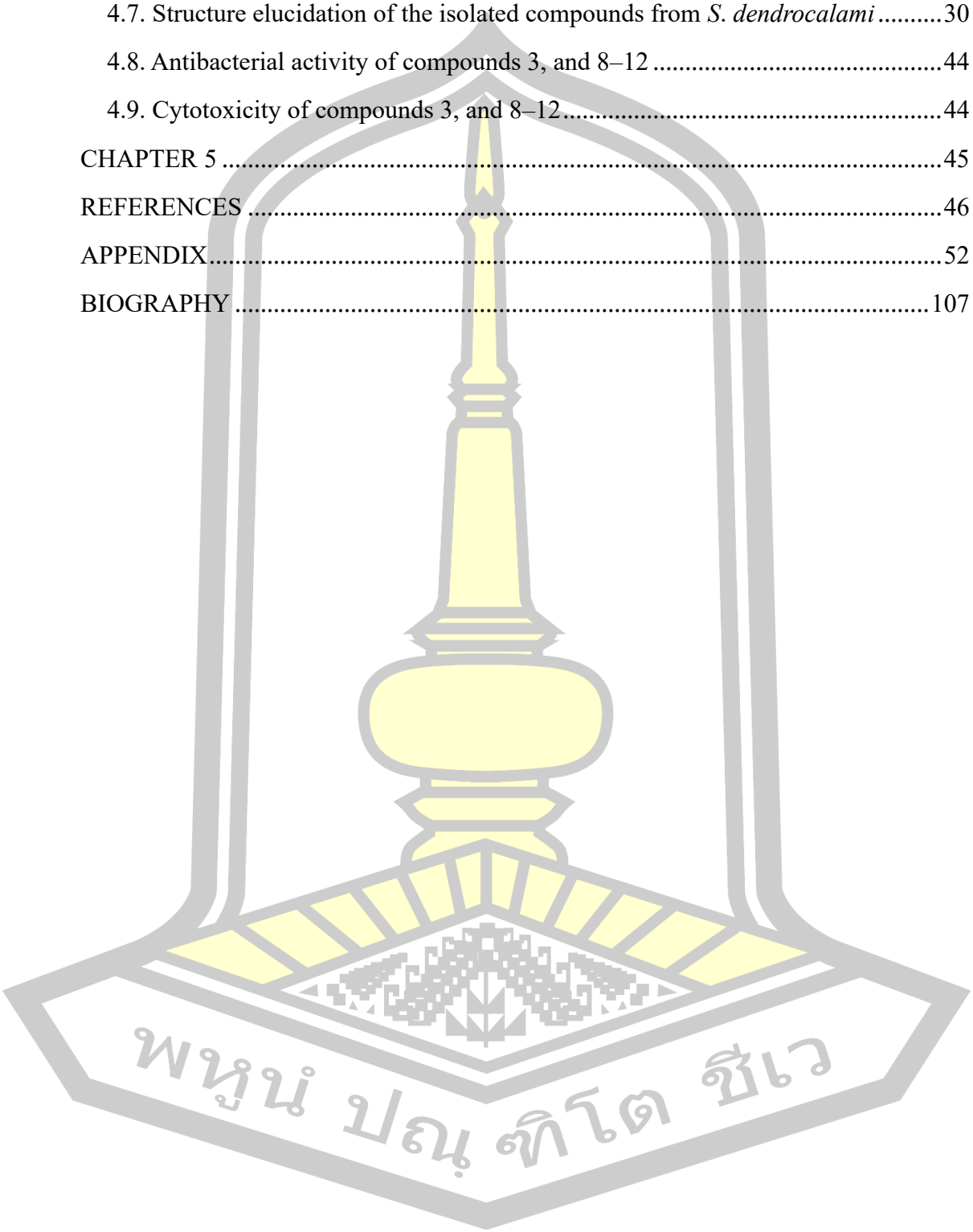

LIST OF TABLES

Page

LIST OF FIGURES

Page

LIST OF FLOWCHARTS

Page

LIST OF ABBREVIATIONS

MTT	3-(4,5-Dimethylthiazolyl-2)-2,5-diphenyltetrazolium bromide
A	Absorbance
ATCC	American type culture collection
BLAST	Basic local alignment search tool
CO_2	Carbon dioxide
PERCH-CIC	Center of excellence for innovation in Chemistry
cm	Centimeter
δ	Chemical shift
$CHCl_3$	Chloroform
CC	Column chromatography
c	Concentration
COSY	Correlation spectroscopy
J	Coupling constant
°C	Degree Celsius
DNA	Deoxyribonucleic acid
DMST	Department of medical sciences Thailand
$CDCl_3$	Deuterated chloroform
DMSO-d_6	Deuterated dimethyl sulfoxide
CD_3OD	Deuterated methanol
DCM	Dichloromethane
DMSO	Dimethyl sulfoxide

DEPT	Distortionless enhancement by polarization transfer
d	Doublet (spectral multiplicity)
dd	Doublet of doublet (spectral multiplicity)
DMEM	Dulbecco's modified eagle's medium
EF	Elongation factor
EtOAc	Ethyl acetate
U.N. FAO	Food and agriculture organization of the United Nations
FTIR	Fourier transform infrared spectroscopy
Fr	Fraction
g	Gram
HMBC	Heteronuclear multiple bond correlation
HSQC	Heteronuclear single quantum coherence spectroscopy
HRESIMS	High-resolution electrospray ionization mass spectrometry
HDAC	Histone deacetylase
h	Hour
HL 60	Human leukemia cell line
A549	Human lung cancer cell line
IR	Infrared radiation
IC_{50}	50% inhibitory concentration
ITS	Internal transcribed spacer
LSU	Large subunit
LPS	Lipopolysaccharide
L	Liter

RAW 264.7	Macrophage-like cells
MSUCC	Mahasarakham University culture collection
MSUT	Mahasarakham University Thailand
MEB	Malt extract broth
MS	Mass spectrometry
ML	Maximum likelihood
MHz	Megahertz
MeOH	Methanol
MRSA	Methicillin-resistant *Staphylococcus aureus*
MSSA	Methicillin-susceptible *Staphylococcus aureus*
µg	Microgram
µL	Microliter
µm	Micrometer
µM	Micromolar
mg	Milligram
mL	Milliliter
mm	Millimeter
MBC	Minimum bacterial concentration
MIC	Minimum inhibitory concentration
min	Minute
MHA	Mueller-Hinton agar
m	Multiplet (spectral multiplicity)
mult.	Multiplicity

nm	Nanometer
NCBI	National center for biotechnology information
NRCT	National research council of Thailand
NO	Nitric oxide
NMR	Nuclear magnetic resonance
NOESY	Nuclear overhauser effect spectroscopy
1D NMR	One-dimensional nuclear magnetic resonance
ppm	Parts per million
H_3PO_4	Phosphoric acid
PCR	Polymerase chain reaction
PDA	Potato dextrose agar
rpm	Revolutions per minute
rDNA	Ribosomal deoxyribonucleic acid
rRNA	Ribosomal ribonucleic acid
s	Singlet (spectral multiplicity)
[α]	Specific rotation
TLC	Thin-layer chromatography
2D NMR	Two-dimensional nuclear magnetic resonance
UV	Ultraviolet radiation
UV-Vis	Ultraviolet-visible
v/v	Volume per volume
v	Wave number
cm^{-1}	Wave number unit

YMG Yeast, malt, and glucose

CHAPTER 1

INTRODUCTION

1.1. Background

Nestled in the heart of Southeast Asia, Thailand is a tropical country with the rich biodiversity of plants, animals, fungi, and microorganisms. Based on the U.N. FAO, 37% or about 18,972,000 ha of Thailand is forested (Butler, 2000). The diverse ecosystem of Thailand is a locality for a variety of organisms with the equatorial climate, varied topography, and abundant rainfall (Doryane, 2004). Thailand supports up to 12,000 species of plants, roughly 15,000 known species of animals and about 10,000 known species of microorganisms (Baimai, 2010). People directly use these biological resources in their locality as sources of agricultural products, traditional medicines, and many things for human survival (Baimai, 2010). Nowadays, studies on the biodiversity including their utilizations have received attention. The purposes of the studies are to gain knowledge, to preserve and to increase value of these natural resources.

Fungi are a kingdom of organisms with the heterotrophic eukaryotic cells (Pedro, 2022). Most of fungi live in a state of decomposition or saprophytism by releasing enzymes to decompose the remains to get their nutrients and absorbing food (Várnai et al., 2014). Currently, about 100,000 described species of fungi distribute around the world (Hyde, 2022). Fungi structure consists of filaments called hyphae. The hyphae are arranged into a network called mycelium which perform in food

attaching and enzymes releasing, and food absorption to mycelium cells of fungi (Bueno & Silva, 2014). The mycelium in some species of fungi will grow into fruiting body to produce spores. The hyphae may be transformed shape to exhibit special functions, including rhizoid which similar to plant roots extending from the mycelium to bind to the food surface and absorb food, this hypha can be found in parasitic fungi such as bread mold (Haustorium or Arbuscules) (Bueno & Silva, 2014). Fungi reproduce by spore formation, both sexual reproduction which occurs in an unappreciated environment, and asexual reproduction by budding or fragmentation (McConnaughey, 2014). They are a diverse kingdom of living things which important in ecosystem as decomposers which play a role in the organic matter breaking down and transformation organic molecules into nutrients (Enrica, 2023). Fungi can be yeasts, rusts, smuts, mildews, molds, and mushrooms (Ahmadjian et al., 2024). There are over 14,000 species of mushrooms in the world have been described (NPS, 2021). Lacking chloroplasts and photosynthesis ability, these reasons show mushrooms differ from plants (Lovett, 2021).

Mushrooms are more closely similar to animals than plants. Phylum Basidiomycota has the highest evolution which plays a role as an efficient digester of organic matter in the ecosystem. The important characteristic of phylum Basidiomycota, there are complete septate hyphae, and sexual reproduction by producing spores called basidiospore. The most evolved mushroom will form basidium on a special structure or fruiting body called basidiocarp or mushrooms. There are four basic of mushroom life cycle, which are spore germination, colonization, fruiting, and sporulation (Acres, 2017). In human life, mushrooms are

natural resources that could serve as functional food for nutrition and medicinal purposes (Adedokun et al., 2022). Mushrooms are sources of secondary metabolites which display the interesting biological activities. *Ganoderma lucidum* or Lingzhi is a well-known medicinal mushroom. Triterpenoids, polysaccharides, proteins, amino acids, nucleosides, alkaloids, steroids, lactones, lectins, fatty acids, and enzymes with biological activities can be isolated from *G. lucidum* (Bulam et al., 2019).

In this research, a polypore mushroom of the genus *Serpula* was investigated. This genus has ribbon-like fruiting bodies color from pale yellow to orange-brown known as dry rot which is the main cause of wooden building decay in the United Kingdom and northern Europe (Moore et al., 2000). The nomenclatural database Index Fungorum indicates 14 species in genus *Serpula* (Kirk, n.d.); *S. atrovirens*, *S. byssoidea*, *S. costaricensis*, *S. crassa*, *S. dendrocalami*, *S. erecta*, *S. fuscescens*, *S. himantioides*, *S. lacrymans*, *S. olivacea*, *S. sclerotiorum*, *S. similis*, *S. tignicola*, and *S. umbrina*. The genus *Serpula* is a rare macrofungus. The mushroom *Serpula dendrocalami* was described in 2019, which discovered from the root of living bamboo genus *Dendrocalamus* (Wang et al., 2019). This mushroom is very rare to find in Thailand. Chemical investigation of this species has never been reported. Herein, the chemical constituents of the mushroom *Serpula dendrocalami* collected from northeastern Thailand was studied.

1.2. Research objective

Biological activities and chemical constituents of *S. dendrocalami* have never been reported. Therefore, chemical constituents of the fruiting bodies of *S. dendrocalami* collected from northeastern Thailand and biological activities of the extracts and the isolated compounds were studied in this research.

1.3. Expected result

Identification of compounds isolated from the fruiting bodies of *S. dendrocalami* and biological activity results of the isolated compounds are expected in this research.

1.4. Scop of research

Extraction of the fruiting bodies of *S. dendrocalami*, purification of the extract, structure elucidation of the isolated pure compounds, and evaluation of biological activities of the extracts and the isolated compounds, are in the scope of this research.

CHAPTER 2

LITERATURE REVIEW

2.1. *Serpula dendrocalami*

Serpula dendrocalami is a brown rot wood-decaying fungus within the genus *Serpula* which was first described from the roots of the living bamboo of *Dendrocalmus* (**Figure 1**). The basidiocarp was characterized by pileate fruiting body, grow either solitarily or clusters. Their texture was soft, containing varying amounts of moisture when fresh. After dying, the basidiocarp was transformed into cork-like and brittle structure and become noticeably lightweight. The pileus was sessile cap, resembling a leaf or a semicircle in shape. Color of pileal surface was cream to light brown when fresh, turning brown upon drying. The pileus texture was smooth but uneven. The hymennophore surface was poroid, with pores which were slightly indented at the edges. The color was yellowish-brown when fresh, transitioning yellowish-brown to brown when dry, with paler edges and darker center. The context was spongy, with a cream-colored surface. The tubes colored yellowish-brown to brown (**Figure 2**).

This species sistered to *S. similis* but differed from *S. dendrocalami* by its smaller basidiocarps and sandy soil-associated habitat. Two other species in genus *Serpula* are similar to *S. dendrocalami*: *S. himantioides* and *S. lacrymans*. The former differed from *S. dendrocalami* by membranaceous basidiocarps with smooth hymenophore and larger basidiospores and found on stumps of *Picea* or *Pinus*. In contrast, *S. lacrymans* distinguished from *S. dendrocalami* by its reflexed basidiocarps

with rhizomorphs and larger basidiospores, and grew on manufactured wood such as in old woody houses (Wang et al., 2019).

(**A**)

(**B**)

Figure 1. *Serpula dendrocalami* C. L. Zhao, sp. nov. (holotype): basidiocarps (**A** and **B**) (Wang et al., 2019).

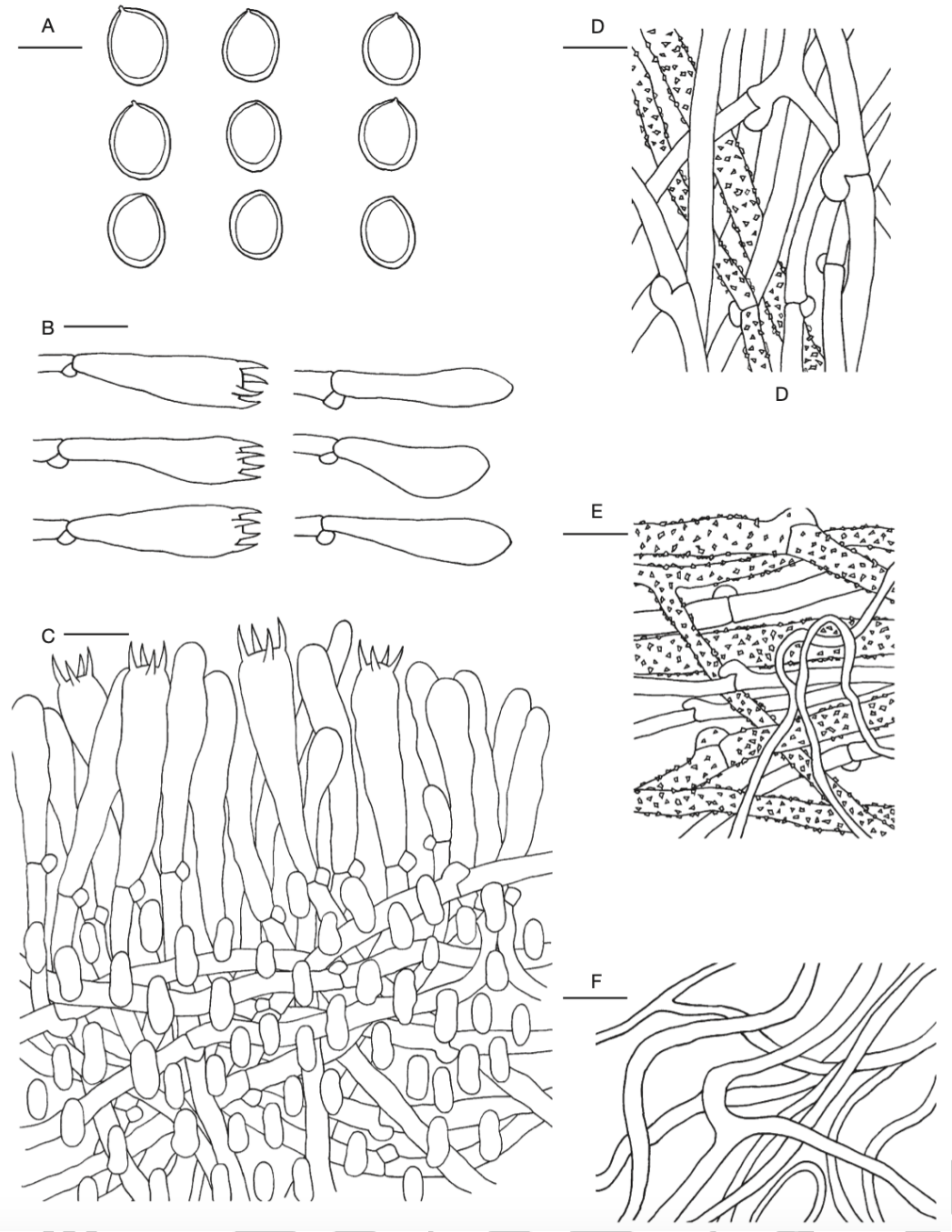

Figure 2. *Serpula dendrocalami* C. L. Zhao, sp. nov. (holotype), microscopic structures: basidiospores (**A**); basidia and basidioles (**B**); a section of hymenium (**C**); hyphae from trama (**D**); hyphae from context (**E**); skeletal hyphae from context (**F**) (Wang et al., 2019).

From literature survey, there have been only a few reports on the isolation of compounds from the genus *Serpula* due to this genus is a rare macrofungus. Based on searching in SciFinder, PubMed, and ScienceDirect databases, there are only two publications on the isolation of compounds from the genus *Serpula*.

2.2. Isolated compounds from *Serpula* sp.

In 2018, Williams et al. reported the isolation of *N*-oxidized tyrosine derivatives serpulaines A–C (**1**–**3**) (**Figure 3**) from the chloroform ($CHCl_3$) fractions of the fruiting bodies of *Serpula* sp. collected from Sri Lanka. The structures of these isolated new compounds were elucidated by spectroscopic and single-crystal X-ray diffraction analyses. Serpulanines A (**1**) and B (**2**) contain the (*E*)-2-hydroxyimino hydroxamic acid which is a rare functional group in natural products. The *E* oxime configuration of compound **1** was confirmed by X-ray diffraction analysis of the crystals. Serpulanine A displayed class I/II histone deacetylases (HDAC) inhibitory activity in murine metastatic lung carcinoma cells in a dose-dependent manner with 50% inhibitory concentration (IC_{50}) value of 7 μM (Williams et al., 2018).

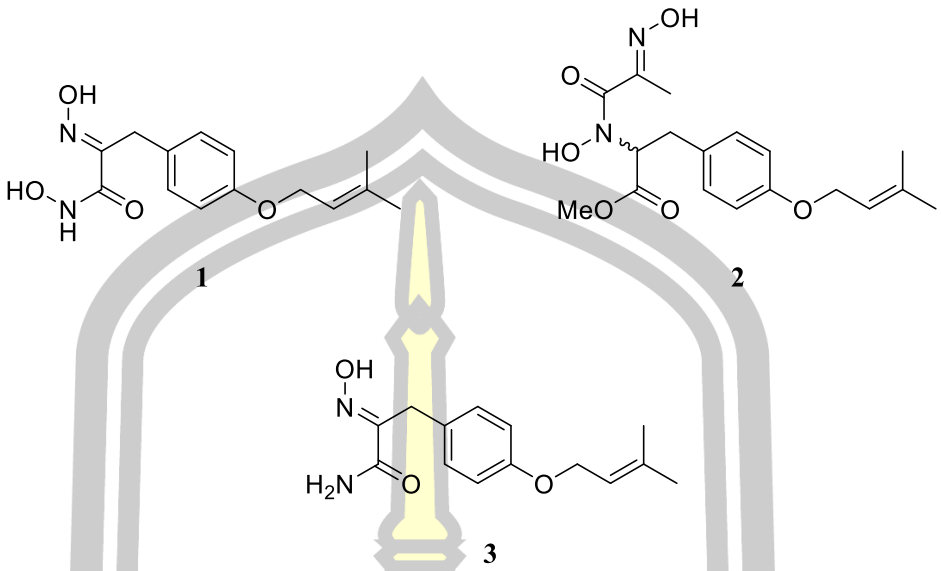

Figure 3. Structures of compounds **1**–**3**.

2.3. Isolated compounds from *Serpula himantioides*

In 2002, Aqueveque et al. reported the isolation of succinimide and maleimide derivatives, himanimides A–D (**4**–**7**) (**Figure 4**) from the cultured broth extract of *Serpula himantioides*. The fruiting bodies of *S. himantioides* were collected in Chile, growing on *Eucalyptus globulus*. Fermentation was carried out in yeast, malt, and glucose (YMG) medium at 24 °C for 10 days. The structures of isolated compounds were elucidated by spectroscopic analysis. Himanimide C exhibited antifungal activity against *Alternaria porri*, *Aspergillus ochraceus* and *Pythium irregulare* with minimum inhibitory concentration (MIC) value of 25 µg/mL and showed cytotoxicity against human leukemia cell line (HL 60) cancer cell with IC_{50} value of 10 µg/mL (Aqueveque et al., 2002).

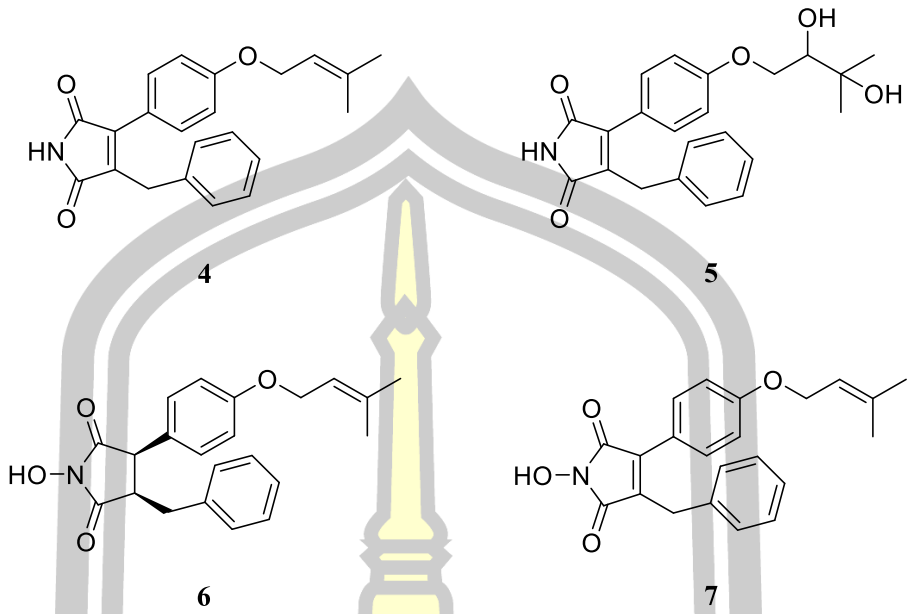

Figure 4. Structures of compounds **4**–**7**.

CHAPTER 3

MATERIALS AND METHODS

3.1. General experimental procedures

Optical rotations were determined using a JASCO P-200 digital polarimeter. Ultraviolet (UV) spectra were recorded on a JASCO V-730 spectrophotometer. Fourier transform infrared (FTIR) spectra were acquired using a Bruker INVENNIO-S spectrometer. Nuclear magnetic resonance (NMR) spectra were recorded on a Bruker Ascend-400 (Prodigy unit) and Avance III HD 400 MHz spectrometers with deuterated solvents; deuterated chloroform ($CDCl_3$) (δ_H 7.26/δ_C 77.0 ppm), deuterated methanol (CD_3OD) (δ_H 3.31/δ_C 49.0 ppm), and deuterated dimethyl sulfoxide (DMSO-d_6) (δ_H 2.50/δ_C 39.5 ppm). High-resolution electrospray ionization mass spectrometry (HRESIMS) spectra were measured using a Bruker micrOTOF mass spectrometer. Column chromatography was performed using silica gel 60 (Merck), silica gel 60H (Merck), and Sephadex LH-20 (Merck). Aluminium-backed silica gel $60F_{254}$ (Merck) was used for analytical thin-layer chromatography (TLC).

3.2. The fungus *S. dendrocalami*

3.2.1. Fungal material

Natural fruiting bodies were collected on dead log of *Pterocarpus macrocapus* from Tha-Uthen District, Nakhon Phanom Province, Thailand, in August 2022. The voucher mushroom collection was deposited at the Medicinal Mushroom Museum, Faculty of Science, Mahasarakham University as Mahasarakham University Thailand 7911 (MSUT-7911) (**Figure 5**).

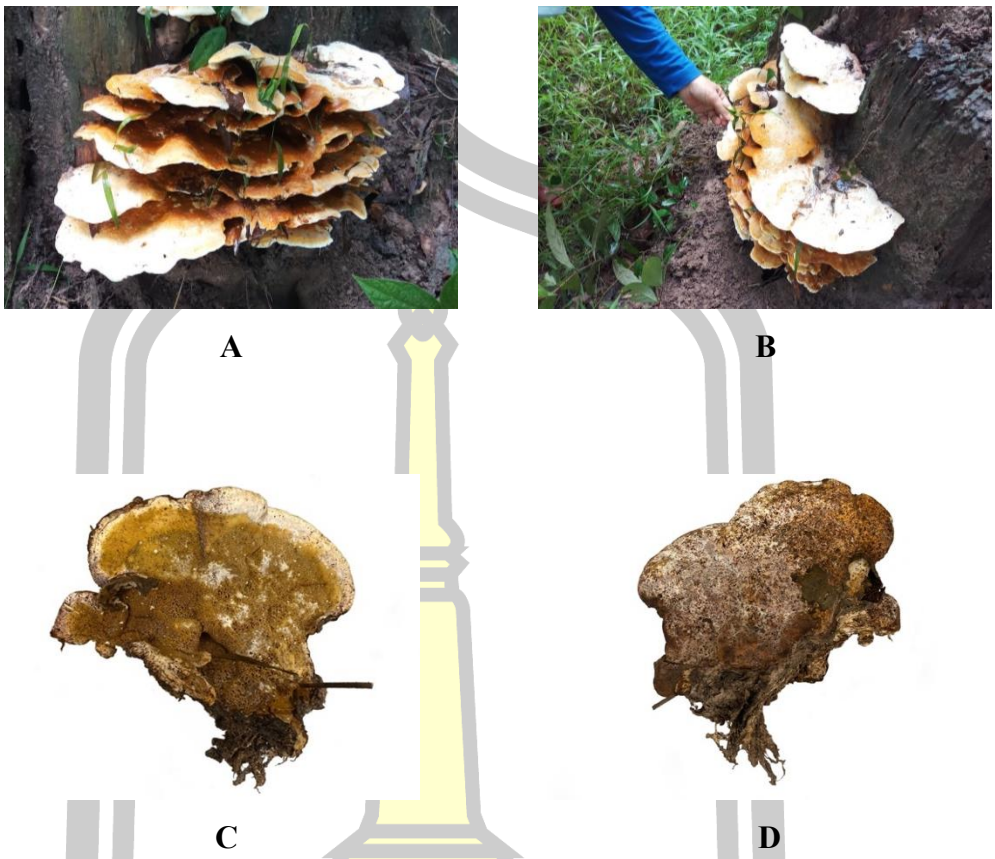

Figure 5. Natural living habitats (**A** and **B**) and fruiting body (front (**C**), back (**D**)) of *Serpula dendrocalami*.

3.2.2. Living isolation

The isolation of living culture of the sample code Mahasarakham University culture collection 032 (MSUCC032) of the natural mushroom specimen of *S. dendrocalami* was performed. The inner tissue of *S. dendrocalami* was cut, then soaked in 10% v/v clorox for 1 min and sterile water for 1 min, and then placed on potato dextrose agar (PDA) for cultivation.

3.2.3. DNA extraction

The pieces of fruiting bodies were homogenized in a cold mortar and pestle. The fruiting bodies powder was transferred into a microcentrifuge tube and genomic deoxyribonucleic acid (DNA) was extracted using the plant DNA extraction kit handbook (Vivantis, Malaysia) (A. Sangdee & Sangdee, 2013). DNA samples were checked on 1% agarose gel electrophoresis and stored at −20 ℃ for further experimental use.

3.2.4. Identification of the *S. dendrocalami*

The fungus was identified on the basis of internal transcribed spacer (ITS) ribosomal ribonucleic acid (rDNA), large subunit of the rRNA (LSU rRNA) and elongation factor 1 alpha (EF - 1α) gene sequencing data. Polymerase chain reaction (PCR) was conducted for the ITS gene (K. Sangdee et al., 2015). The resulting PCR products were purified using the Gel/PCR DNA Fragments Extraction Kit (Vivantis, Malaysia). Sequencing was carried out by Macrogen Inc. (Korea). The partial ITS sequence data were compared with those in the national center for biotechnology information (NCBI) database using the nucleotide basic local alignment search tool (BLAST) program (www.ncbi.nih.gov/blast). The novel partial sequence was deposited in the GenBank nucleotide sequence database. Reference sequences from related species were downloaded and aligned using ClustalW (www.genome.jp/tools/clustalw/). Phylogenetic analysis of the ITS region was performed using MEGA program (Tamura et al., 2013), and a maximum likelihood (ML) tree was constructed with 1000 bootstrap replicates using the Kimura 2-parameter method for pairwise deletion at uniform rates.

3.3. Small scale fermentation

The culture of *S. dendrocalami* was maintained on PDA at room temperature. The inoculum was prepared by growing initial fungus on PDA plate for 7 days at room temperature. Then, a 1 × 1 cm fungal colony was cut with a sterile inoculation needle and transferred to 25 mL of malt extract broth (MEB) (6 g/L of malt extract, 1.8 g/L of maltose, 6 g/L of dextrose, and 1.2 g/L of yeast extract in a 250 mL Erlenmeyer flask and incubated at room temperature on rotary shaker (125 rpm) for 7 days. After incubation, the culture was transferred into a 1 L erlenmeyer flask containing 250 mL of the same liquid medium (MEB) and carried out at room temperature for 20 days under static conditions (**Figure 6**).

(A) **(B)**

Figure 6. Colony of *Serpula dendrocalami* in 25 mL (**A**) and 250 mL (**B**) of MEB.

3.3.1. Extraction of the culture broth

The culture was filtered through 0.2 µm filter membrane, the filtrate was extracted with ethyl acetate (250 mL × 2). The ethyl acetate layer was concentrated under reduced pressure to obtain crude ethyl acetate extract from culture broth (**Flowchart 1**).

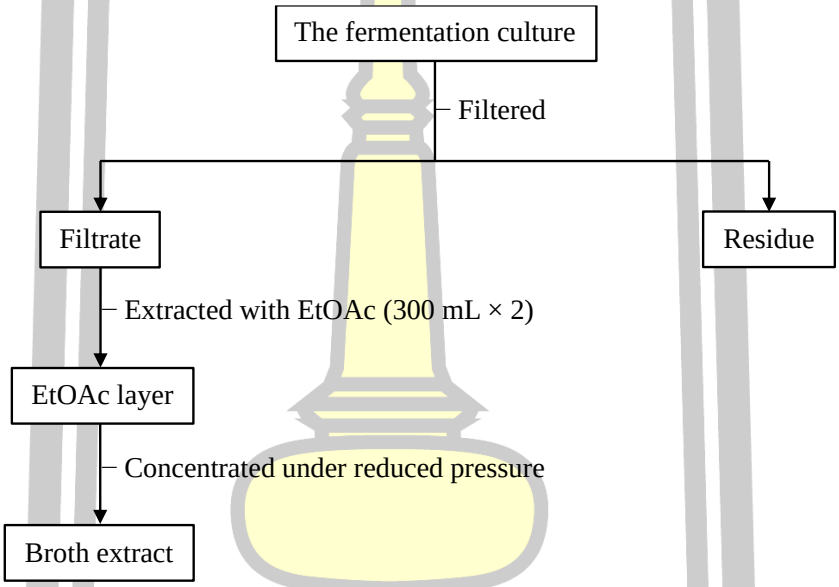

Flowchart 1. Extraction of the culture broth.

3.3.2. Extraction of the fungal mycelium

The residual mycelium was macerated in 300 mL of acetone for 5 days under static conditions and filtered. The filtrate was concentrated under reduced pressure to afford crude extract from mycelium (**Flowchart 2**).

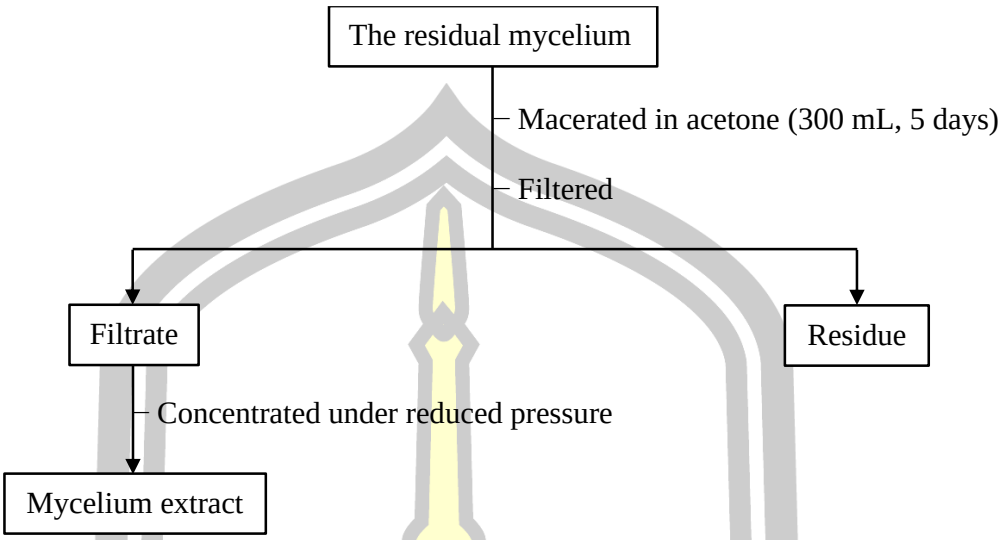

Flowchart 2. Extraction of the fungal mycelium.

3.4. Extraction of the natural fruiting bodies

Natural fruiting bodies of *S. dendrocalami* were cut into small pieces and dried at 60 ℃ for 2 days to remove moisture. The dried fruiting bodies were macerated in dichloromethane (DCM) (5 L) at room temperature for 5 days (**Figure 7**). The mixture was filtered, and the filtrate was concentrated under reduced pressure. This extraction was repeated to obtain a combined dark brown gum of dichloromethane (DCM) extract. The residual fungal material was then extracted with methanol using the same procedure as described above to dark brown gum of methanol (MeOH) extract. The methanol extract was suspended in water (800 mL) and then partitioned with ethyl acetate (EtOAc) (1 L × 6) to afford a combined dark brown gum ethyl acetate (EtOAc) extract (**Flowchart 3**).

(A) **(B)**

(C)

Figure 7. Dried fruiting bodies of *Serpula dendrocalami* (**A**) and maceration of the natural fruiting bodies (**B** and **C**).

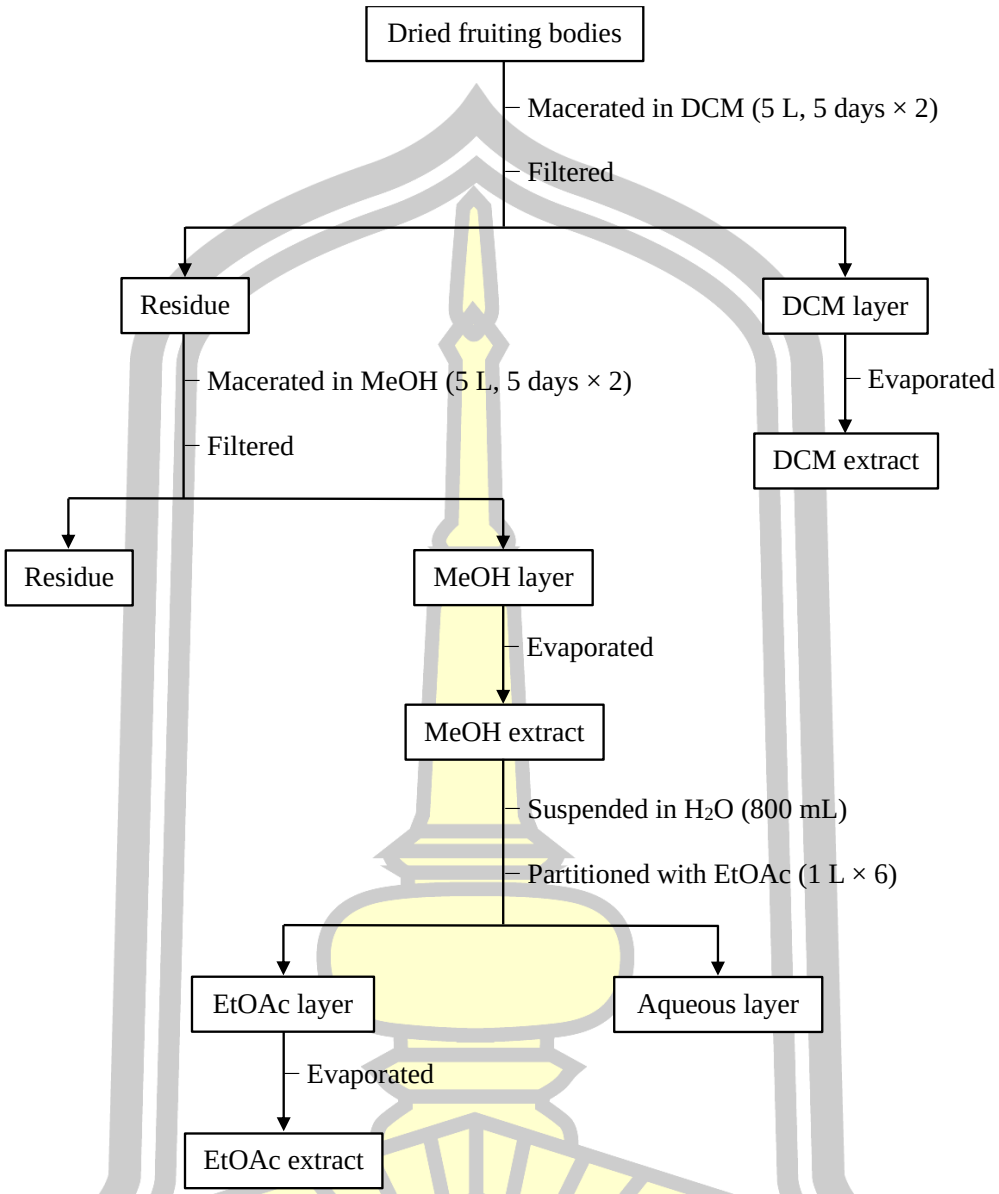

Flowchart 3. Extraction of the natural fruiting bodies.

3.5. Isolation

The dichloromethane extract was subjected to column chromatography (CC) on silica gel (7.5 × 30 cm, hexane/acetone, step gradient elution 0:100, 20:80, 40:60, 60:40, 80:20, and 100:0, and then with acetone/EtOAc, 80:20 and 60:40) (**Figure 8**) to afford nine fractions (Fr-A–Fr-I). Fr-B (6.89 g) was separated by CC on silica gel

(5 × 28 cm, hexane/acetone, 100:0, 80:20, 60:40,40:60, 20:80, and 0:100, and then with acetone/EtOAc 80:20, and 60:40) to furnish **13** (1.05 g) and **14** (347 mg). Fr-D (464 mg) and Fr-E (248 mg) were combined and further chromatographed over silica gel (2.5 × 26 cm) followed by silica gel (2 × 18 cm) using hexane/EtOAc 80:20, 70:30, 60:40, 50:50, and 40:60, as eluent. Selected fractions were subjected to further purification by Sephadex LH-20 column (0.8 × 10 cm, MeOH) to furnish **8** (4.1 mg) and **9** (1.2 mg). A combined fraction (776 mg) of Fr-F and Fr-G was separated by silica gel column (2.5 × 28 cm, hexane/EtOAc, 80:20, 70:30, 60:40, 50:50, 40:60, 30:70, 20:80, 10:90, and 0:100, and then with EtOAc/MeOH, 90:10, 80:20, and 70:30) followed by Sephadex LH-20 column (0.8 × 10 cm, MeOH) to furnish **3** (8.8 mg), **12** (3.5 mg), and a mixture of **11** and **12** (82 mg). Fr-H (48 mg) was fractionated by CC on silica gel (1.5 × 15 cm, hexane/EtOAc, 80:20, 70:30, 60:40, 50:50, 40:60, 30:70, 20:80, 10:90, and 0:100, and then with EtOAc/MeOH, 90:10, 80:20, and 70:30) followed by purification over Sephadex LH-20 (0.8 × 10 cm, MeOH) to furnish **10** (1.2 mg) and **12** (2.4 mg) (**Flowchart 4**).

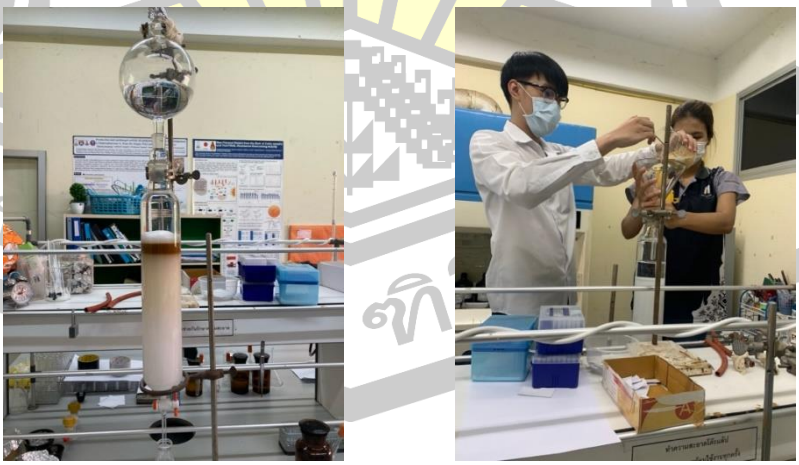

(**A**) (**B**)

Figure 8. Isolation of the DCM extract using column chromatography (**A** and **B**).

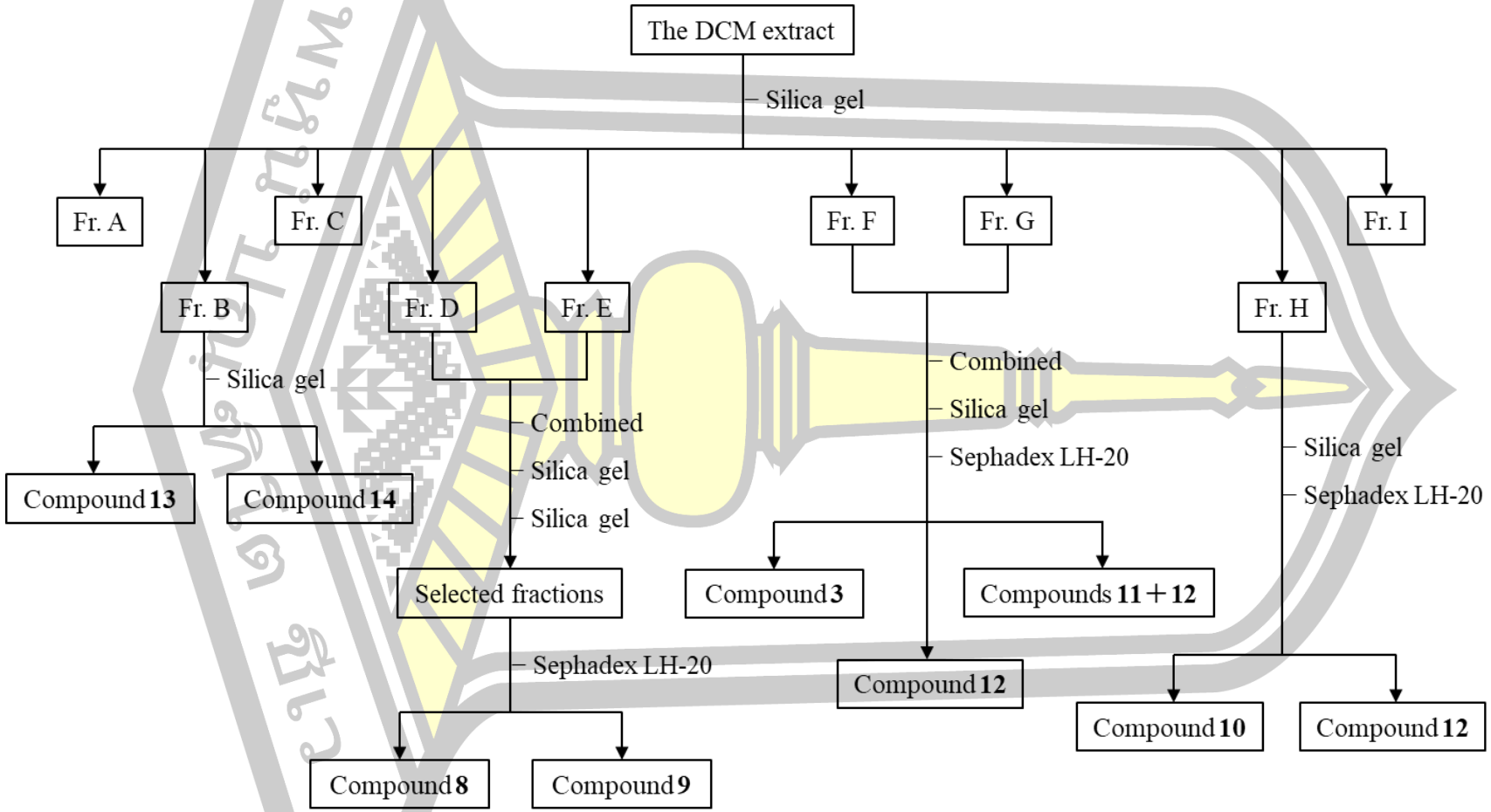

Flowchart 4. Isolation of the DCM extract.

3.6. Structure elucidation

The structures of the pure isolated compounds were elucidated based on spectroscopic methods (1D and 2D nuclear magnetic resonance (NMR) spectroscopy, mass (MS) spectrometry, infrared (IR) spectroscopy, and ultraviolet-visible (UV-Vis) spectroscopy). The structures of the known compounds were confirmed by the comparison of their spectroscopic data to those reported in literatures.

3.7. Antibacterial activity assay

3.7.1. Bacterial strains and cultivation

The antibacterial activity was assayed against three Gram-positive bacteria, including methicillin-resistant *Staphylococcus aureus* (MRSA) DMST 20651, methicillin-susceptible *Staphylococcus aureus* (MSSA) DMST 2933, and *Bacillus cereus* ATCC 11778. These bacterial strains were cultured on Mueller-Hinton agar (MHA) at 37 ℃ for 16−18 h.

3.7.2. Agar well diffusion method

The agar well diffusion method was performed to determine antibacterial activity of the samples (Sangdee et al., 2018). The sample solutions (50 mg/mL) were added to each well (0.1 mL per well) and incubated at 37 °C for 16−18 h. The zone of inhibition was measured after incubation of the plates. The negative controls of 10% (v/v) methanol and 10% dimethyl sulfoxide (DMSO) were used. A standard positive control was tetracycline (250 μg/mL).

3.7.3. MIC and MBC determination

The minimum inhibitory concentration (MIC) and minimum bactericidal concentration (MBC) values were evaluated using the microdilution method (Sangdee et al., 2018). MICs were determined by identifying the solutions that were clear after incubation compared with the control well. MBCs were determined by transferring bacterial suspensions from the MIC assay onto MHA plates. The MBC referred to the lowest concentration that showed no growth after incubation for 24 h. A reference standard antibiotic tetracycline (250 µg/mL) was used in the study.

3.8. NO inhibitory activity assay

Inhibition of nitric oxide (NO) production were evaluated in lipopolysaccharide (LPS)-activated murine macrophage RAW 264.7 cells, using a method modified from previous report (Makchuchit et al., 2017). RAW 264.7 cells were cultured in Dulbecco's modified eagle's medium (DMEM) supplement with 10% fetal bovine serum and 1% antibiotic-antimycotic solution (10×10^3 units/mL of penicillin, 10 mg/mL of streptomycin, and 25 µg/mL of amphotericin B. The cells were maintained at 37 °C in an incubator with 5% CO_2 and 95% humidity. For the NO inhibitory assay, the RAW 264.7 cells (1×10^6 cells/well) in DMEM were seeded into 96-well plates containing 100 µL of culture medium and incubated for 24 h. Subsequently, the medium was replaced with fresh medium containing 2 µg/mL of LPS, and test samples were added to each well at the final concentrations of 20 µg/mL. DMSO was used in the solvent control wells. After 24 h of incubation, 100 µL of supernatant was transferred to new 96-well plates, and 100 µL of Griess reagent

(1% sulfanilamide in 0.1% *N*-(1-naphtyl)ethylenediamine dihydrochloride in 2.5% H_3PO_4 solution) was added to each well. The absorbances (A) of samples and control were measured at 520 nm using a microplate reader, and the percentage of NO inhibition was determined according to the formula below. Diclofenac sodium was used as a positive control.

$$\%\text{Inhibition of NO production} = [(A\ sample - A\ control)/A\ control] \times 100$$

To evaluate the cytotoxic effect of samples in RAW 264.7 cells in the assay condition, a 3-(4,5-dimethylthiazolyl-2)-2,5-diphenyltetrazolium bromide (MTT) assay was performed. Briefly, after removing the supernatant from the incubated plate, a 5 mg/mL MTT solution was added to each well, and incubated at 37 ℃, 5% CO_2, for 2 h. Then the medium was removed, and 50 µL of DMSO was added to dissolve the formazan product. The absorbance was measured at 570 nm using a microplate reader. The percentage of cell survival was considered acceptable if it remained above 70% compared to the control.

3.9. Cytotoxicity assay

The cytotoxic activity against human lung cancer (A549) cell lines was assayed using the previously described method with some modifications (Su et al., 2009) (Min et al., 2023). Briefly, cell suspensions in culture medium (100 µL per well) were seeded into 96-well plates and incubated at 37 °C in a humidified 5% CO_2 atmosphere. After 24 h, 100 µL of culture medium containing the test sample was added to each well, followed by an additional 72 h incubation. Half of the medium

was removed then added 10 µL of 5 mg/mL MTT in phosphate buffer saline, and the cells were incubated for 4 h at 37 °C. Afterward, the medium was removed, DMSO (50 µL per well) was added, and absorbance was measured at 570 nm on a microplate reader. The absorbance values were used to calculate cell viability relative to the control. All assays were performed in duplicate, and results were expressed as %cytotoxicity compared to the control group.

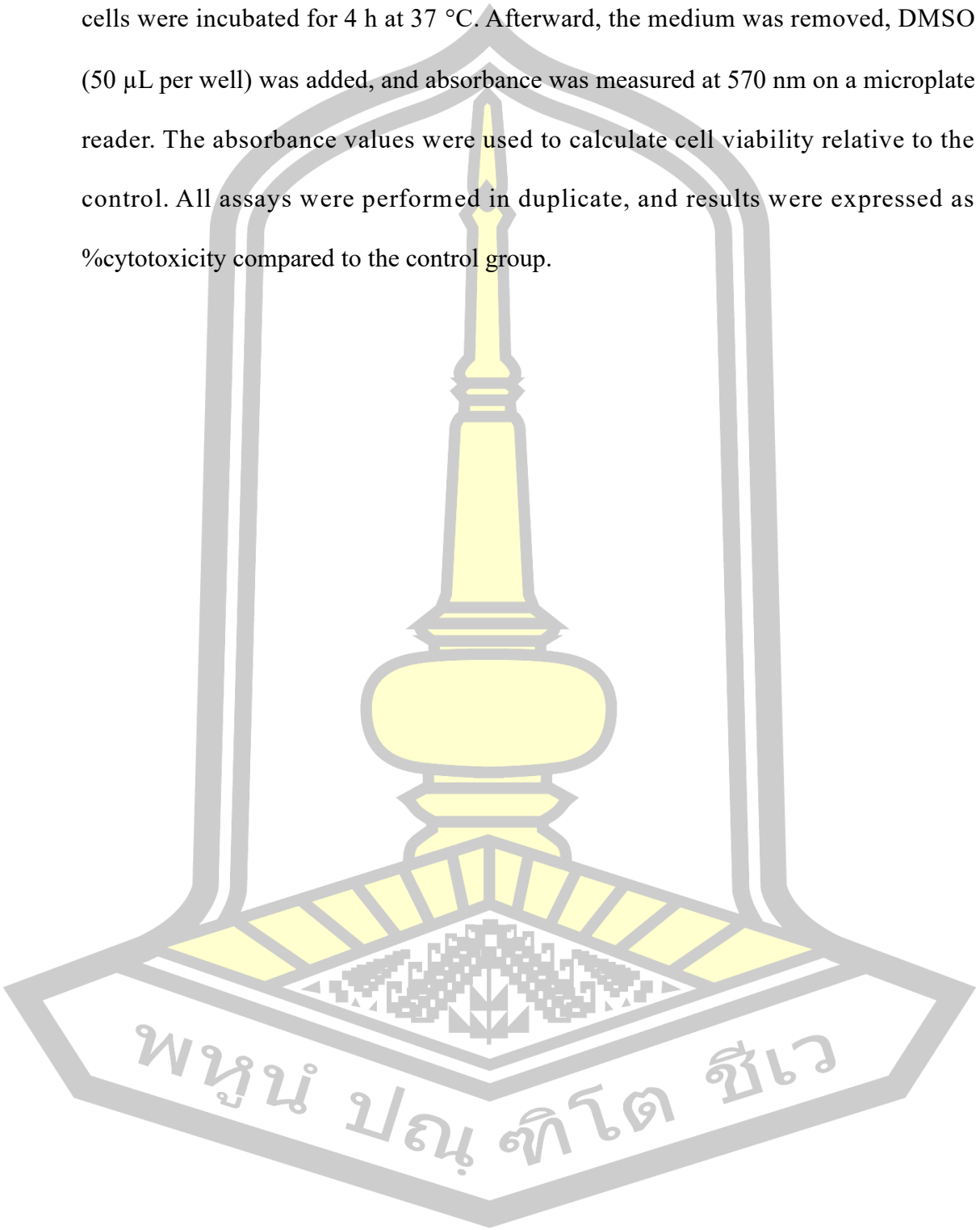

CHAPTER 4

RESULTS AND DISCUSSION

4.1. The fungus *S. dendrocalami*

4.1.1. Living isolation

The mycelium of *S. dendrocalami* was grown on potato dextrose agar (PDA) plate. The living culture was maintained in sterile distilled water and preserved at the Department of Biology, Faculty of Science, Mahasarakham University, as MSUCC032 (**Figure 9**).

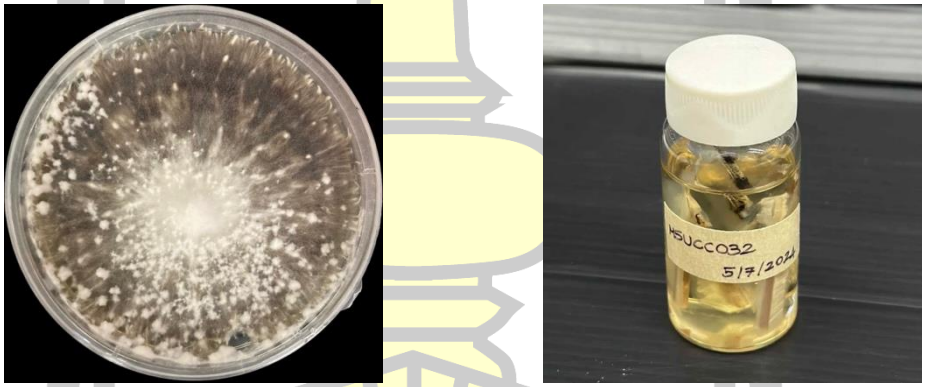

A **B**

Figure 9. Mycelium of *Serpula dendrocalami* on PDA (**A**) and fungal strain in sterile distilled water (**B**).

4.1.2. Identification of the *S. dendrocalami*

This fungus was identified as *Serpula dendrocalami* (Serpulaceae) based on the ITS rDNA, large subunit of the rRNA (LSU rRNA) and elongation factor 1 alpha (EF-1α) gene sequencing data (GenBank accession number: PP838810,

PQ372921 and PQ416623, respectively). Maximum likelihood (ML) tree depicting the fungal isolate *Serpula dendrocalami* (strain MSUCC032) alongside related species, constructed from partial ITS rDNA, LSU rRNA and EF-1α gene sequences. The tree was rooted at the midpoint and developed using the GTR + GAMMA model. Branch lengths indicate the expected number of substitutions per site, and support values above branches represent bootstrap percentages (**Figure 10**).

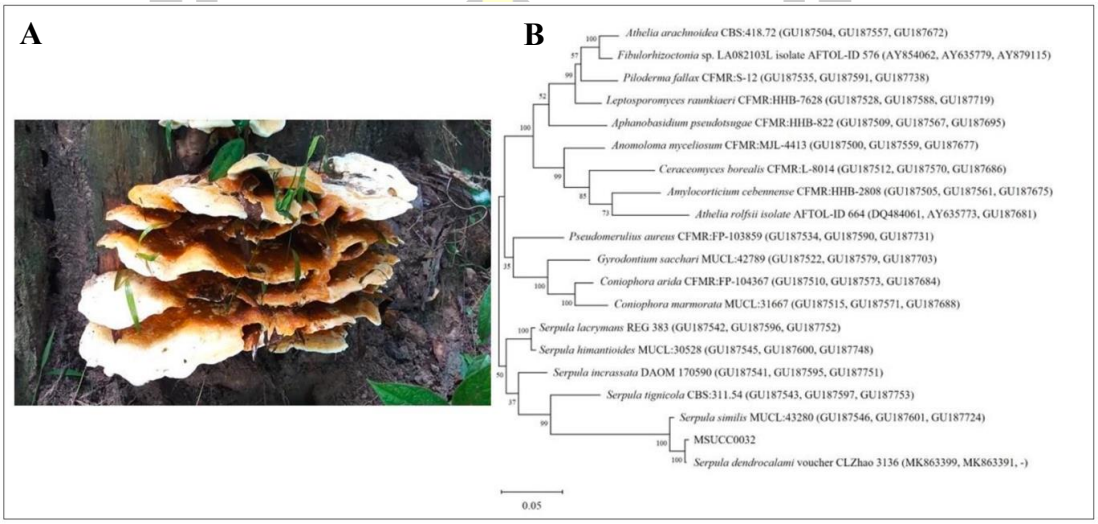

Figure 10. Basidiocarp of the fungus *Serpula dendrocalami* (MSUT-7911) (**A**) and maximum likelihood (ML) tree (**B**).

4.2. Small scale fermentation

4.2.1. Extraction of the culture broth and cell mycelium

From the results, the crude extracts from the small scale extraction of the culture broth and the cell mycelium were 22.7 mg and 30.3 mg, respectively (**Table 1**).

Table 1. Fermentation and extraction yield of the culture broth and fungal mycelium.

25 mL of MEB		250 mL of MEB		Weight (mg)	
Started	**Collected**	**Started**	**Collected**	**Broth**	**Mycelium**
04/04/2023	11/04/2023	11/04/2023	03/05/2023	27.7	30.0

4.3. Extraction of the natural fruiting bodies

The quantity of the DCM, MeOH, and EtOAc extracts is shown in **Table 2**.

Table 2. Extraction yield of the natural fruiting bodies *Serpula dendrocalami.*

Crude extract	Weight (g)
DCM	22.5
EtOAc	8.9
MeOH	36.6

4.4. Biological activities of the crude extracts

4.4.1. Antibacterial activity

The extracts were evaluated for antibacterial activity against three Gram-positive bacteria, including *S. aureus* (MRSA), *S. aureus* (MSSA), and *B. cereus* using agar well diffusion method. A standard positive control was tetracycline (**Table 3**). The assay was performed by Assoc. Prof. Dr. Aphidech Sangdee from the Department of Biology, Faculty of Science, Mahasarakham University.

Table 3. Antibacterial activity of the crude extracts.

Crude extract	Inhibition zone (mm)		
	B. cereus	***S. aureus* (MRSA)**	***S. aureus* (MSSA)**
Broth	-	-	-
Mycelium	14 × 15	-	-
DCM	8 × 8	-	-
EtOAc	13 × 13	12 × 12	11 × 11
MeOH	13 × 13	22 × 22	20 × 20

Sample were tested at 50 mg/mL. Tetracycline was used as a positive control.

4.4.2. NO inhibitory activity

The inhibition effects of the extracts on NO production in LPS-activated RAW 264.7 cells. Diclofenac was used as a positive control. The cytotoxic effect of the extracts in RAW 264.7 cells was evaluated by MTT method (**Table 4**). The assay was performed by Asst. Prof. Dr. Ruchilak Rattarom from Faculty of Pharmacy, Mahasarakham University.

Table 4. NO inhibitory activity of the crude extracts.

Crude extract	% Inhibition	% Cell survival
Broth	56.03	94.52
Mycelium	76.46	65.26
DCM	49.35	82.42
EtOAc	64.24	96.03
MeOH	18.09	89.09

Diclofenac was used as a positive control. Sample were tested at 100 µg/mL.

4.5. ^{1}H NMR spectrum of the crude extracts

The broth and mycelium extracts from small scale fermentation, and the DCM, EtOAc, and MeOH extracts of the natural fruiting bodies were subjected to ^{1}H NMR analyses. All the extracts obviously illustrated the aromatic proton signals of their chemical constituents except broth and mycelium extracts (**Figure A1**).

From the ^{1}H NMR spectrum, antibacterial and NO inhibitory activities, and the previous report on the isolation of active compounds from the $CHCl_3$ extract of the genus *Serpula*, the DCM extract was selected to chemical investigate in this study.

4.6. Isolation

The purification of dichloromethane extract led to the isolation of three undescribed *O*-prenyl-tyrosime oxime derivatives, serpulanine D−F (**8**−**10**), together with five know compounds, serpulanine C (**3**) (Williams et al., 2018), valencic acid (**11**) (Ito et al., 1988), 4-prenyloxyphenylacetic acid (**12**) (Awad et al., 2005), ergosterol (**13**), and ergosterol endoperoxide (**14**) (**Figure 11**). The structures were elucidated on the basis of ^{1}H and ^{13}C NMR, UV, IR spectroscopic and mass spectrometry data, including 2D NMR techniques (COSY, HSQC, HMBC, and NOESY). The structures of known compounds were confirmed by comparison of their spectroscopic data to those reported in literatures.

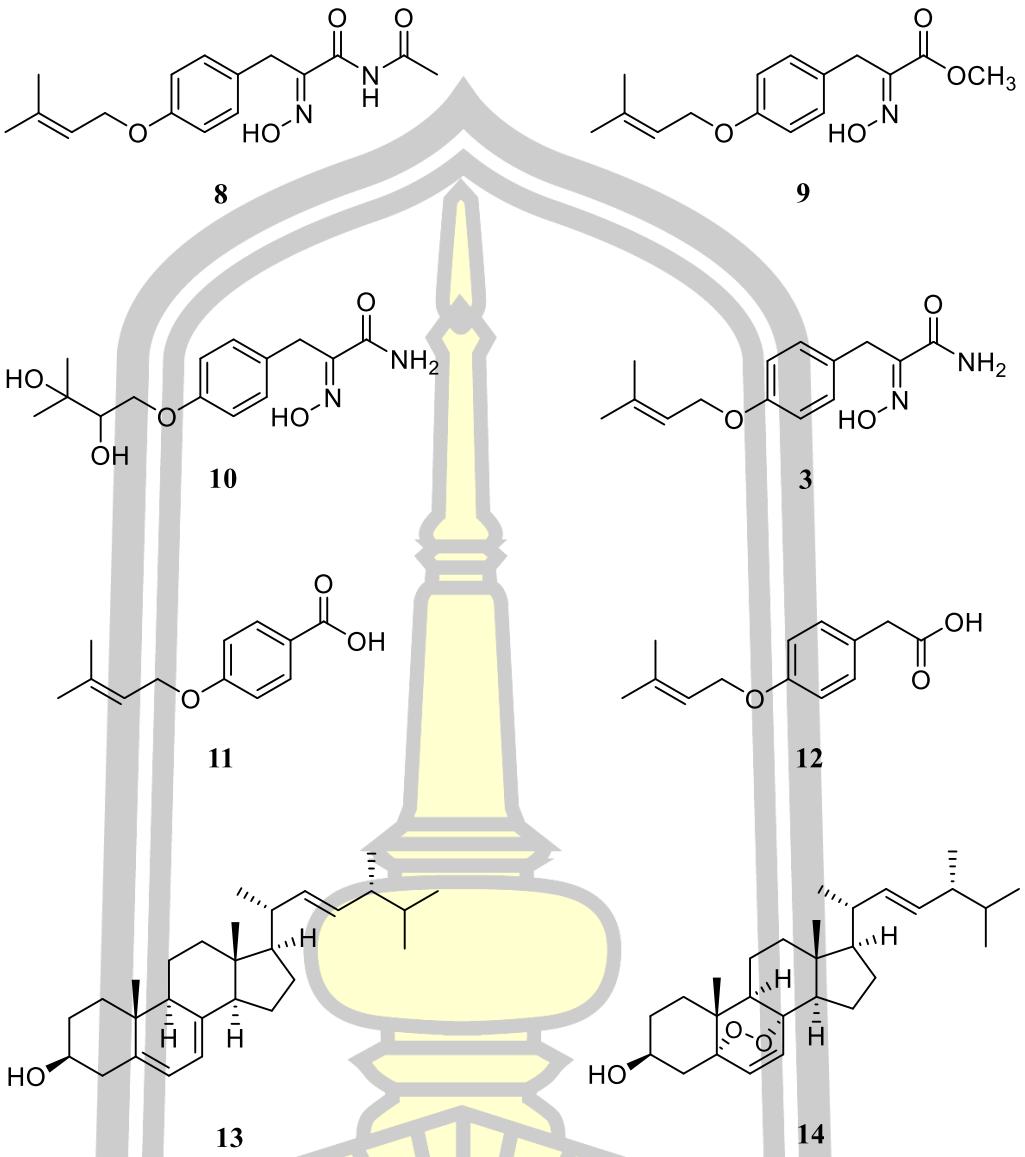

Figure 11. Isolated compounds from the natural fruiting bodies *Serpula dendrocalami.*

4.7. Structure elucidation of the isolated compounds from *S. dendrocalami*

Serpelanine D (**8**) was isolated as a white amorphous solid. The molecular formula was determined to be $C_{16}H_{20}N_2O_4$ by HRESIMS. The IR spectrum exhibited a broad absorption band of hydroxy group and *N*H at ν_{max} 3340 cm^{-1} and the carbonyl absorption bands at ν_{max} 1694–1668 cm^{-1}. The ^{13}C NMR, DEPT-135, and HSQC spectroscopic data indicated the presence of sixteen carbons categorised as two

carbonyl carbons (δ_C 170.5 and 162.4), four sp^2 tetrasubstituted carbons, five sp^2 methine carbons (δ_C 114.5 × 2, 129.7 × 2, and 120.0), two methylene carbons, and three methyl carbons (**Table 5**). The presence of a *para*-substituted benzene ring (C-4–C-9) was revealed based on COSY correlations between two sets of doublets aromatic H-5/H-9 (δ_H 7.10, d, J = 8.7 Hz) and H-6/H-8 (δ_H 6.82, d, J = 8.7 Hz), the HMBC correlations from H-5/H-9 and H-6/H-8 to the sp^2 tetrasubstituted carbons C-7 (δ_C 156.9) and C-4 (δ_C 127.8) (**Figure A15**). The presence of a prenyl group (C-10–C-14) was demonstrated by COSY correlation of H_2-10 and H-11 (δ_H 5.39, m) and the HMBC correlations from H_2-10, H_3-13, and H_3-14 to C-12 (**Figure A15**). The prenyl ether linkage to the benzene ring was indicated by the intense HMBC correlation from H_2-10 to C-7. The other side of the benzene ring (C-4) was bonded to a methylene carbon C-3 (δ_C 27.6; δ_H 3.74, 2H, s), which was revealed by the HMBC correlations from H_2-3 to C-4 and C-5/C-9, and from H-5/H-9 to C-3. The HMBC correlations from H_2-3 to a sp^2 carbon (δ_C 151.5, C-2) and a carbonyl carbon (δ_C 162.4, C-1) demonstrated the carbon linkage of C-3/C-2/C-1. Elucidation of the imide moiety was based on the HMBC data from *N*H (δ_H 9.99, s) of the imide to a carbonyl carbon C-1 and a methyl carbon of an acetyl group (δ_C 25.1, C-2′), and from H_3-2′ to an acetyl carbonyl carbon (δ_C 170.5, C-1′). Intense HMBC correlation from *N*OH (δ_H 12.47, s) to C-2 (δ_C 151.5) indicated the presence of an oxime unit (**Figure A15**).

Compound **8** is closely related to the known co-metabolite serpulanine C (**3**) which was first isolated from fruiting bodies of *Serpula* sp. (Williams et al., 2018). The difference was only the presence of the imide moiety in the structure of **8** instead of the carboxyamide in **3**. Therefore, **8** was identified as a derivative of **3**, wherein the

C-1 carboxyamide of **3** is acetylated to form an imide. NMR data for **8** and **3** in DMSO-d_6 were similar. The configuration of the oxime group of **8** was elucidated based on the comparison of ^{13}C NMR chemical shift of its methylene carbon C-3 (δ_C 27.6) with (*E*,*Z*)-pasmmaplin A, which the structure contains both (*E*) and (*Z*)-oxime moieties. The ^{13}C NMR data of methylene carbons adjacent to the (*E*)-oxime; δ_C 28.7, and (*Z*)-oxime; δ_C 37.5, groups in this compound were reported (Park et al., 2003). Additionally, ^{13}C NMR chemical shift of the methylene carbon next to the (*Z*)-oxime unit (δ_C 39.7) in the structure of maydisone was referenced (Tran et al., 2021). Based on these supporting data, the *E*-configuration of the oxime group of **8** was proposed. The ^{13}C NMR data (in DMSO-d_6) at C-3 position of **8** was the same with serpulanine C (δ_C 27.7) which the *E*-configuration of the oxime was reported (Williams et al., 2018). For comparison with other related compounds (**9** and **3**), 1D and 2D NMR spectra of **8** were taken also in $CDCl_3$ (**Table 6**). Interpretation of the NMR data ($CDCl_3$) (**Figure A30**) further supported the proposed structure of **8**.

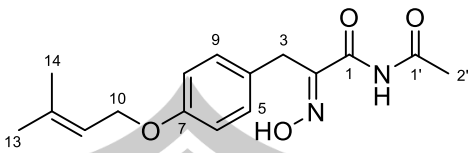

Table 5. ^{1}H and ^{13}C NMR spectroscopic data and 2D NMR data of **8** in DMSO-d_6.

position	δ_H, mult. (J in Hz)	δ_C	COSY	HMBC	NOESY
1	-	162.4	-	-	-
2	-	151.5	-	-	-
3	3.74, s	27.6	5/9, 6/8	1, 2, 5/9, 4	5/9
4	-	127.8	-	-	-
5/9	7.10, d (8.7)	129.7	3, 6/8	7, 5/9, 6/8, 3	3, 6/8
6/8	6.82, d (8.7)	114.5	3, 5/9	7, 4, 6/8	10, 5/9
7	-	156.9	-	-	-
10	4.46, d (6.7)	64.1	14, 13, 11	7, 12, 11	14, 11, 6/8
11	5.39, m	120.0	14, 13, 10	13, 14	13, 10
12	-	136.9	-	-	-
13	1.72, s	25.4	10, 11, 14	12, 11, 14	11, 14
14	1.68, s	18.0	10, 11, 13	12, 11, 13	10, 13
1′	-	170.5	-	-	-
2′	2.25, s	25.1	N*H*	1′	N*H*
N*H*	9.99, s	-	2′	2′, 1	2′, NO*H*
NO*H*	12.47, s	-	-	2	N*H*

Calibration of DMSO-d_6 δ_H 2.50/δ_C 39.5

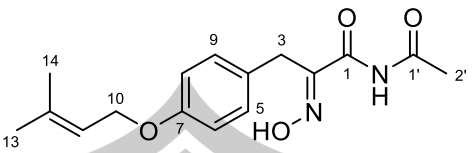

Table 6. ^{1}H and ^{13}C NMR spectroscopic data and 2D NMR data of **8** in $CDCl_3$.

position	δ_H, mult. (*J* in Hz)	δ_C	COSY	HMBC	NOESY
1	-	161.4	-	-	-
2	-	152.6	-	-	-
3	3.91, s	27.9	5/9, 6/8	1, 2, 5/9, 4	5/9
4	-	127.3	-	-	-
5/9	7.23, d (8.7)	130.3	3, 6/8	7, 5/9, 6/8, 3	3, 6/8
6/8	6.82, d (8.7)	114.7	3, 5/9	7, 4, 6/8	10, 5/9
7	-	157.7	-	-	-
10	4.46, d (6.7)	64.7	14, 13, 11	13, 12, 11, 7	14, 11, 6/8
11	5.47, m	119.6	14, 13, 10	13, 14, 10	13, 10
12	-	138.2	-	-	-
13	1.78, s	25.8	10, 11, 14	12, 11, 14	11, 14
14	1.72, s	18.1	10, 11, 13	12, 11, 13	10, 13
1′	-	173.3	-	-	-
2′	2.54, s	25.4	N*H*	1′	-
N*H*	9.22, s	-	2′	2′, 1, 1′	-
NO*H*	9.85, s	-	-	-	-

Calibration of $CDCl_3$ δ_H 7.26/δ_C 77.0

Serpelanine E (**9**) was isolated as a white amorphous solid. The molecular formula was determined as $C_{15}H_{19}NO_4$ by HRESIMS. Its NMR spectroscopic data in $CDCl_3$ were similar to those of **8** (in $CDCl_3$) with the only structural difference being the presence of a methoxy group (δ_H 3.82, 3H, s; δ_C 52.8) in **9** instead of the

acetamide in **8** (**Table 7**). The HMBC correlation (**Figure A43**) from the methoxy protons to carbonyl carbon C-1 (δ_C 163.8) indicated the C-1 methoxycarbonyl group. The structures of *para*-substituted benzene ring, prenyl ether, and C-3/C-2/C-1 unit, the same as **8** and **3**, were elucidated based on the COSY and HMBC data (**Figure A43**). Thus, the prenyl ether linkage was indicated by the HMBC correlation from H_2-10 to C-7. The C-3/C-2/C-1 unit of **9** was elucidated by the HMBC correlations from H_2-3 to C-1 (δ_C 163.8), C-2 (δ_C 151.9), C-4, and C-5/C-9. The ^{13}C NMR chemical shift of methylene carbon C-3 (δ_C 29.7) indicated the *E*-configuration of the oxime.

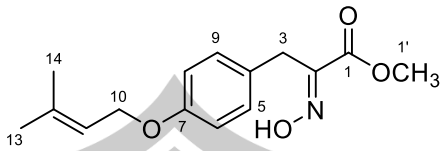

Table 7. ^{1}H and ^{13}C NMR spectroscopic data and 2D NMR data of **9** in $CDCl_3$.

position	δ_H, mult. (*J* in Hz)	δ_C	COSY	HMBC	NOESY
1	-	163.8	-	-	-
2	-	151.9	-	-	-
3	3.91, s	29.7	5/9	1, 2, 5/9, 4	5/9, 1′
4	-	127.4	-	-	-
5/9	7.22, d (8.7)	130.2	6/8, 3	7, 5/9, 3	6/8, 3
6/8	6.82, d (8.7)	114.7	5/9	7, 4, 6/8	5/9, 10
7	-	157.7	-	-	-
10	4.47, d (6.8)	64.7	11, 13, 14	7, 12, 11	6/8, 11, 14
11	5.47, m	119.7	10, 13, 14	14, 13	10, 13
12	-	138.2	-	-	-
13	1.78, s	25.8	10, 11, 14	12, 11, 14	11, 10, 14
14	1.72, s	18.2	10, 11, 13	12, 11, 13	10, 13
1′	3.82, s	52.8	-	1	3

Calibration of $CDCl_3$ δ_H 7.26/δ_C 77.0

Serpelanine F (**10**) was isolated as a white amorphous solid. The molecular formula of serpulanine F (**10**) was determined to be $C_{14}H_{20}N_2O_5$ by HRESIMS. Due to the reasons of sample solubility and limitation of sample quantity, the NMR spectra of **10** were recorded in CD_3OD. Interpretation of the ^{1}H, ^{13}C, DEPT-135, and 2D (HSQC, HMBC, COSY, and NOESY) NMR data (**Table 8**) led to the elucidation of the same structure of the tyrosine-derived core (C-1–C-9) as serpulanine C (**3**). ^{13}C NMR data at the position C-3 (δ_C 28.0) indicated *E*-configuration of the oxime. On

the other hand, compound **10** possessed a modified prenyl unit (C-10–C-14). The olefinic double bond of the prenyl group (C-11/C-12) was absent, which was replaced by a secondary alcohol (δ_C 77.6, C-11; δ_H 3.70, dd, J = 8.0, 2.7 Hz, H-11) and a tertiary alcohol (δ_C 72.8, C-12). This partial structure was indicated by the COSY correlations between H_2-10 and H-11, and HMBC correlations from H-11 to C-10 (δ_C 70.5), C-12 (δ_C 72.8), from H_3-13 (δ_H 1.25, s) to C-11, C-12 and C-14 (δ_C 16.7), and from H_3-14 (δ_H 1.22, s) to C-11, C-12 and C-13 (**Figure A62**). Consequently, serpulanine F (**10**) was identified as a derivative of serpulanine C (**3**), wherein the prenyl double bond was dihydroxylated. Due to the limitation of the sample quantity, configuration of the secondary alcohol (C-11) remains unassigned. The low specific rotation value of **10**, $[\alpha]^{26}_D = -2.0$ (c = 0.06, MeOH), which was within the range of standard deviation (±4.8) suggested that it was likely either a racemic mixture (50:50) or a non-racemic mixture of enantiomers with close composition. Asymmetric synthesis of a structurally related natural product possessing the same phenyl isopentyl ether with a 1,2-diol (corresponding to C-4–C-14 unit in **10**) was reported (Yang, 2016). The specific rotation of the synthetic (*S*)-isomer (92% ee) was reported to be $[\alpha]^{25}_D = -27.3$ (c = 0.6, MeOH).

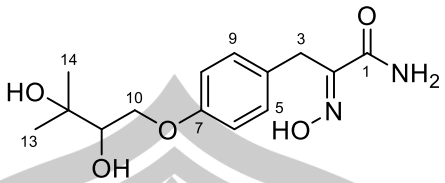

Table 8. ^{1}H and ^{13}C NMR spectroscopic data and 2D NMR data of **10** in CD_3OD.

position	δ_H, mult. (*J* in Hz)	δ_C	COSY	HMBC	NOESY
1	-	168.3	-	-	-
2	-	153.3	-	-	-
3	3.82, s	28.7	-	1, 2, 5/9	5/9
4	-	130.4	-	-	-
5/9	7.19, d (8.7)	131.1	6/8	7, 5/9, 6/8, 3	6/8, 3
6/8	6.83, d (8.7)	115.5	5/9	7, 4, 6/8	5/9, 10a, 10b, 11
7	-	158.9	-	-	-
10	4.19, dd (9.9, 2.7)	70.5	10b, 11	7, 11	6/8, 10b, 11, 13, 14
	3.87, dd (9.9, 8.0)		10a, 11	7, 11	6/8, 10a, 11, 13, 14
11	3.70, dd (8.0, 2.7)	77.6	10a, 10b	10, 12	6/8, 10a, 10b, 13, 14
12	-	72.8	-	-	-
13	1.25, s	25.0	14	11, 12, 14	10a, 10b, 11, 14
14	1.22, s	26.7	13	11, 12, 13	10a, 10b, 11, 13

Calibration of CD_3OD δ_H 3.31/δ_C 49.0

Compound **3** was isolated as a colorless amorphous solid. The molecular formula was identified to be $C_{14}H_{18}N_2O_3$ by HRESIMS. The ^{1}H NMR spectroscopic data of **3** in DMSO-d_6 (**Table 10**) related to the previously described serpulanine C which was first reported from the isolation of *Serpula* sp. (Williams et al., 2018). The 1D and 2D NMR and data of **3** were also recorded in $CDCl_3$ (**Table 9**). The comparison of NMR data confirmed that compound **3** was a serpulanine C.

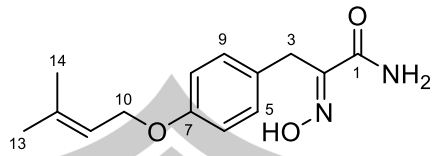

Table 9. ^{1}H and ^{13}C NMR spectroscopic data and 2D NMR data of **3** in $CDCl_3$.

position	δ_H, mult. (*J* in Hz)	δ_C	COSY	HMBC	NOESY
1	-	165.0	-	-	-
2	-	153.6	-	-	-
3	3.90, s	28.0	5/9	4, 5/9, 2, 1	5/9
4	-	127.9	-	-	-
5/9	7.25, d (8.8)	130.3	3, 6/8	7, 5/9, 6/8, 3	3, 6/8
6/8	6.81, d (8.8)	114.6	5/9	7, 4, 6/8	10, 5/9
7	-	157.5	-	-	-
10	4.46, d (6.7)	64.7	13, 14, 11	12, 11, 7	11, 6/8
11	5.47, m	119.7	13, 14, 10	14, 13	13, 10
12	-	138.1	-	-	-
13	1.78, s	25.8	10, 11	14, 11, 12	14, 11
14	1.72, s	18.1	10, 11	13, 11, 12	10, 13

Calibration of $CDCl_3$ δ_H 7.26/δ_C 77.0

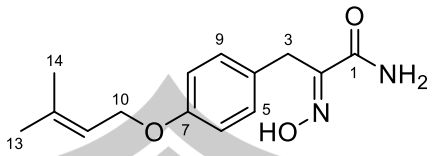

Table 10. ^{1}H NMR spectroscopic data for compound **3** compared with literature.

Position	**3** (in DMSO-d_6)[a]	Serpulanine C (in DMSO-d_6)[b]	
	δ_H, mult. (J in Hz)	δ_H, mult. (J in Hz)	δ_C
1	-	-	165.1
2	-	-	152.1
3	3.71, s	3.69, s	27.7
4	-	-	128.7
5/9	7.09, d (8.7)	7.08, d (8.7)	129.7
6/8	6.80, d (8.7)	6.79, d (8.7)	114.3
7	-	-	156.7
10	4.45, d (6.7)	4.44, bd (6.7)	64.1
11	5.32, m	5.39, tm (6.7)	120.1
12	-	-	136.8
13	1.72, s	1.71, brs	25.4
14	1.68, s	1.67, brs	18.0
N*H*	7.27, s	7.28, brs/7.19, brs	-
NO*H*	11.74, s	11.75, s	-

[a]Calibration of DMSO-d_6 δ_H 2.50/δ_C 39.5, [b]Calibration of DMSO-d_6 δ_H 2.49/δ_C 39.5

Compounds **11** and **12** were isolated as colorless solid. The ^{1}H and ^{13}C NMR spectrum displayed a 1:1 ratio mixture of the compounds (**Figure A79**). The 1D and 2D NMR data of compounds **11** and **12** were recorded in $CDCl_3$ (**Table 11** and **Table 13**). The delocalization of electrons in the α,β-unsaturated system indicated the deshielded aromatic proton (δ_H 8.02, d, J = 8.8 Hz) in **11**. From the comparison

(**Table 12**), compound **11** was identified as valencic acid which was first reported from the phytochemical investigation of roots and root barks of *Citrus sinensis* OSBECK (valencia orange) (Ito et al., 1988).

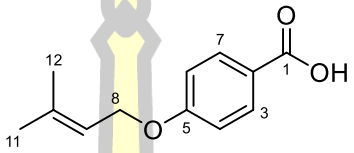

Table 11. ^{1}H and ^{13}C NMR spectroscopic data and 2D NMR data of **11** in $CDCl_3$.

position	δ_H, mult. (*J* in Hz)	δ_C	COSY	HMBC	NOESY
1	-	171.5	-	-	-
2	-	121.3	-	-	-
3/7	8.02, d (8.8)	132.3	4/6	1, 5, 3/7, 4/6	4/6
4/6	6.93, d (8.8)	114.4	3/7	5, 2, 4/6	3/7, 8
5	-	163.4	-	-	-
8	4.58, d (6.7)	65.0	9, 11, 12	5, 10, 9	4/6, 9, 11
9	5.49, m	118.9	8, 11, 12	11, 12, 8	8, 11, 12
10	-	139.0	-	-	-
11	1.80, s	25.8	9, 8	10, 9, 12	9
12	1.76, s	18.2	9, 8	10, 9, 11	8

Calibration of $CDCl_3$ δ_H 7.26/δ_C 77.0

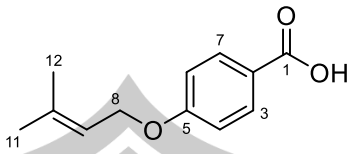

Table 12. ^{1}H NMR spectroscopic data for compound **11** compared with literature.

Position	**11** (in $CDCl_3$)[a]	Valencic acid (in $CDCl_3$)
	δ_H, mult. (*J* in Hz)	δ_H, mult. (*J* in Hz)
1	-	-
2	-	-
3/7	8.02, d (8.8)	8.05, d (8.7)
4/6	6.93, d (8.8)	6.95, d (8.7)
5	-	-
8	4.58, d (6.7)	4.59, d (7.1)
9	5.49, m	5.49, t (7.1)
10	-	-
11	1.80, s	1.81, s
12	1.76, s	1.76, s

[a]Calibration of $CDCl_3$ δ_H 7.26/δ_C 77.0

The ^{1}H NMR signal of methylene protons (δ_H 3.60, s) illustrated the presence of methylene in phenylacetic acid moiety of **12** which was differed from valencic acid (**11**). The comparison of ^{1}H NMR data confirmed that compound **12** was a 4-prenyloxyphenyl acetic acid (**Table 14**) which was first reported from the isolation of *Aspergillus ochraceus* (Awad et al., 2005).

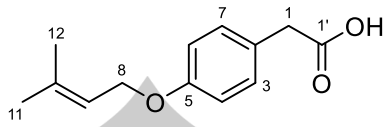

Table 13. ^{1}H and ^{13}C NMR spectroscopic data and 2D NMR data of **12** in $CDCl_3$.

position	δ_H, mult. (*J* in Hz)	δ_C	COSY	HMBC	NOESY
1	3.60, s	40.1	3/7, 4/6	1′, 3/7, 2	3/7
2	-	125.3	-	-	-
3/7	7.20, d (8.5)	130.3	4/6, 1	5, 3/7, 4/6, 1	4/6, 1
4/6	6.88, d (8.5)	114.8	3/7	5, 2, 4/6	3/7, 8
5	-	158.1	-	-	-
8	4.49, d (6.7)	64.7	9, 11, 12	5, 10, 9	4/6, 9, 11
9	5.49, m	119.6	8, 11, 12	11, 12, 8	8, 11, 12
10	-	138.2	-	-	-
11	1.79, s	25.8	9, 8	10, 9, 12	9
12	1.73, s	18.2	9, 8	10, 9, 11	8
1′	-	177.7	-	-	-

Calibration of $CDCl_3$ δ_H 7.26/δ_C 77.0

Erosterol (**13**) and erogosterol endoperoxide (**14**) were isolated as a major constituent which was commonly found in natural fruiting body. The primary component in the cell membrane of mushrooms, ergosterol is a type of sterol that plays a crucial role in the cell membrane of fungi, including mushrooms. Its function is analogous to that of cholesterol in animal cells, making ergosterol one of the most abundant compounds in the structural composition of mushrooms.

4.8. Antibacterial activity of compounds 3, and 8–12

The undescribed compounds, **8**–**10**, and known compounds, **3**, **11**–**12**, were tested for their antibacterial activities against Gram-positive pathogenic bacteria; *S. aureus* (MRSA), *S. aureus* (MSSA), and *B. cereus*. All of them were inactive in these assays at the test concentration of 1 mg/mL.

4.9. Cytotoxicity of compounds 3, and 8–12

Compounds **3**, and **8**–**12** were evaluated for their cytotoxicity against A549 cell lines. All of them were inactive in these assays at the test concentration of 20 mg/mL.

CHAPTER 5

CONCLUSION

Three previously undescribed *O*-prenyl-tyrosine oxime derivatives, serpulanines D–F (**8**–**10**) together with five known compounds, serpulanine C (**3**) (Williams et al., 2018), valencic acid (**11**) (Ito et al., 1988), 4-prenyloxyphenylacetic acid (**12**) (Awad et al., 2005), ergosterol (**13**), and ergosterol endoperoxide (**14**) were isolated from the natural fruiting bodies of *S. dendrocalami*. There have been a few reports on the chemical investigation of *Serpula*. The present results demonstrate that this genus is a source of structurally unique compounds. Compounds **8**–**10** have been evaluated for their antibacterial activities against *S. aureus* (MRSA and MSSA) and *B. cereus* and cytotoxicity against A549 cell lines. These compounds were inactive in antibacterial and cytotoxic activities assays.

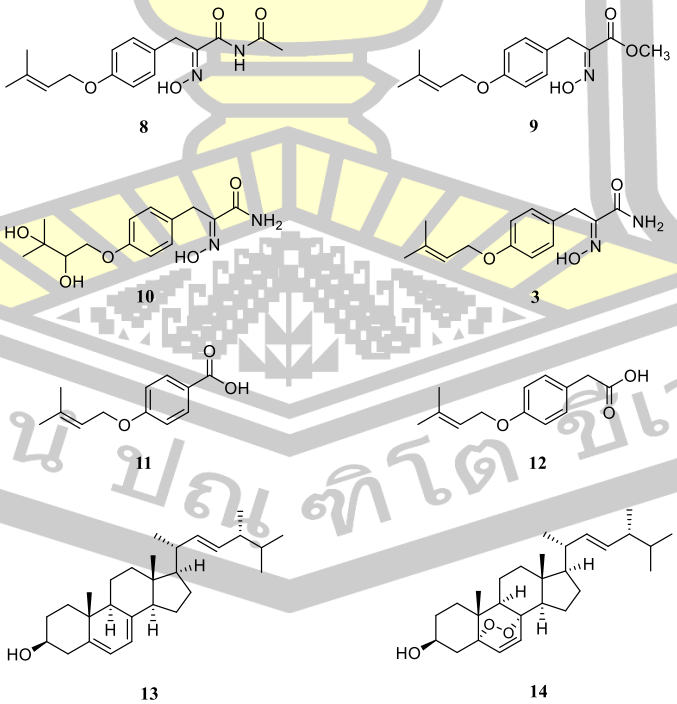

Figure 12. Isolated compounds from the natural fruiting bodies *Serpula dendrocalami*.

REFERENCES

REFERENCES

Acres, B. (2017). *Biology and Life Cycle of a Mushroom*. Mycologic. https://www.mycologic.nz/life-cycle

Adedokun, O. M., Odiketa, J. K., Afieroho, O. E., & Afieroho, M. C. (2022). Importance of Mushrooms for Food Security in Africa. In *Food Security for African Smallholder Farmers. Sustainability Sciences in Asia and Africa* (pp. 343–360). Springer.

Ahmadjian, V., Alexopoulos, C. J., & Moore, D. (2024). *Fungus*. Encyclopedia Britannica. https://www.britannica.com/science/fungus

Aqueveque, P., Anke, T., & Sterner, O. (2002). The Himanimides, New Bioactive Compounds from Serpula himantoides (Fr.)Karst. In *Z. Naturforsch* (Vol. 57). www.znaturforsch.com

Awad, G., Mathieu, F., Coppel, Y., & Lebrihi, A. (2005). Characterization and regulation of new secondary metabolites from Aspergillus ochraceus M18 obtained by UV mutagenesis. *Canadian Journal of Microbiology*, *51*(1), 59–67. https://doi.org/10.1139/w04-117

Baimai, V. (2010). Biodiversity in Thailand. *The Journal of the Royal Institute of Thailand*, *2*, 107–113.

Bueno, D. J., & Silva, J. O. (2014). Fungi: The Fungal Hypha. In *Encyclopedia of Food Microbiology: Second Edition* (pp. 11–19). Elsevier Inc. https://doi.org/10.1016/B978-0-12-384730-0.00132-4

Bulam, S., Üstün, N. Ş., & Pekşen, A. (2019). Health Benefits of Ganoderma lucidum as a Medicinal Mushroom. *Turkish Journal of Agriculture - Food Science and Technology*, *7*, 84–93. https://doi.org/10.24925/turjaf.v7isp1.84-93.2728

Butler, R. A. (2000). *Thailand Forest Information and Data*. https://worldrainforests.com/deforestation/2000/Thailand.htm

Doryane, K. T. (2004). *Atlas of Thailand: Spatial Structures and Development*. IRD Editions.

Enrica, G. (2023). *Journal of Biodiversity & Endangered Species Mini Review Decomposers and Collaborators: Fungal Ecology Unraveled*. https://doi.org/10.37421/2332-2543.2023.11.494

Hyde, K. D. (2022). The numbers of fungi. In *Fungal Diversity* (Vol. 114, Issue 1, p. 1). Springer Science and Business Media B.V. https://doi.org/10.1007/s13225-022-00507-y

Ito, C., Mizuno, T., Matsuoka, M., Kimura, Y., Sato, K., Kajiura, I., Omura, M., Ju-ichi, M., & Furukawa, H. (1988). A New Flavonoid and Other New Components from Citrus Plants. *Chemical & Pharmaceutical Bulletin*, *36*, 3292–3295.

Kirk, P. (n.d.). *Index Fungorum*. Retrieved March 26, 2024, from https://www.indexfungorum.org/names/names.asp

Lovett, B. (2021). *Three Reasons Fungi are Not Plants*. American Society for Microbiology. https://asm.org/articles/2021/january/three-reasons-fungi-are-not-plants

Makchuchit, S., Rattarom, R., & Itharat, A. (2017). The anti-allergic and anti-inflammatory effects of Benjakul extract (a Thai traditional medicine), its constituent plants and its some pure constituents using in vitro experiments.

Biomedicine and Pharmacotherapy, *89*, 1018–1026. https://doi.org/10.1016/j.biopha.2017.02.066

McConnaughey, M. (2014). Physical Chemical Properties of Fungi☆. In *Reference Module in Biomedical Sciences*. Elsevier. https://doi.org/10.1016/b978-0-12-801238-3.05231-4

Min, S. J., Lee, H., Shin, M. S., & Lee, J. W. (2023). Synthesis and Biological Properties of Pyranocoumarin Derivatives as Potent Anti-Inflammatory Agents. *International Journal of Molecular Sciences*, *24*(12). https://doi.org/10.3390/ijms241210026

Moore, D., Robson, G. D., & Trinci, A. P. J. (2000). 21st Century Guidebook to Fungi. In *21st Century Guidebook to Fungi*. Cambridge University Press. https://doi.org/10.1017/cbo9780511977022

NPS. (2021). *Mushrooms and Other Fungi*. National Park Service. https://www.nps.gov/chir/learn/nature/mushrooms.htm

Park, Y., Liu, Y., Hong, J., Lee, C. O., Cho, H., Kim, D. K., Im, K. S., & Jung, J. H. (2003). New Bromotyrosine Derivatives from an Association of Two Sponges, Jaspis wondoensis and Poecillastra wondoensis. *Journal of Natural Products*, *66*(11), 1495–1498. https://doi.org/10.1021/np030162j

Pedro, S. F. (2022). Fungal protein. In *Advances in Food and Nutrition Research* (Vol. 101, pp. 153–179). Academic Press.

Sangdee, A., & Sangdee, K. (2013). Isolation, identification, culture and production of adenosine and cordycepin from cicada larva infected with entomopathogenic fungi in Thailand. *African Journal of Microbiology Research*, *7*(2), 137–146. https://doi.org/10.5897/AJMR

Sangdee, A., Sangdee, K., Buranrat, B., & Thammawat, S. (2018). Effects of mycelial extract and crude protein of the medicinal mushroom, ophiocordyceps sobolifera, on the pathogenic fungus, candida albicans. *Tropical Journal of Pharmaceutical Research*, *17*(12), 2449–2454. https://doi.org/10.4314/tjpr.v17i12.21

Sangdee, K., Nakbanpote, W., & Sangdee, A. (2015). Isolation of the Entomopathogenic Fungal Strain Cod-MK1201 from a Cicada Nymph and Assessment of Its Antibacterial Activities. *International Journal of Medicinal Mushrooms*, *17*(1), 51–63. https://doi.org/https://doi.org/10.1615/intjmedmushrooms.v17.i1.60

Tamura, K., Stecher, G., Peterson, D., Filipski, A., & Kumar, S. (2013). MEGA6: Molecular evolutionary genetics analysis version 6.0. *Molecular Biology and Evolution*, *30*(12), 2725–2729. https://doi.org/10.1093/molbev/mst197

Tran, T. M. D., Nguyen, V. K., Duong, T. H., Tran, T. N., Nguyen, N. H., Devi, A. P., Chavasiri, W., Dinh, M. H., Tran, N. M. A., & Sichaem, J. (2021). Maydisone, a novel oxime polyketide from the cultures of Bipolaris maydis. *Natural Product Research*, *36*(1), 102–107. https://doi.org/10.1080/14786419.2020.1765339

Várnai, A., Mäkelä, M. R., Djajadi, D. T., Rahikainen, J., Hatakka, A., & Viikari, L. (2014). Carbohydrate-Binding Modules of Fungal Cellulases. Occurrence in Nature, Function, and Relevance in Industrial Biomass Conversion. In *Advances in Applied Microbiology* (Vol. 88, pp. 103–165). Academic Press Inc. https://doi.org/10.1016/B978-0-12-800260-5.00004-8

Wang, X.-H., Das, K., Bera, I., Chen, Y.-H., Bhatt, R. P., Ghosh, A., Hembrom, E., Hofstetter, V., Parihar, A., Vizzini, A., Xu, T.-M., Zhao, C.-L., & Buyck, B.

(2019). *Fungal Biodiversity Profiles 81* (Vol. 40, Issue 5). www.cryptogamie.com/mycologie

Williams, D. E., Gunasekara, N. W., Ratnaweera, P. B., Zheng, Z., Ellis, S., Dada, S., Patrick, B. O., Wijesundera, R. L. C., Nanayakkara, C. M., Jefferies, W. A., De Silva, E. D., & Andersen, R. J. (2018). Serpulanines A to C, N-Oxidized Tyrosine Derivatives Isolated from the Sri Lankan Fungus Serpula sp.: Structure Elucidation, Synthesis, and Histone Deacetylase Inhibition. *Journal of Natural Products*, *81*(1), 78–84. https://doi.org/10.1021/acs.jnatprod.7b00680

Yang, Y. Q. (2016). Evidence against the structure proposed for a natural phenylethanol isolated from mangrove Avicennia marina. *Synthetic Communications*, *46*(15), 1263–1267. https://doi.org/10.1080/00397911.2016.1198813

APPENDIX

LIST OF FIGURES

Figure **Page**

Figure **Page**

Figure **Page**

Figure **Page**

Figure **Page**

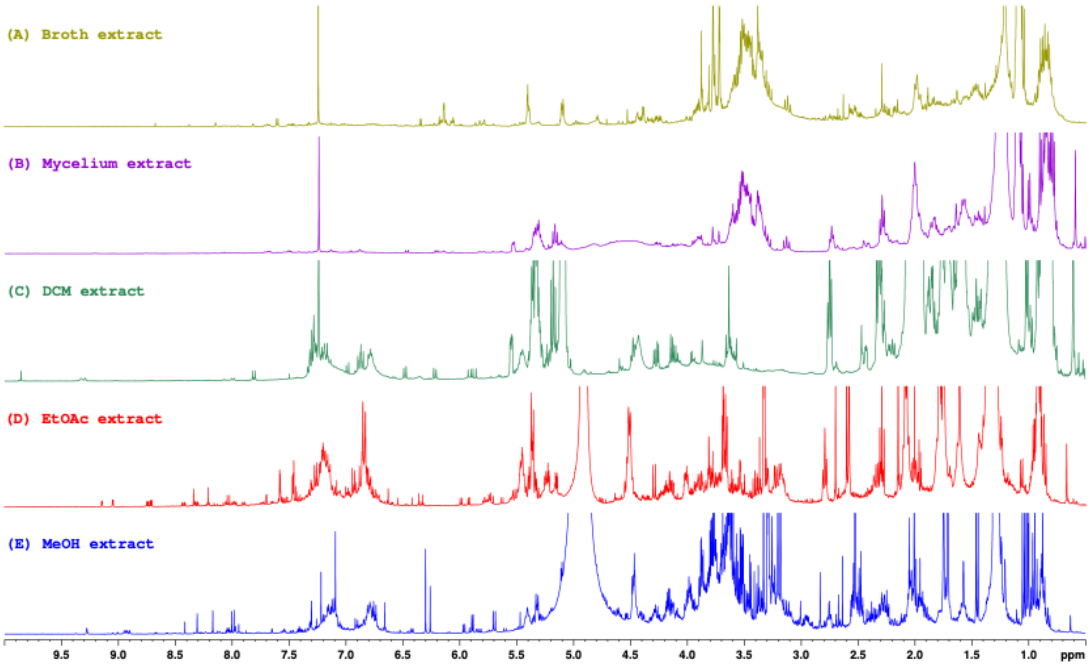

Figure A1. ^{1}H NMR spectrum (400 MHz) of broth extract in $CDCl_3$ (**A**), mycelium extract in $CDCl_3$ (**B**), DCM extract in $CDCl_3$ (**C**), EtOAc extract in CD_3OD (**D**), and MeOH extract in CD_3OD (**E**).

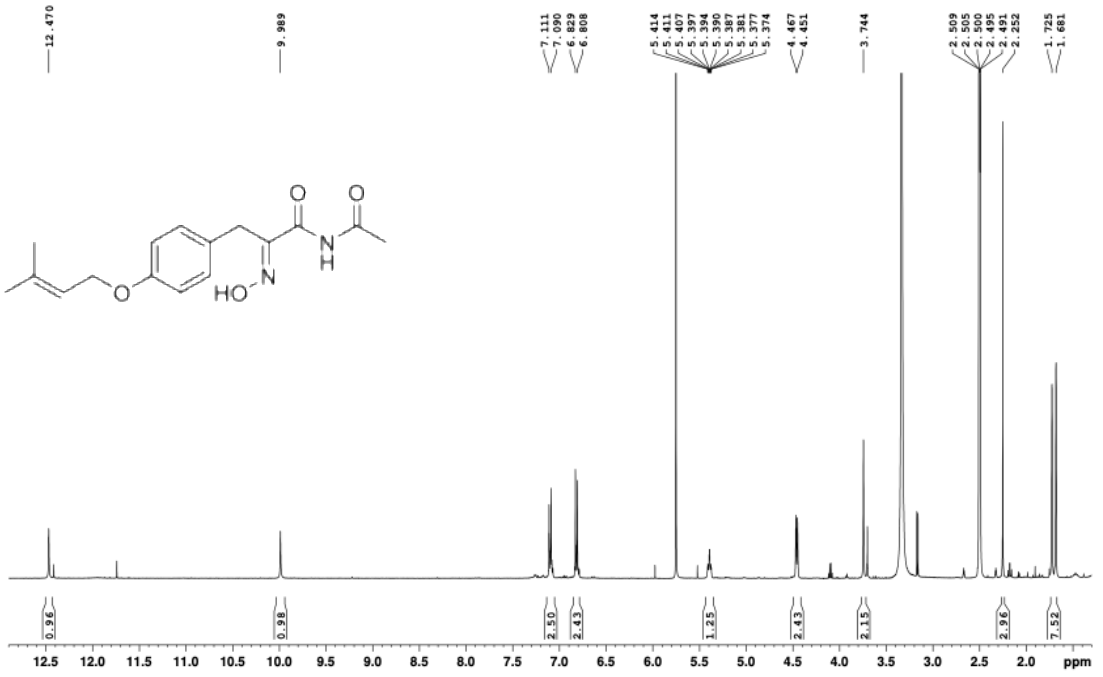

Figure A2. ^{1}H NMR spectrum of **8** (DMSO-d_6, 400 MHz).

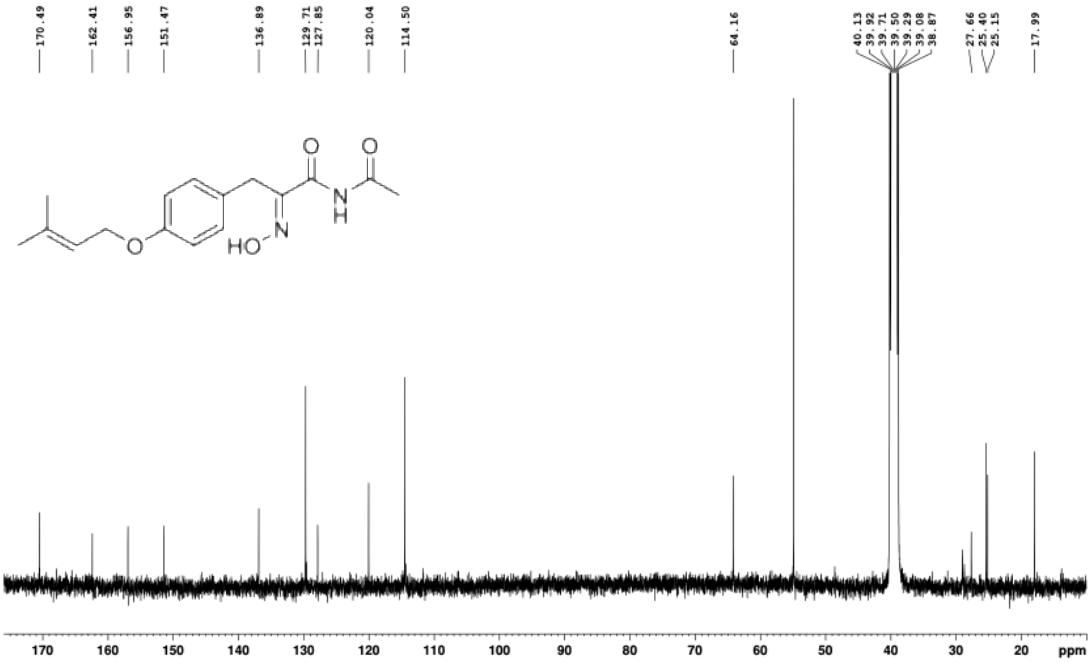

Figure A3. ^{13}C NMR spectrum of **8** (DMSO-d_6, 100 MHz).

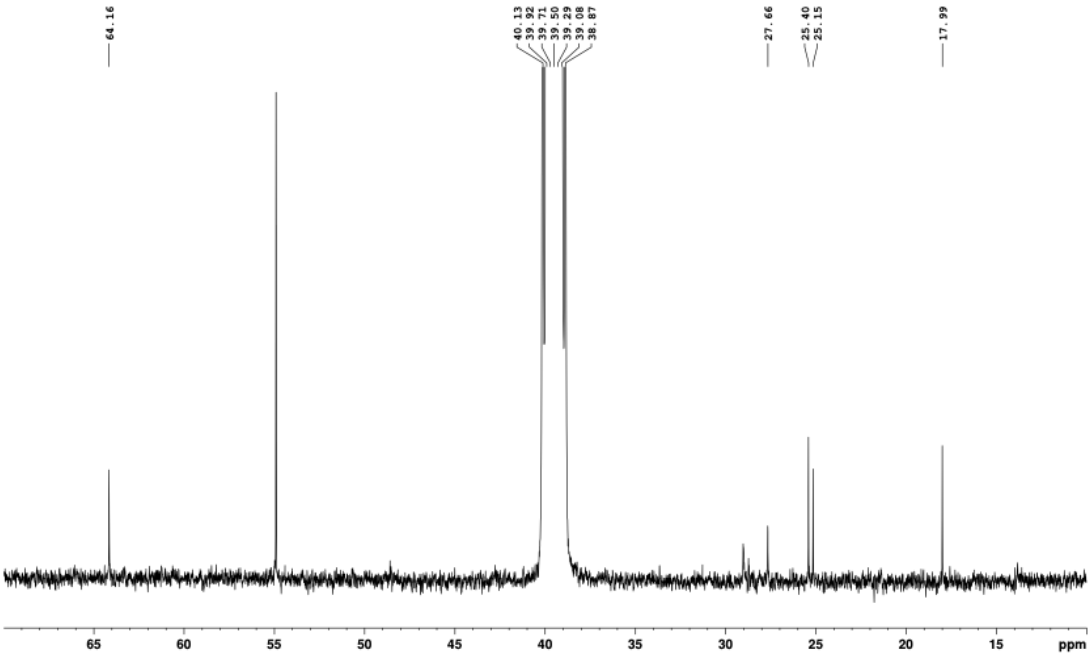

Figure A4. ^{13}C NMR (expansion-1) spectrum of **8** (DMSO-d_6, 100 MHz).

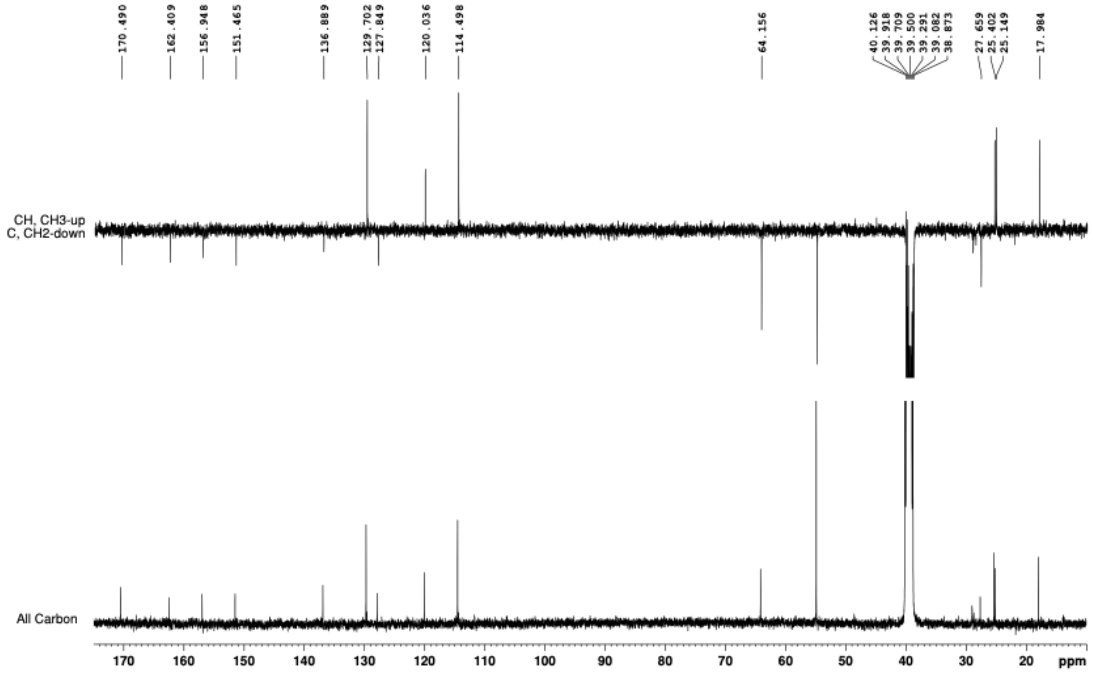

Figure A5. DEPT-135 spectrum of **8** (DMSO-d_6, 100 MHz).

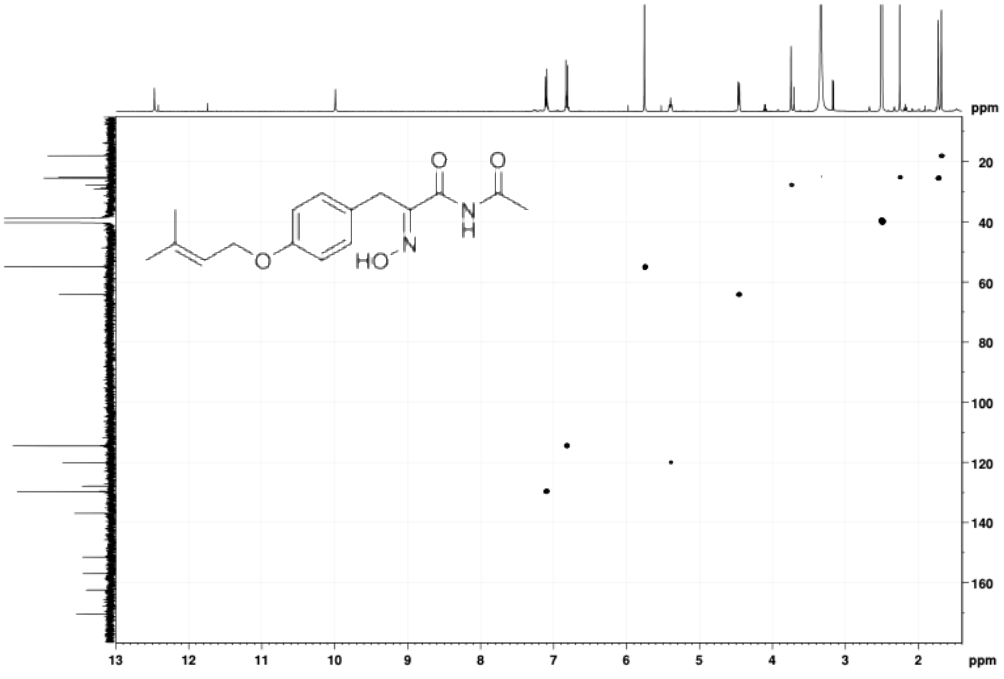

Figure A6. HSQC spectrum of **8** (DMSO-d_6, 400 MHz).

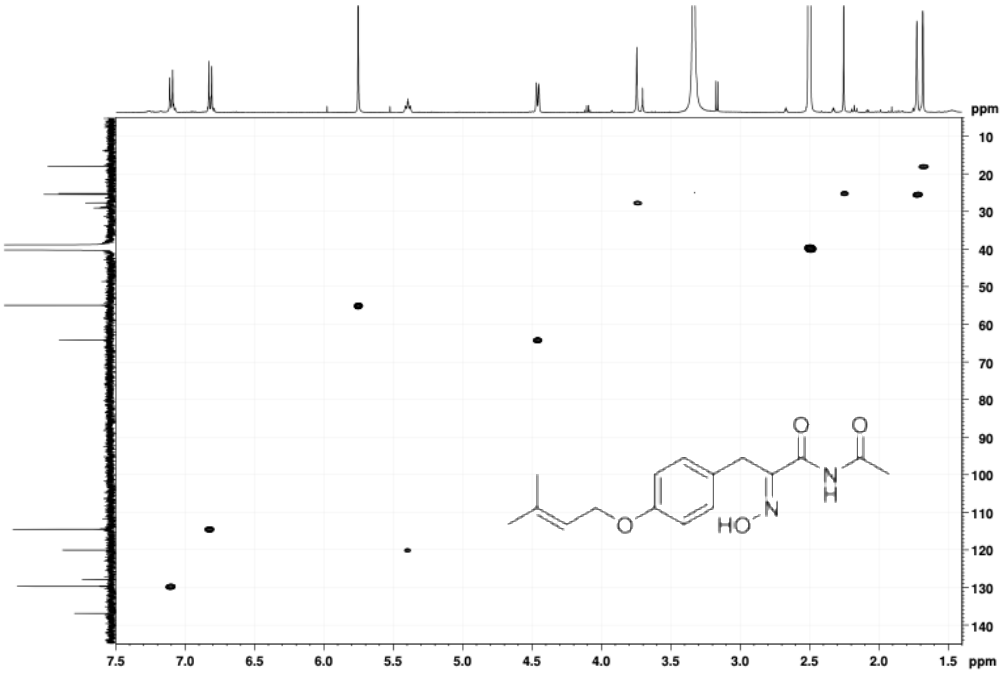

Figure A7. HSQC (expansion-1) spectrum of **8** (DMSO-d_6, 400 MHz).

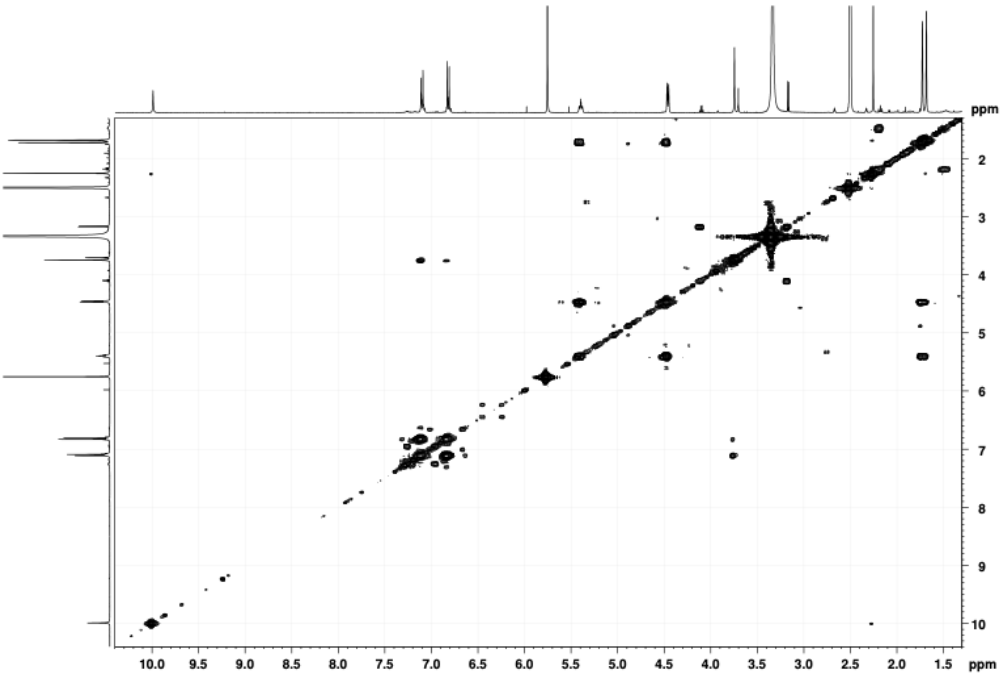

Figure A8. COSY spectrum of **8** (DMSO-d_6, 400 MHz).

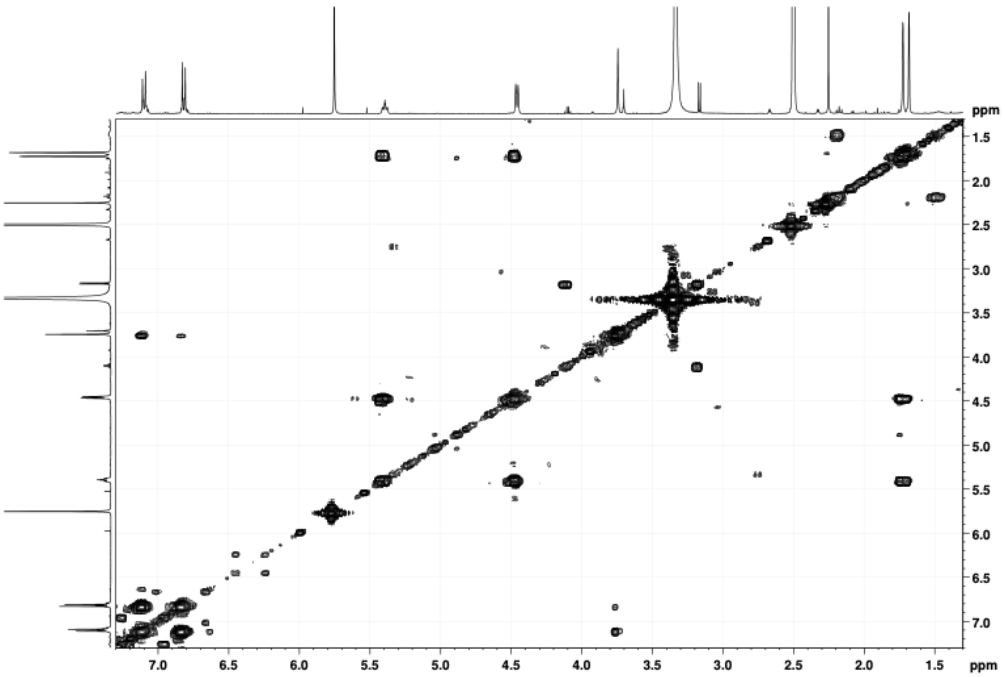

Figure A9. COSY (expansion-1) spectrum of **8** (DMSO-d_6, 400 MHz).

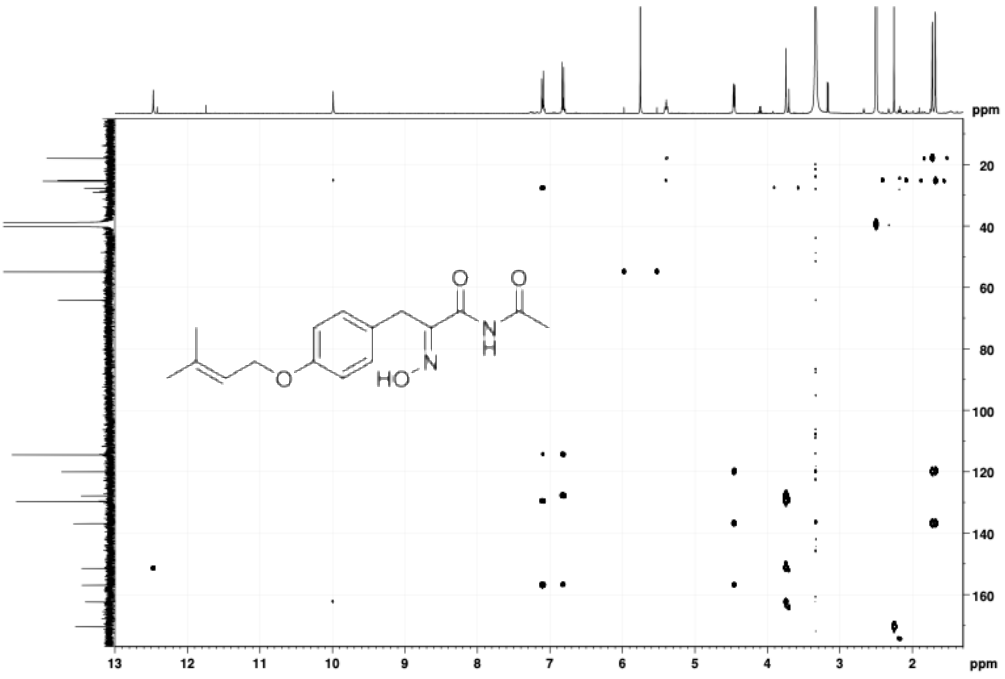

Figure A10. HMBC spectrum of **8** (DMSO-d_6, 400 MHz).

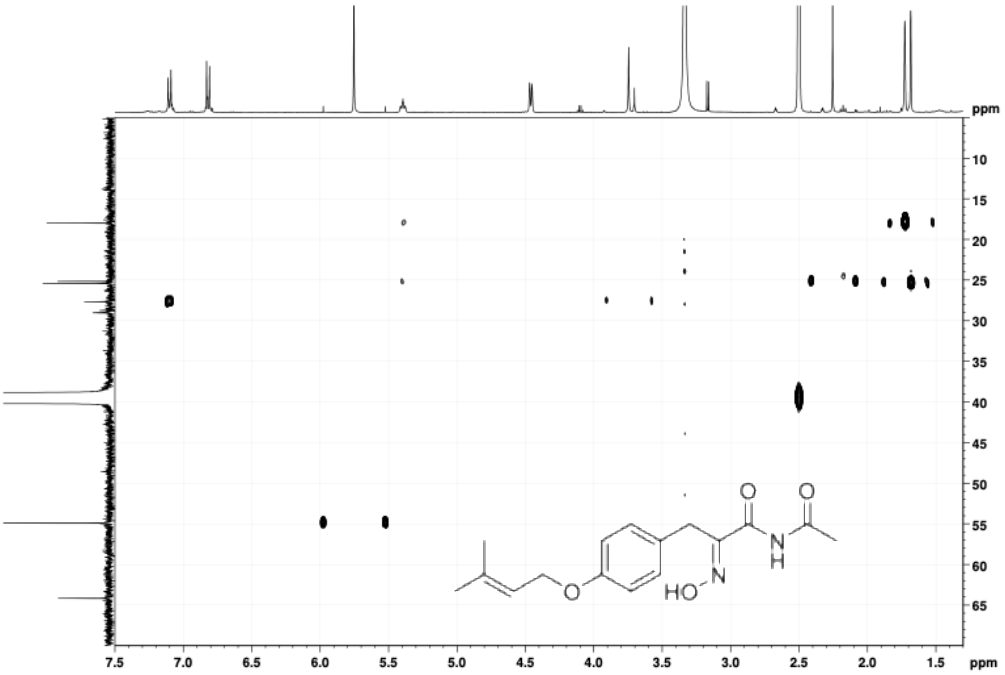

Figure A11. HMBC (expansion-1) spectrum of **8** (DMSO-d_6, 400 MHz).

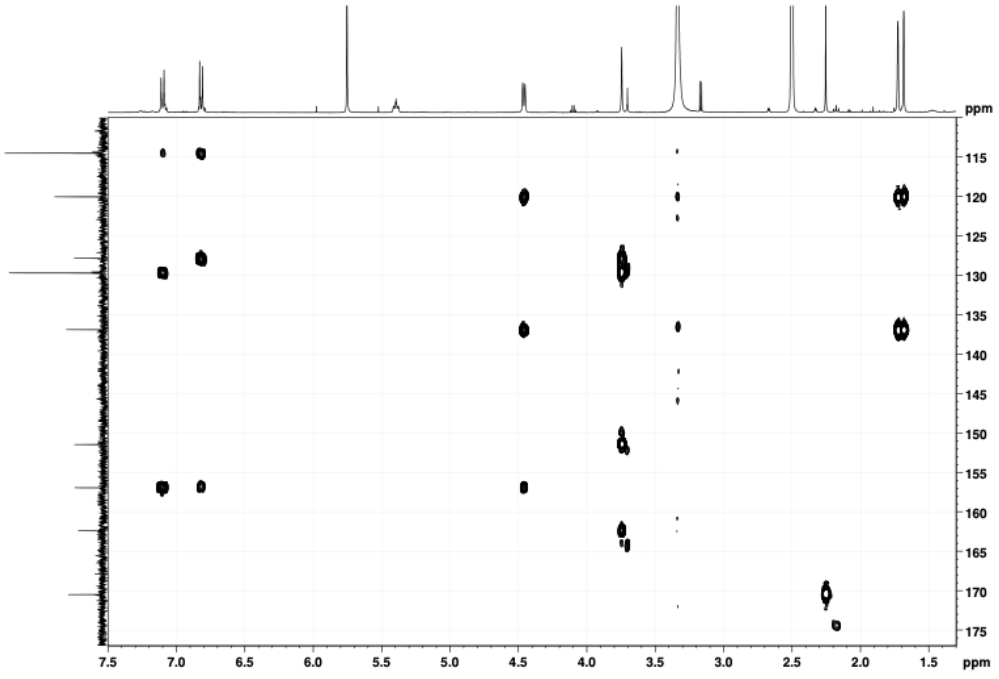

Figure A12. HMBC (expansion-2) spectrum of **8** (DMSO-d_6, 400 MHz).

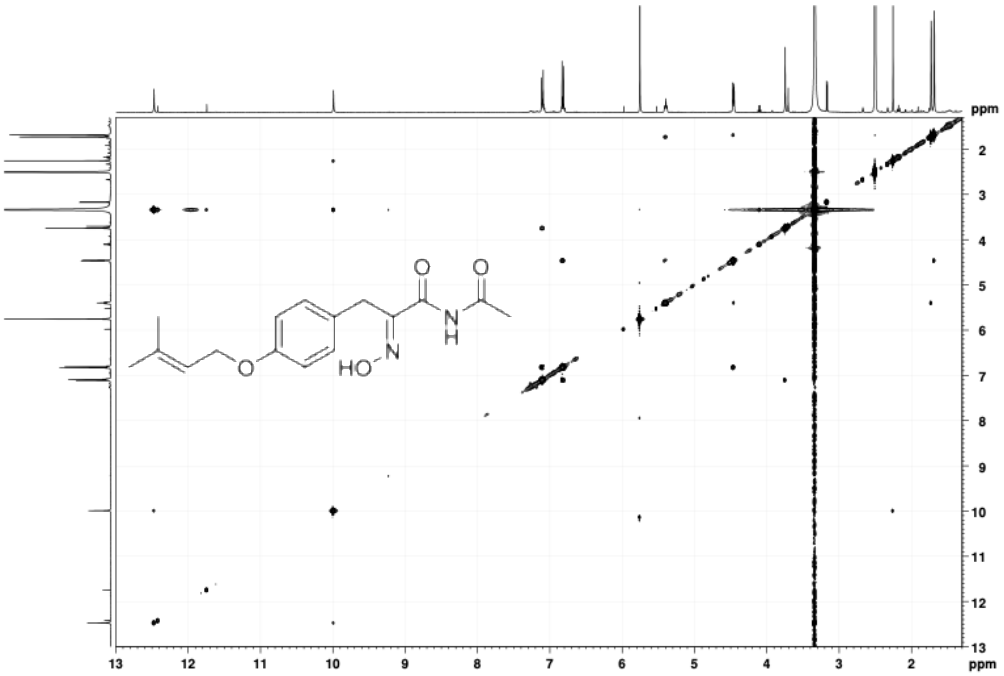

Figure A13. NOESY spectrum of **8** (DMSO-d_6, 400 MHz).

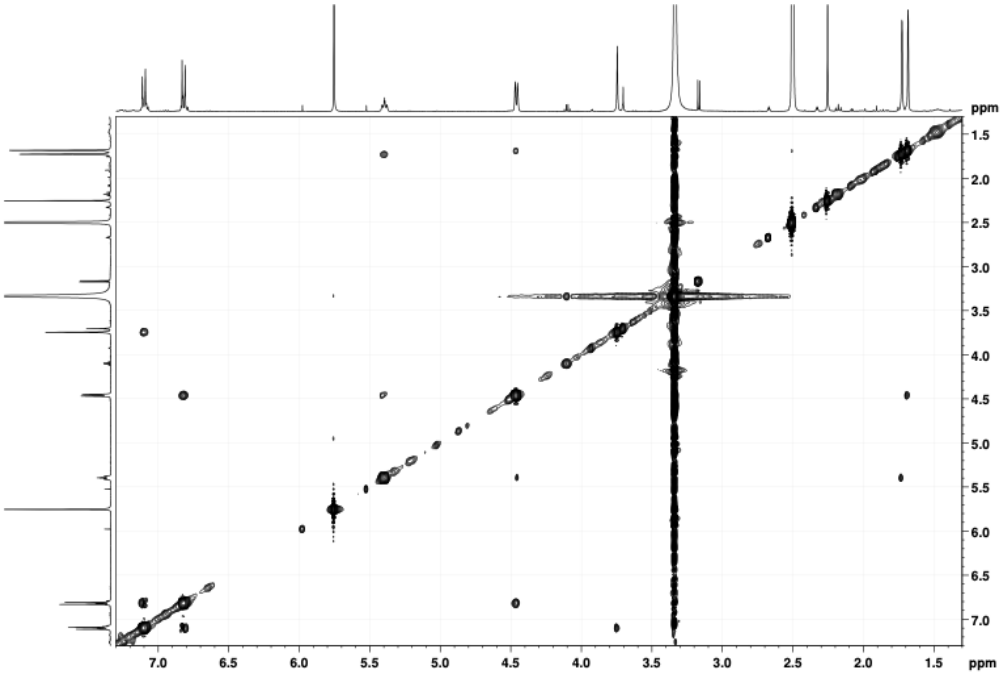

Figure A14. NOESY (expansion-1) spectrum of **8** (DMSO-d_6, 400 MHz).

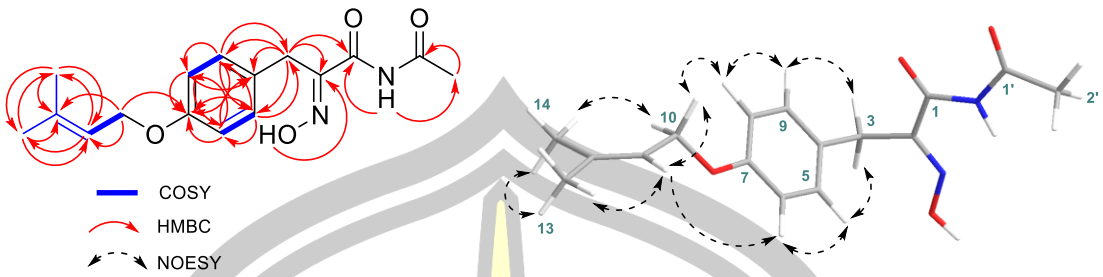

Figure A15. COSY, HMBC, and NOESY correlations of **8** (DMSO-d_6).

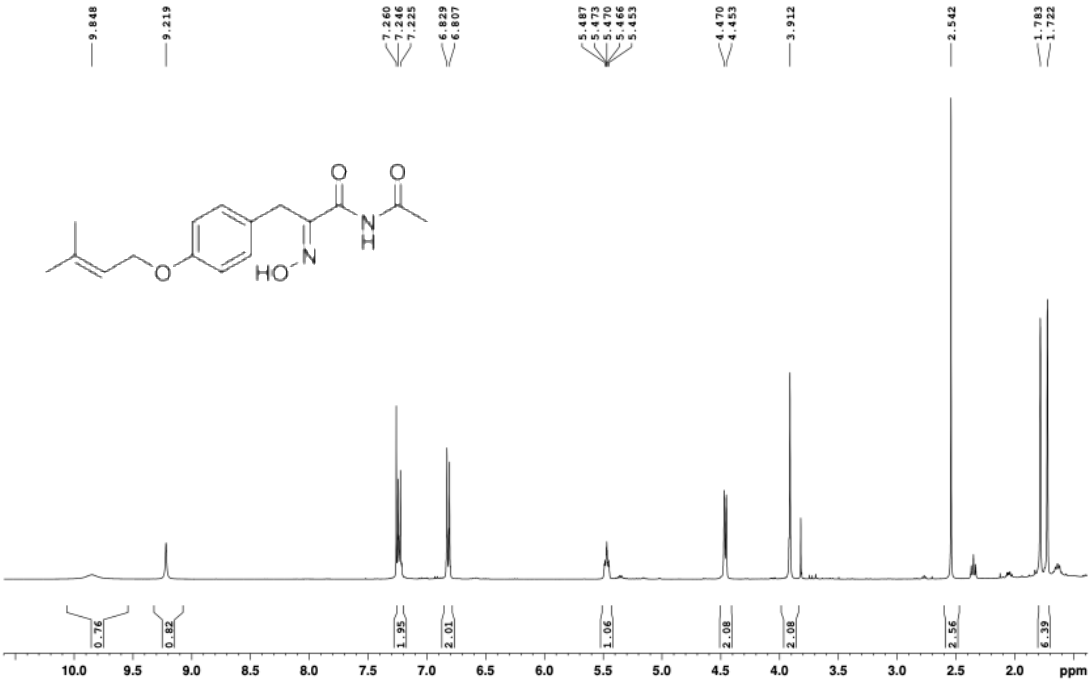

Figure A16. ^{1}H NMR spectrum of **8** ($CDCl_3$, 400 MHz).

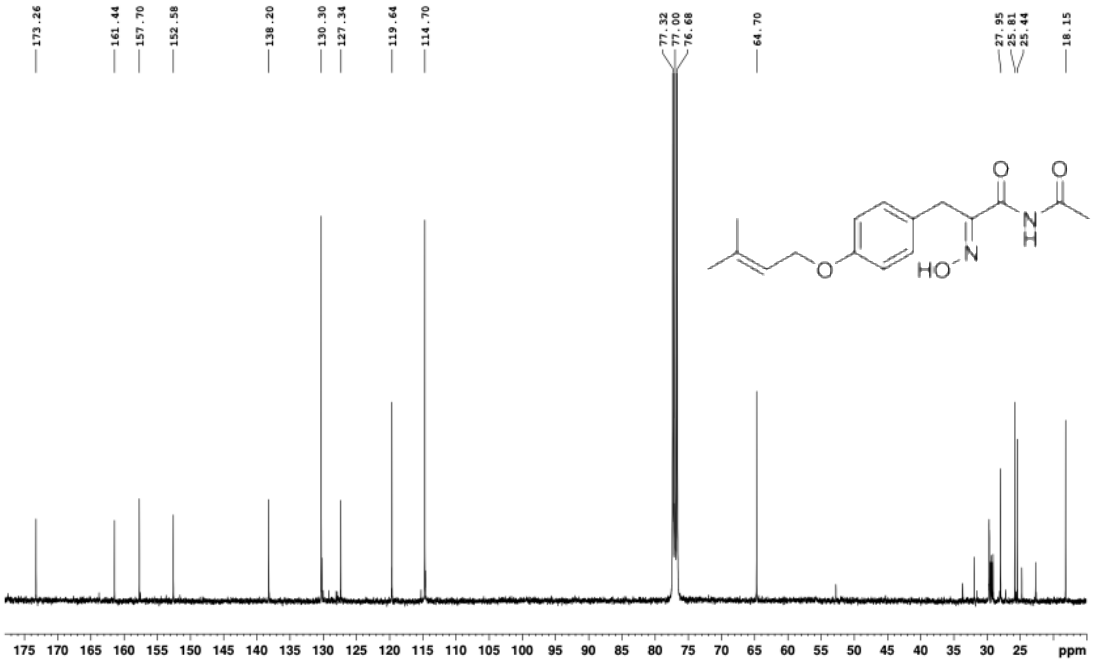

Figure A17. ^{13}C NMR spectrum of **8** ($CDCl_3$, 100 MHz).

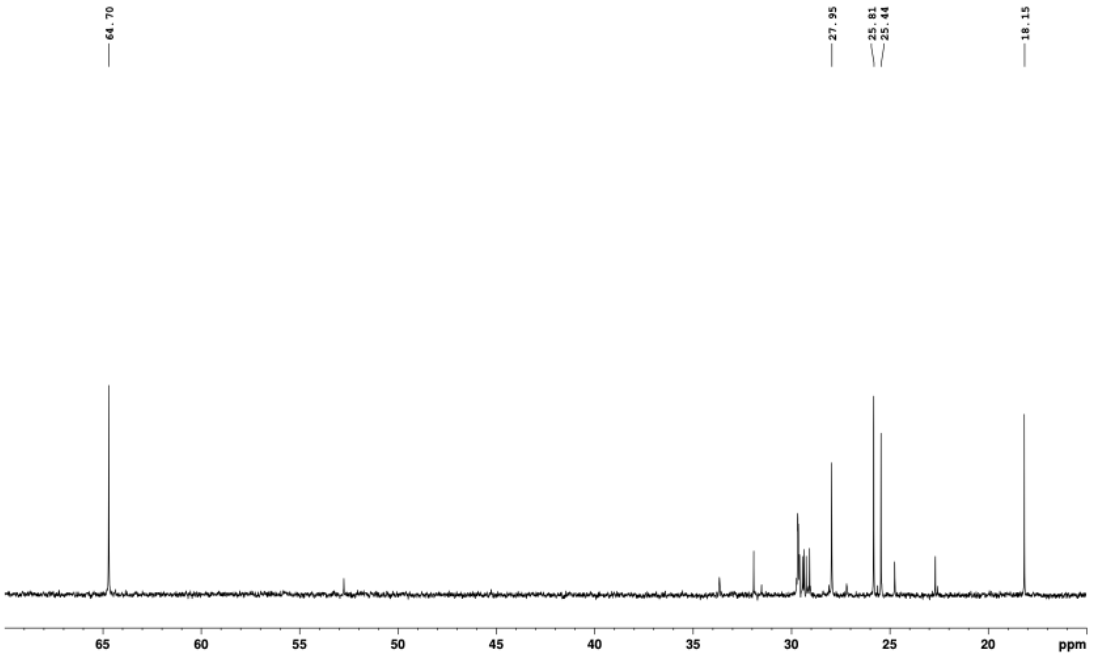

Figure A18. ^{13}C NMR (expansion-1) spectrum of **8** ($CDCl_3$, 100 MHz).

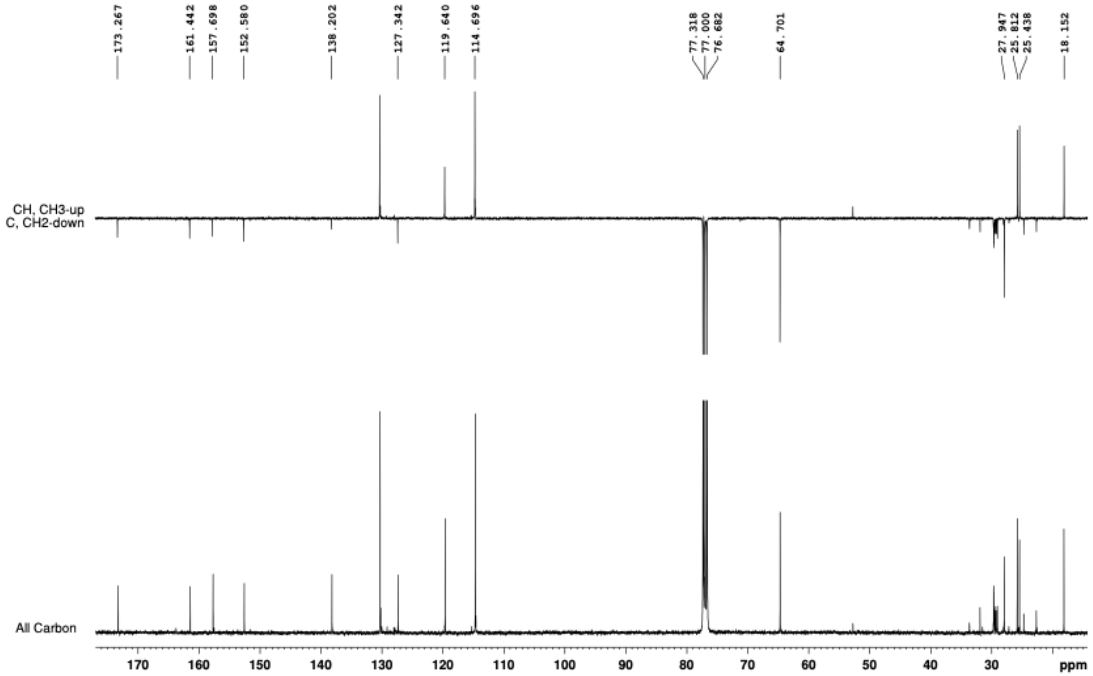

Figure A19. DEPT-135 spectrum of **8** ($CDCl_3$, 100 MHz).

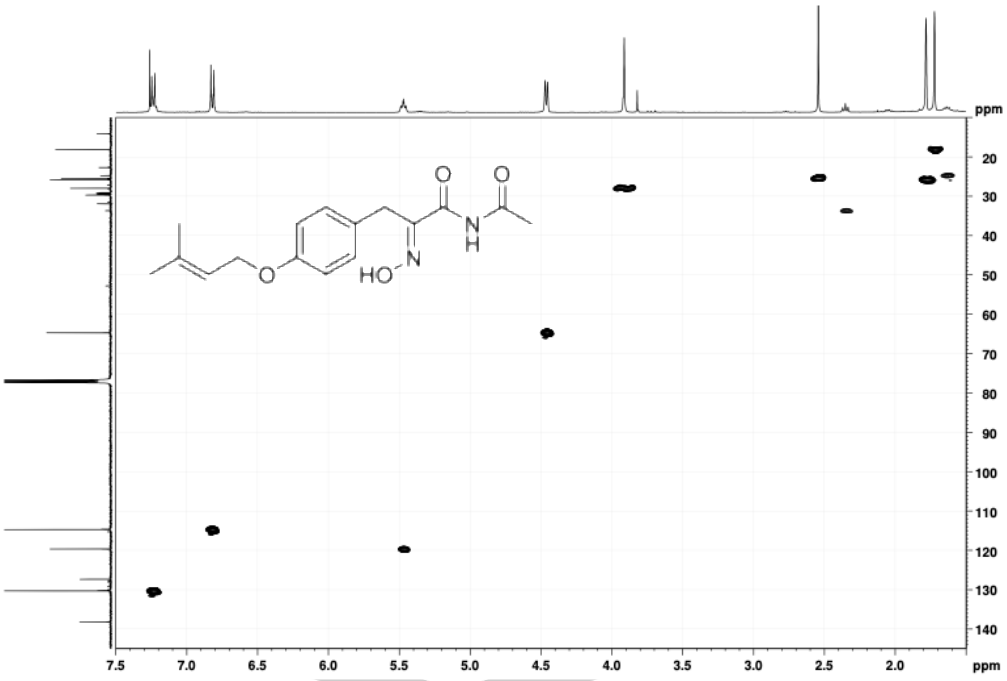

Figure A20. HSQC spectrum of **8** ($CDCl_3$, 400 MHz).

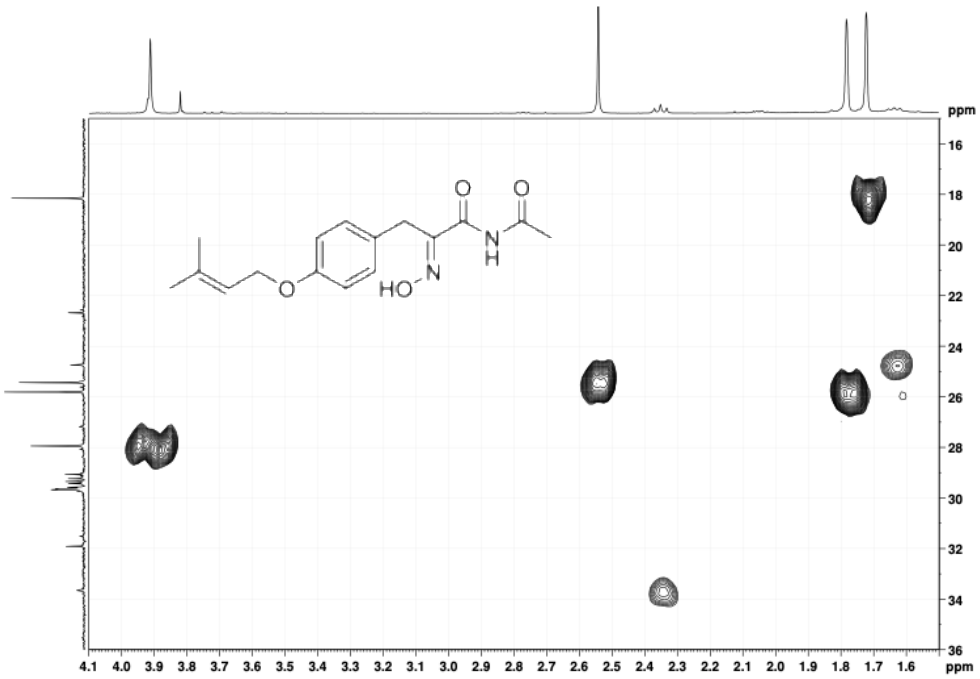

Figure A21. HSQC (expansion-1) spectrum of **8** ($CDCl_3$, 400 MHz).

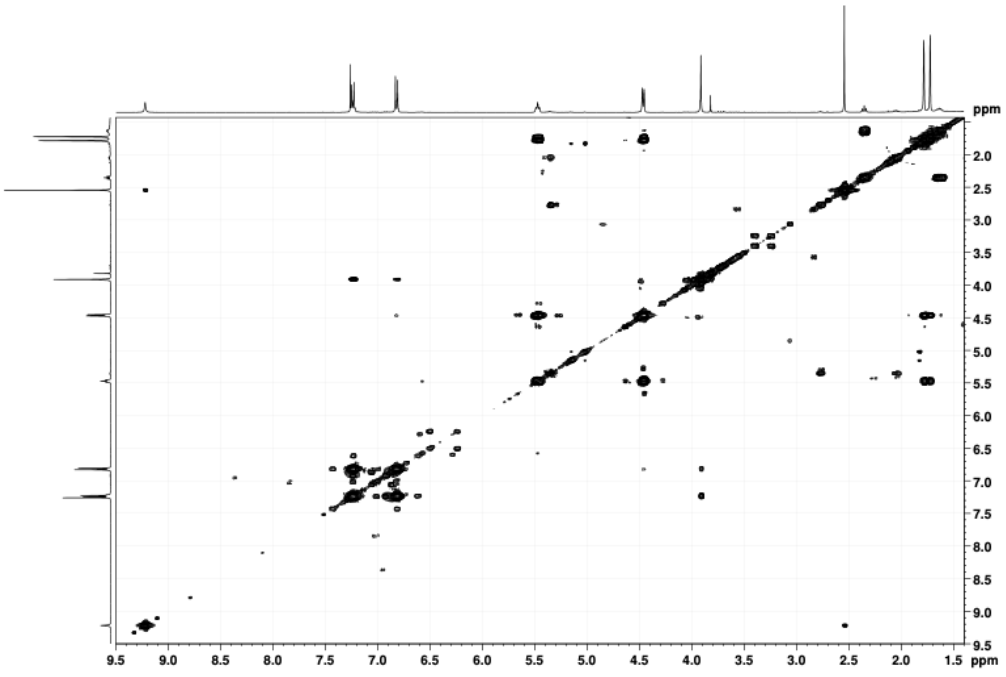

Figure A22. COSY spectrum of **8** ($CDCl_3$, 400 MHz).

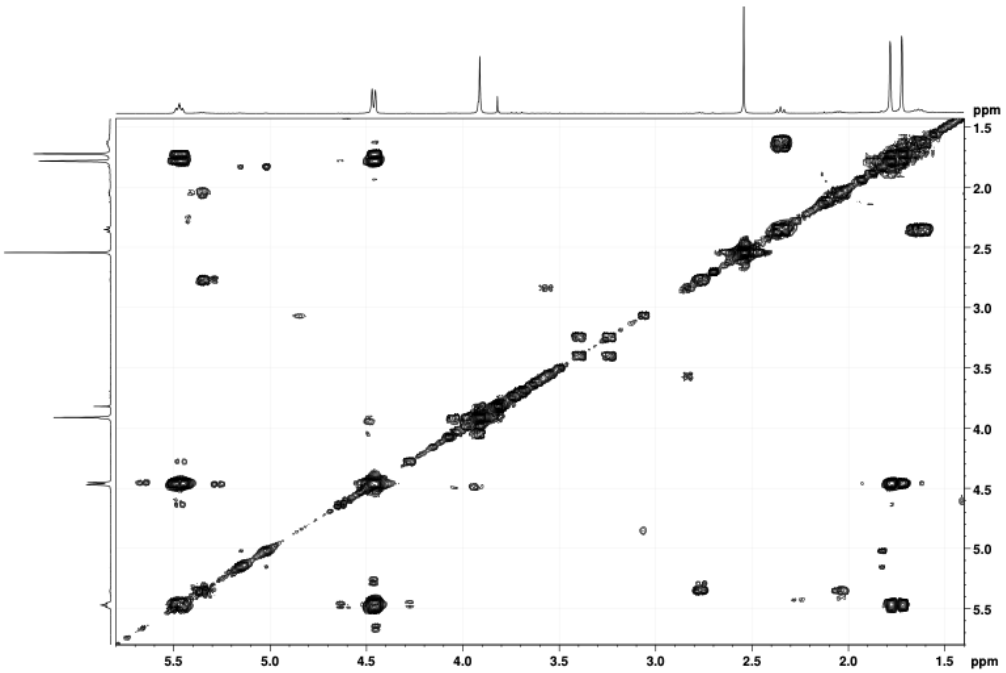

Figure A23. COSY (expansion-1) spectrum of **8** ($CDCl_3$, 400 MHz).

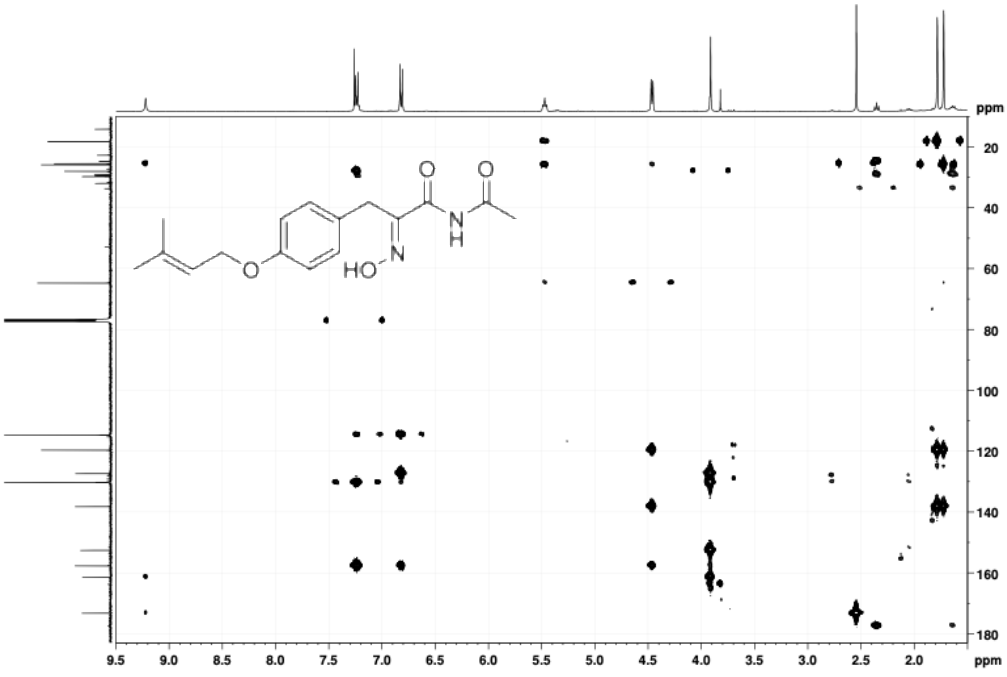

Figure A24. HMBC spectrum of **8** ($CDCl_3$, 400 MHz).

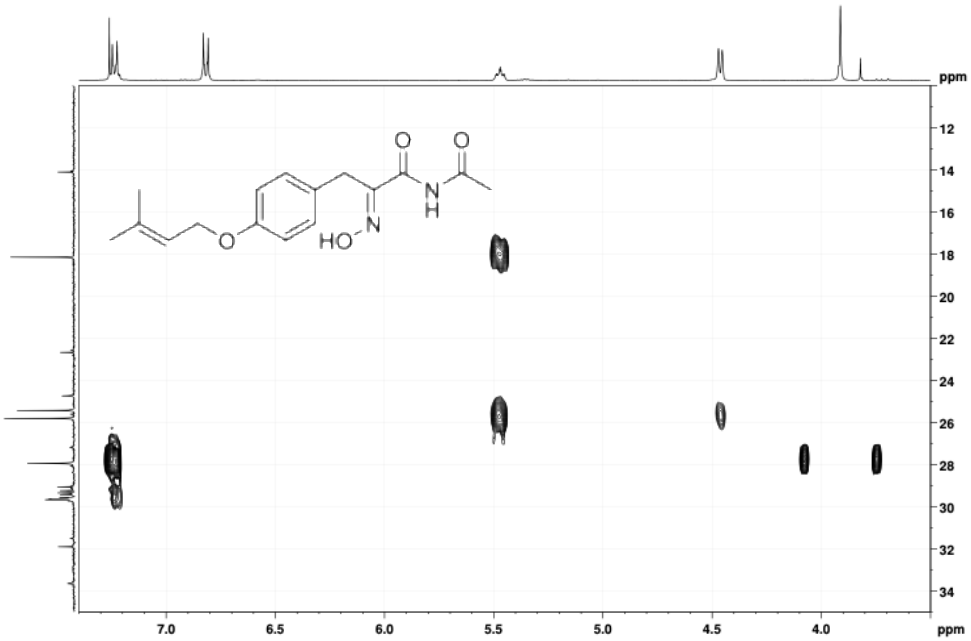

Figure A25. HMBC (expansion-1) spectrum of **8** ($CDCl_3$, 400 MHz).

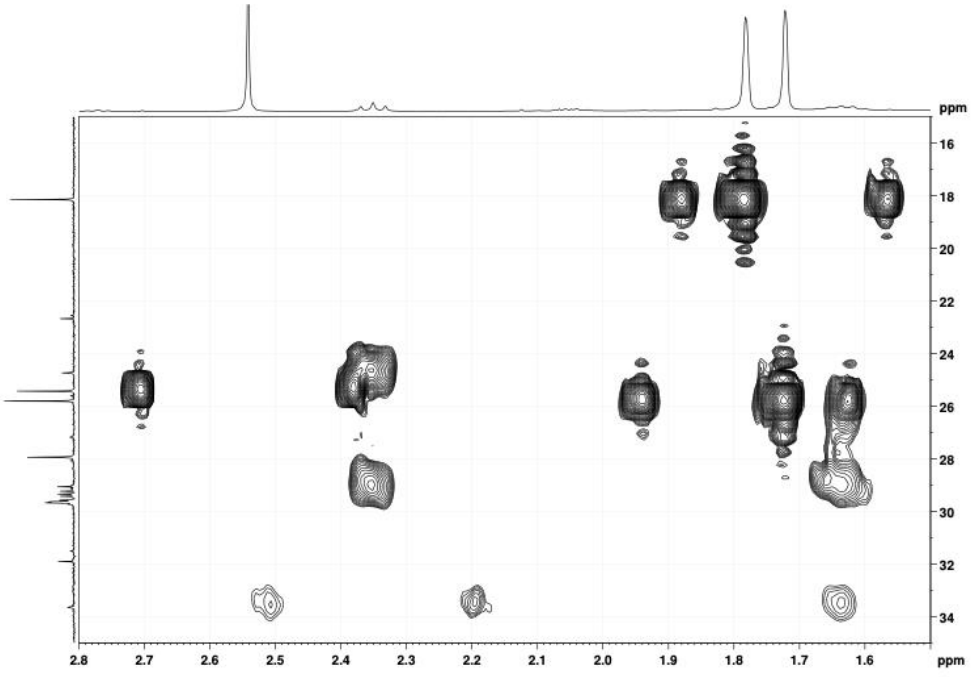

Figure A26. HMBC (expansion-2) spectrum of **8** ($CDCl_3$, 400 MHz).

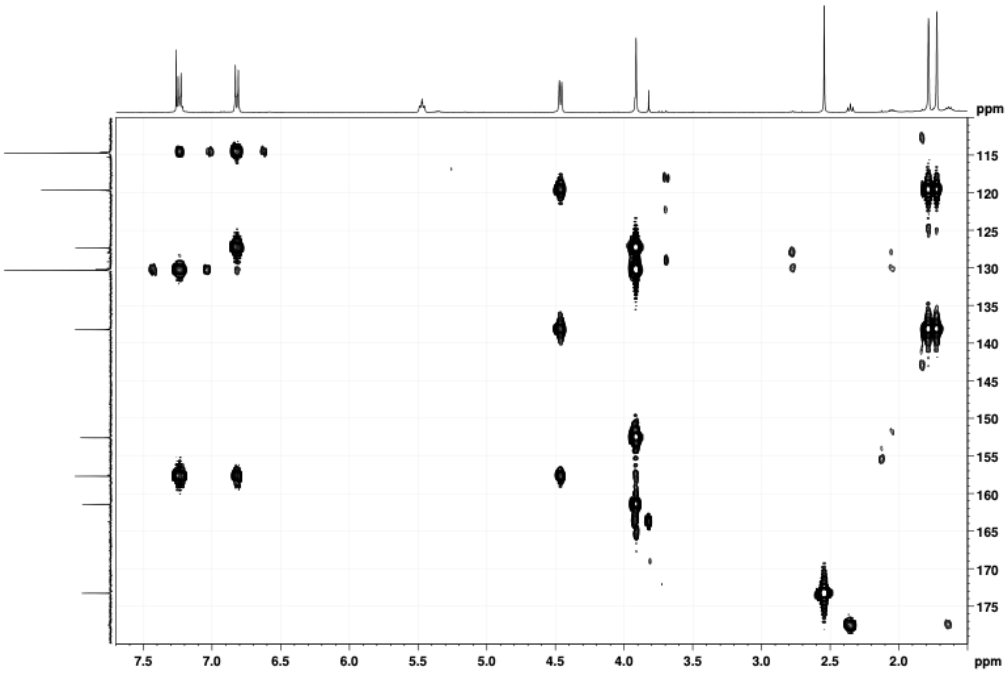

Figure A27. HMBC (expansion-3) spectrum of **8** ($CDCl_3$, 400 MHz).

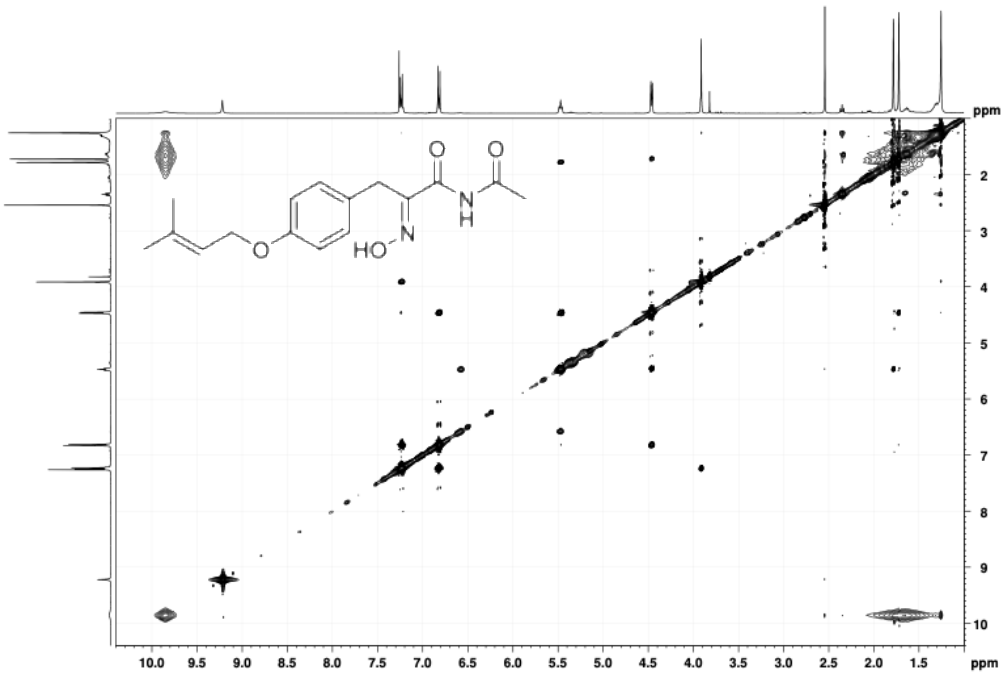

Figure A28. NOESY spectrum of **8** ($CDCl_3$, 400 MHz).

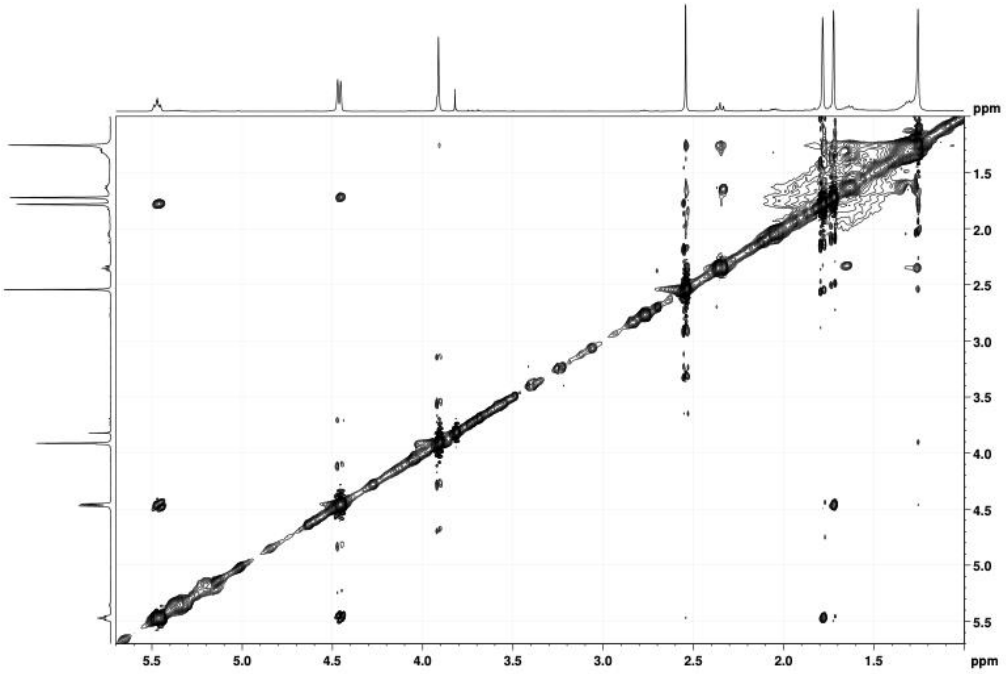

Figure A29. NOESY (expansion-1) spectrum of **8** ($CDCl_3$, 400 MHz).

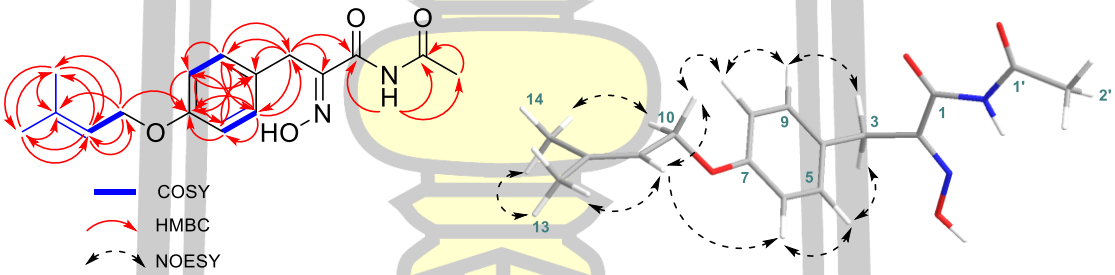

Figure A30. COSY, HMBC, and NOESY correlations of **8** ($CDCl_3$).

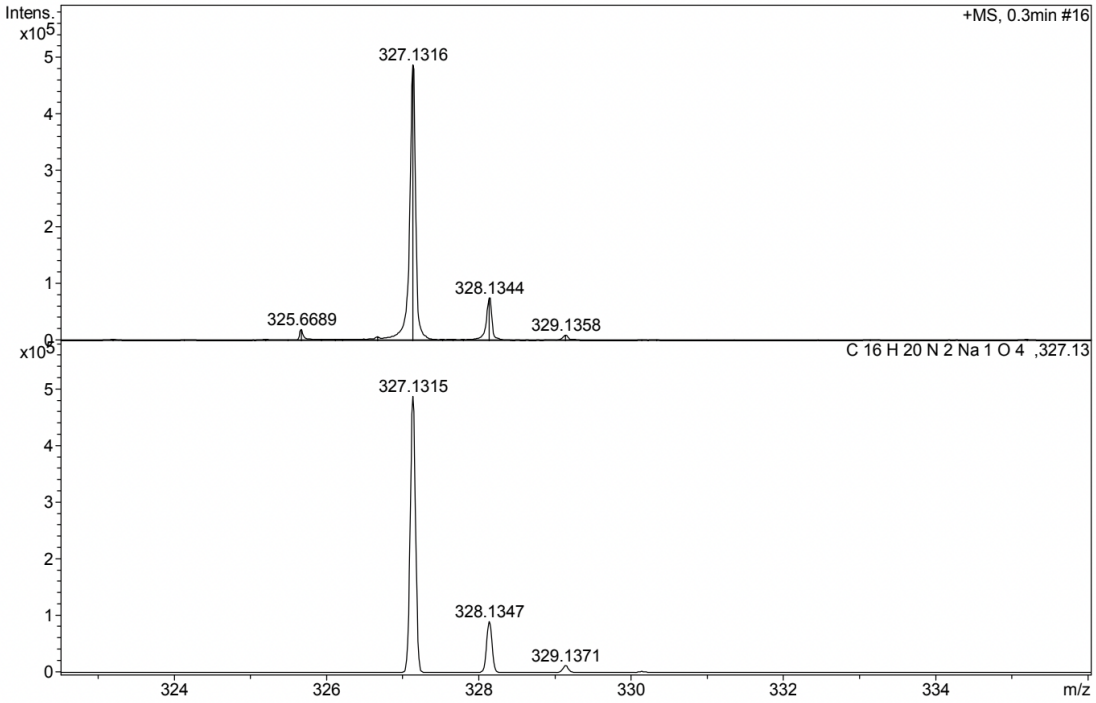

Figure A31. HRESIMS of **8** (positive ion mode).

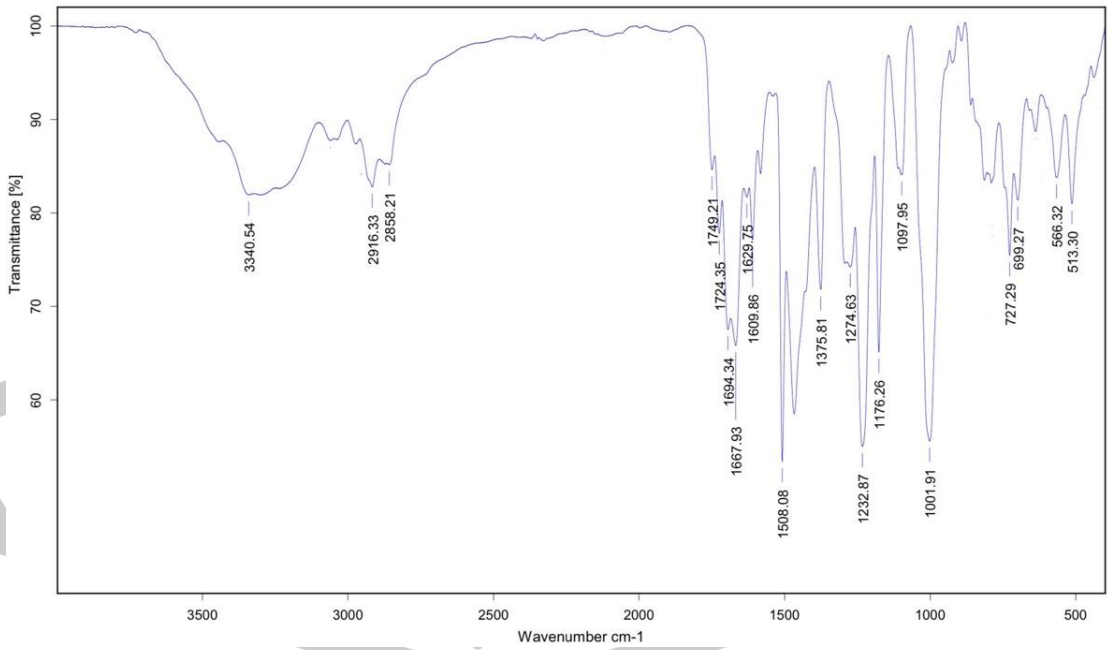

Figure A32. FTIR spectrum of **8**.

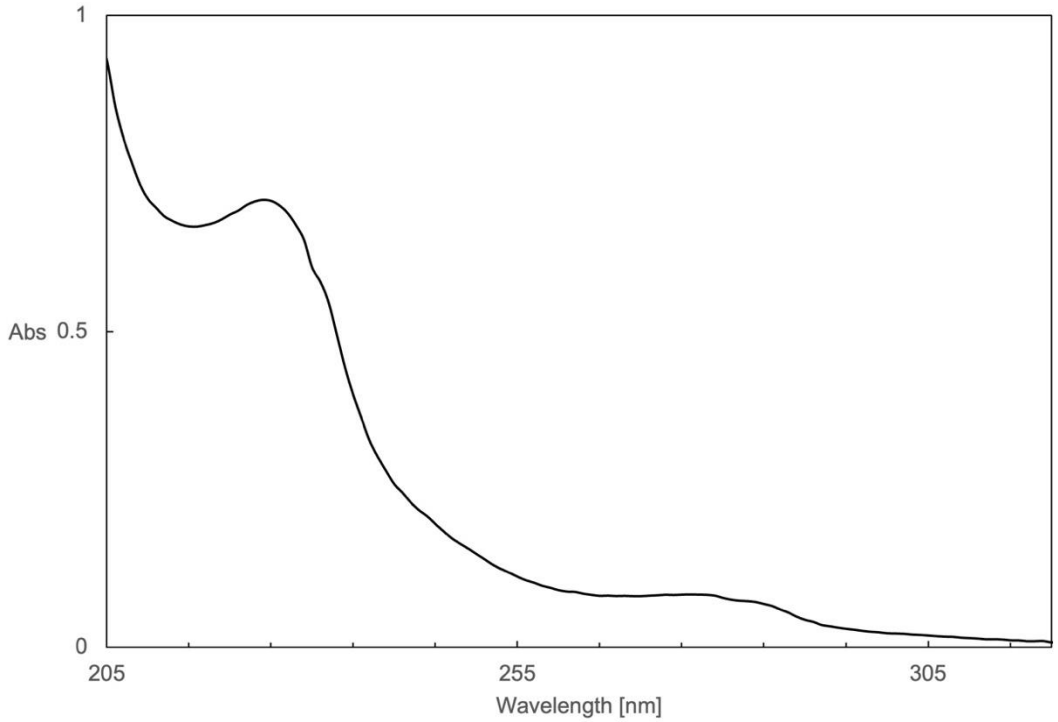

Figure A33. UV spectrum of **8**.

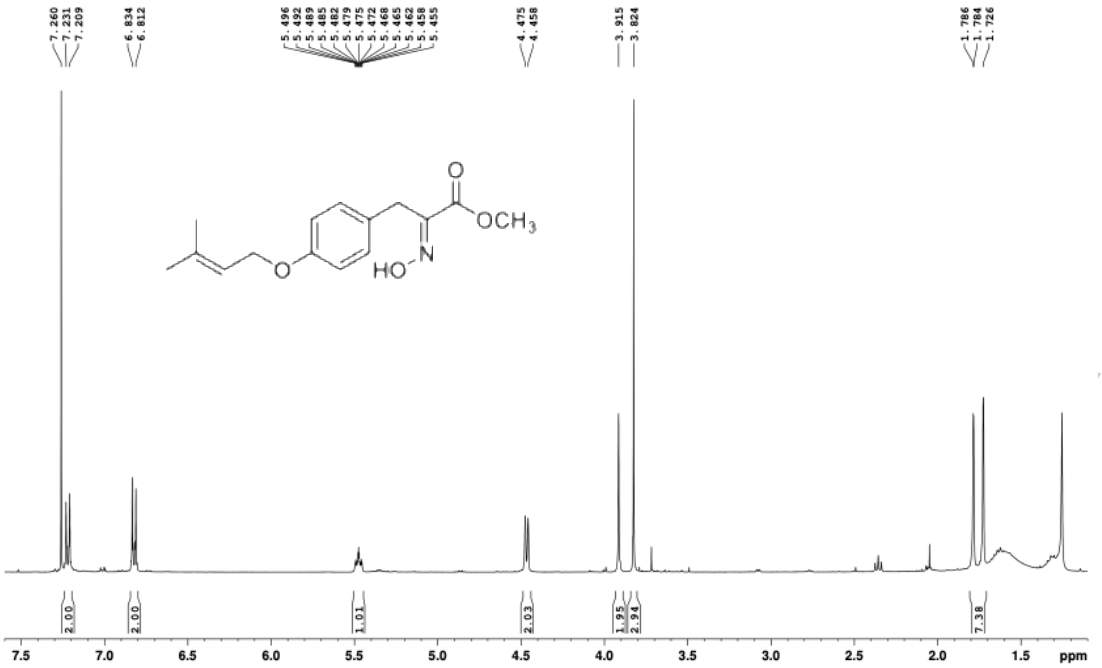

Figure A34. ^{1}H NMR spectrum of **9** ($CDCl_3$, 400 MHz).

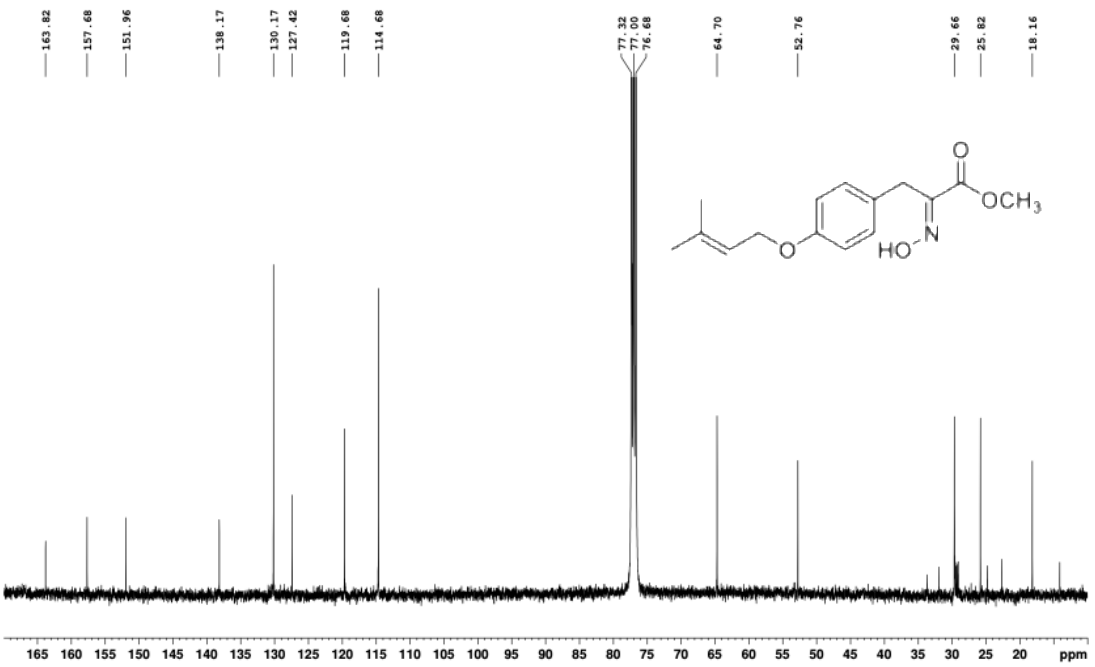

Figure A35. ^{13}C NMR spectrum of **9** ($CDCl_3$, 100 MHz).

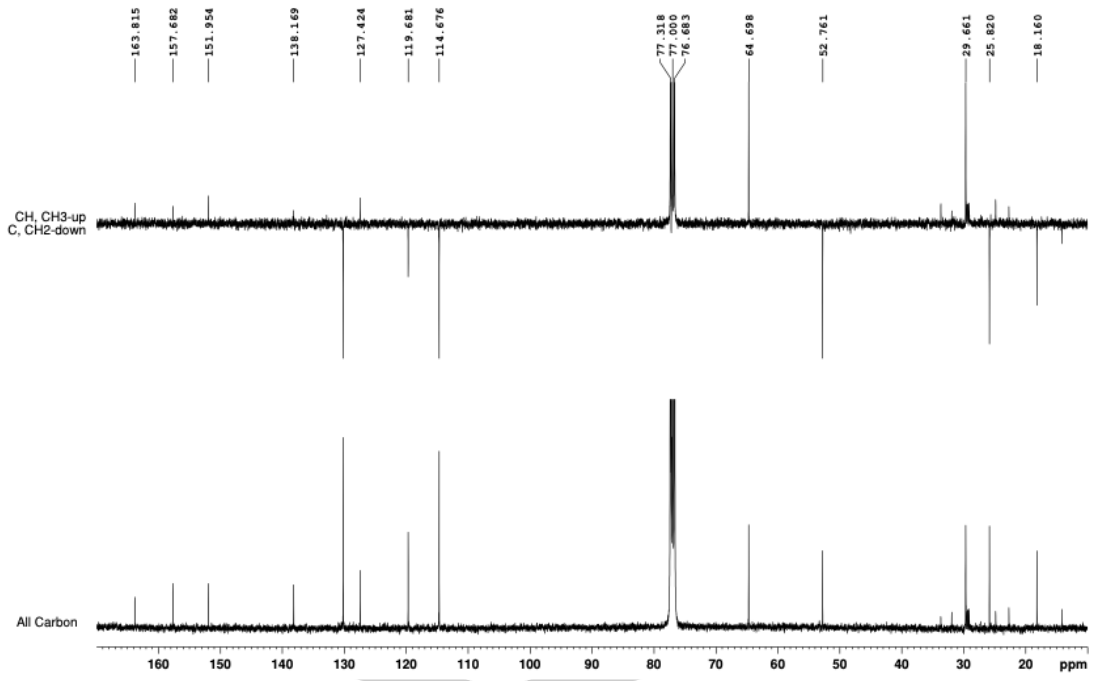

Figure A36. DEPT-135 spectrum of **9** ($CDCl_3$, 100 MHz).

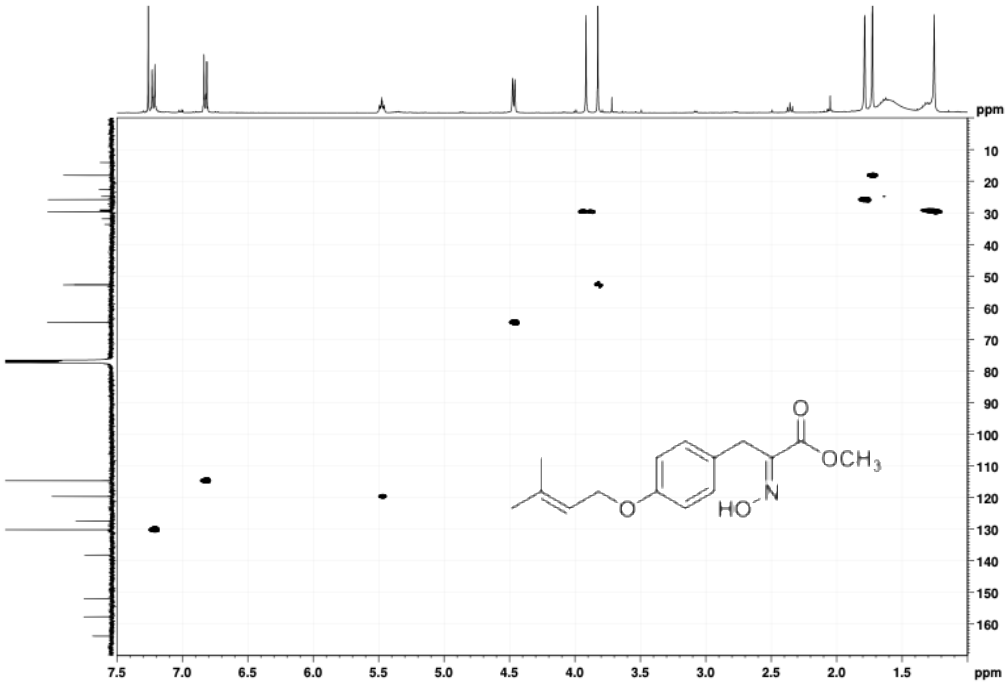

Figure A37. HSQC spectrum of **9** ($CDCl_3$, 400 MHz).

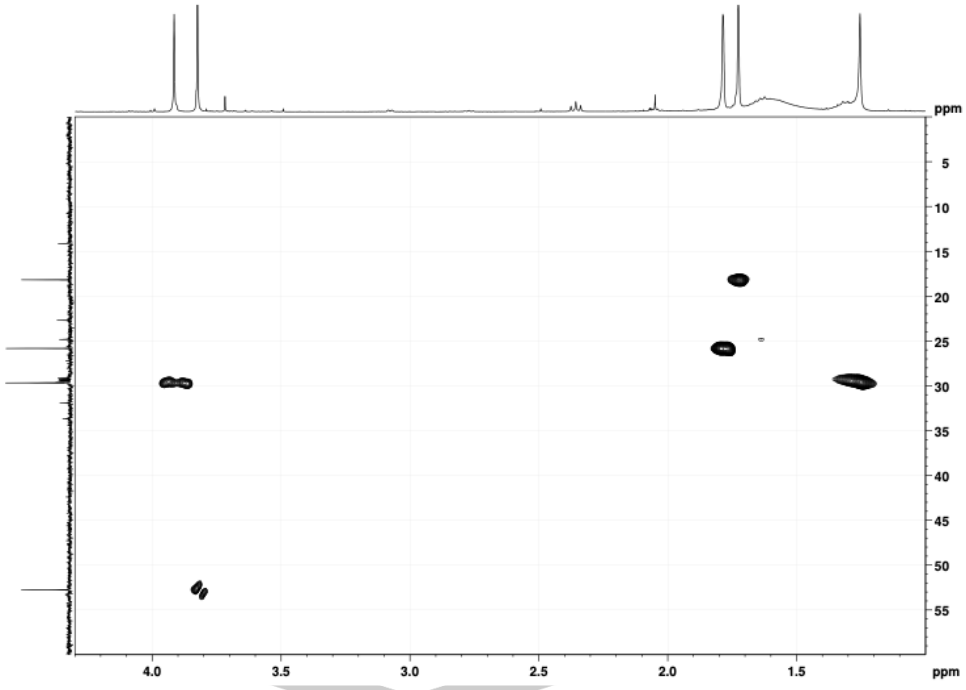

Figure A38. HSQC (expansion-1) spectrum of **9** ($CDCl_3$, 400 MHz).

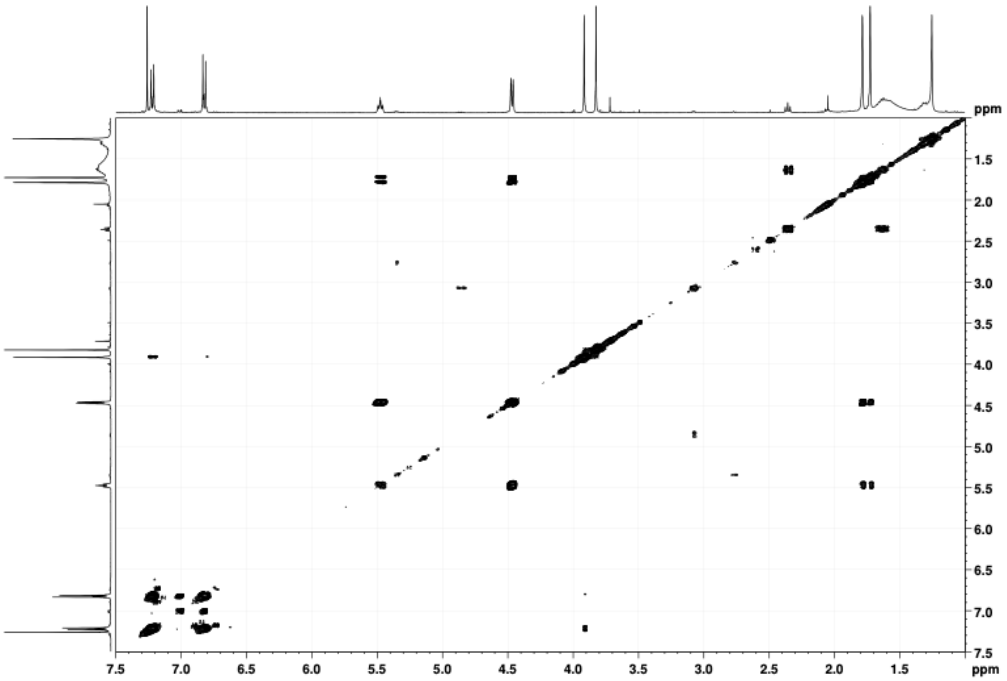

Figure A39. COSY spectrum of **9** ($CDCl_3$, 400 MHz).

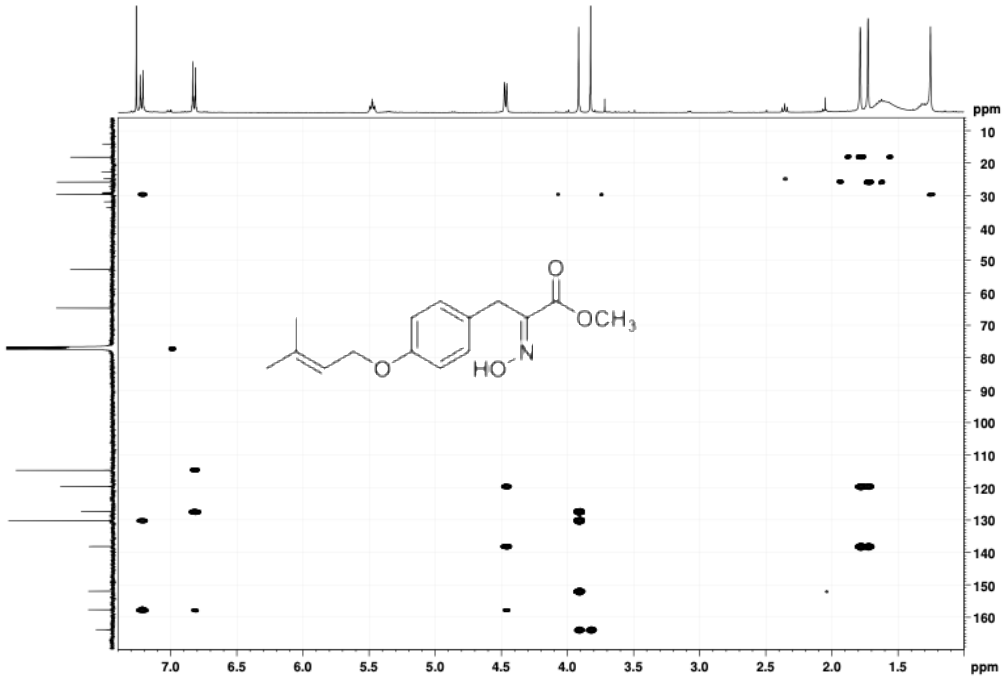

Figure A40. HMBC spectrum of **9** ($CDCl_3$, 400 MHz).

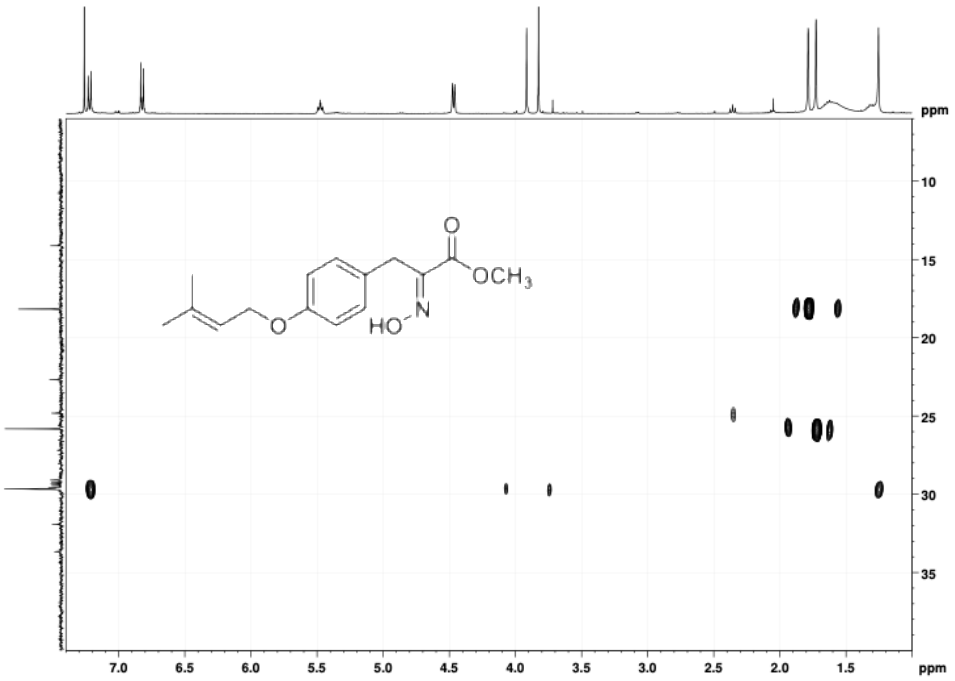

Figure A41. HMBC (expansion-1) spectrum of **9** ($CDCl_3$, 400 MHz).

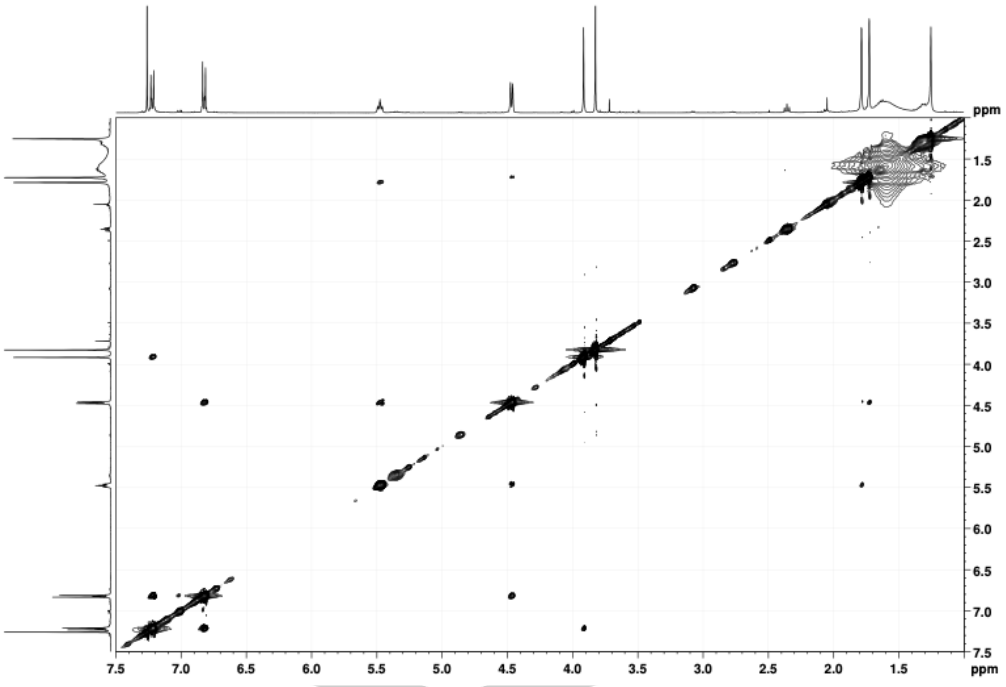

Figure A42. NOESY spectrum of **9** ($CDCl_3$, 400 MHz).

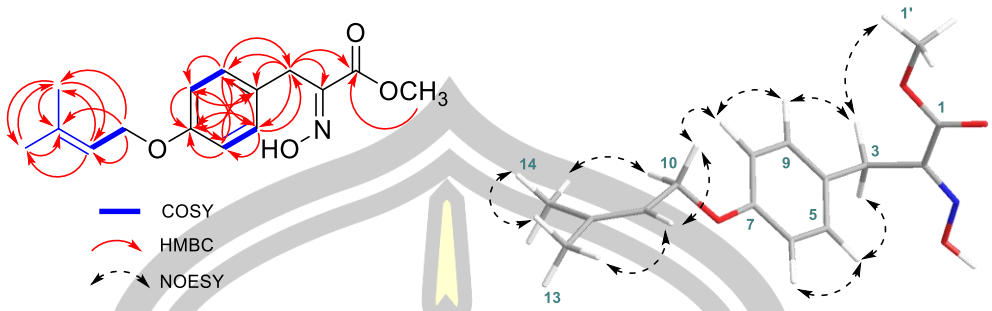

Figure A43. COSY, HMBC, and NOESY correlations of **9** ($CDCl_3$).

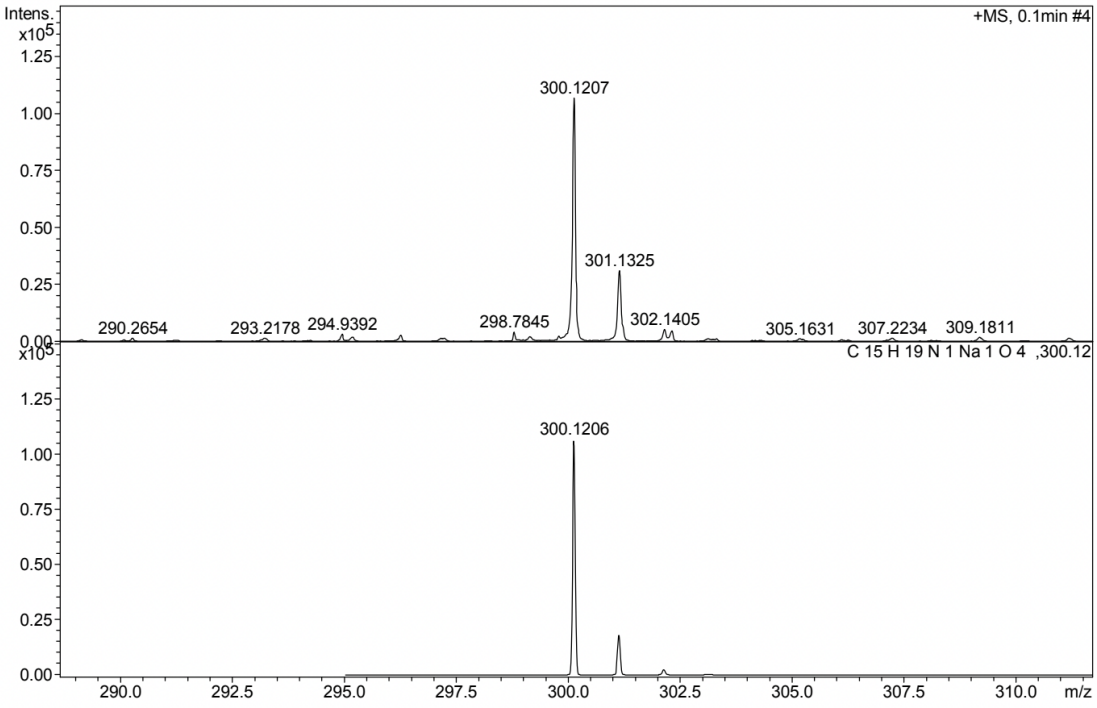

Figure A44. HRESIMS of **9** (positive ion mode).

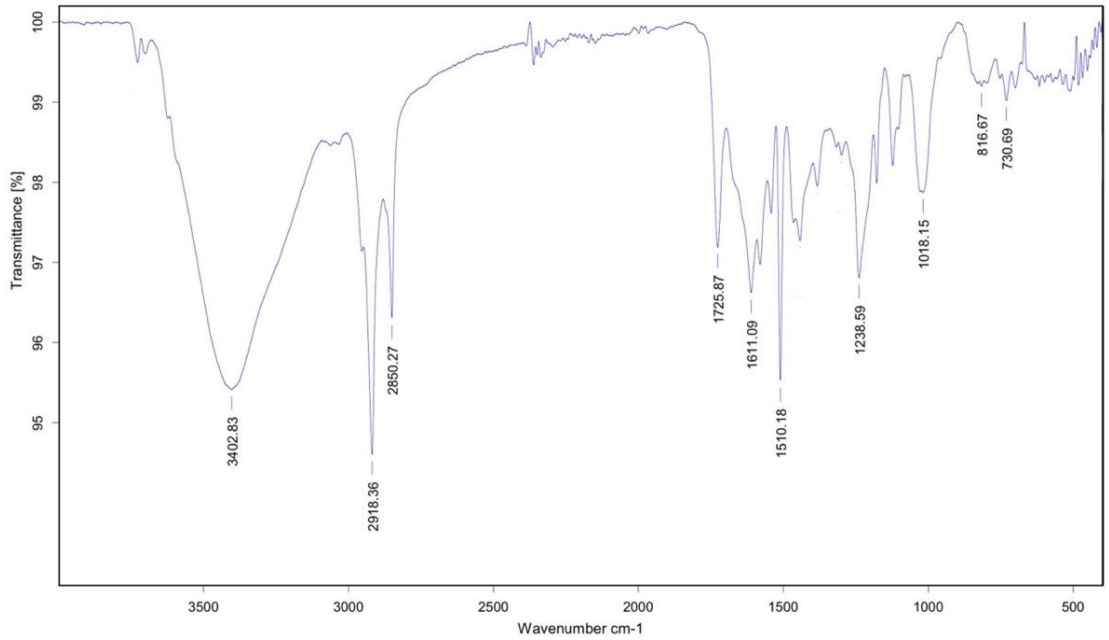

Figure A45. FTIR spectrum of **9**.

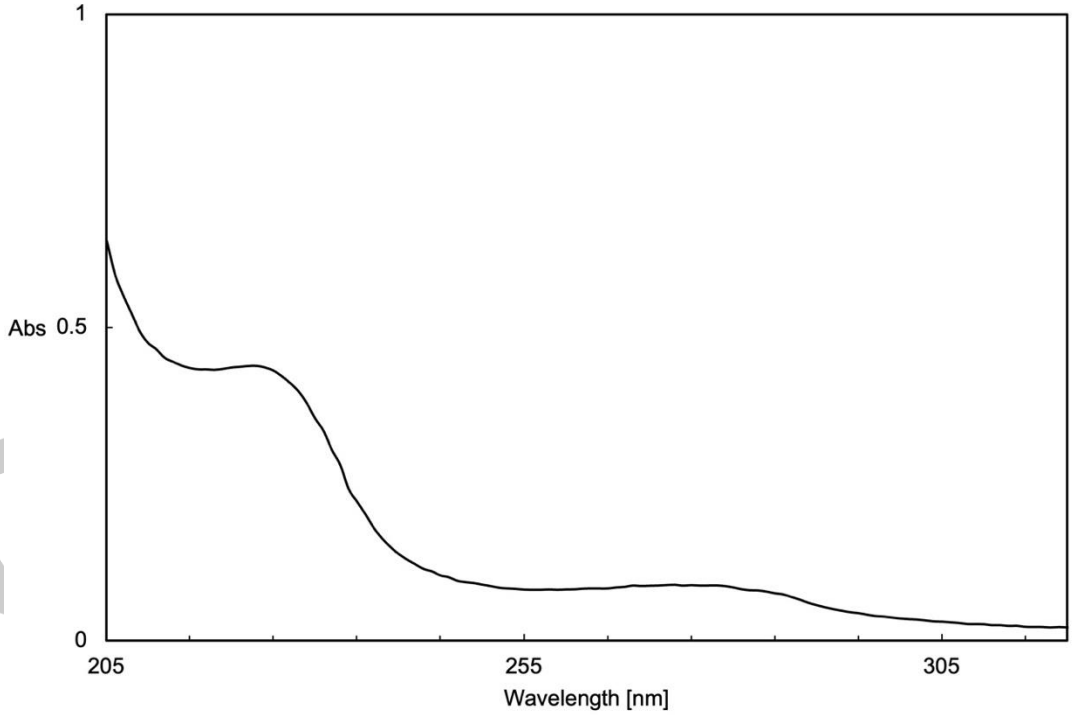

Figure A46. UV spectrum of **9**.

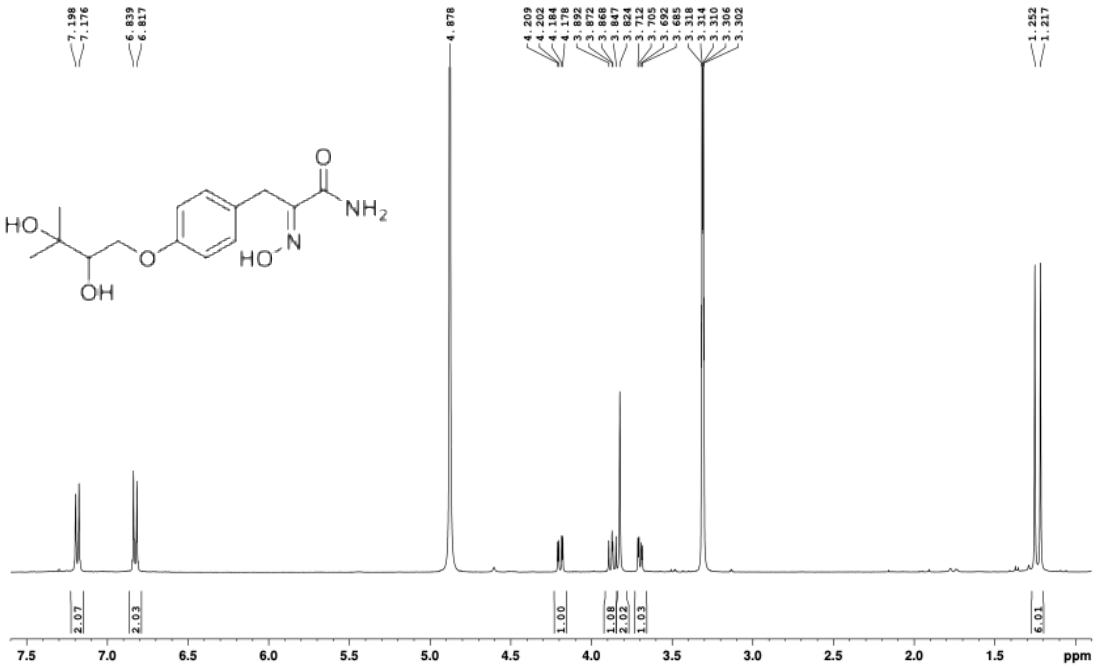

Figure A47. ^{1}H NMR spectrum of **10** (CD_3OD, 400 MHz).

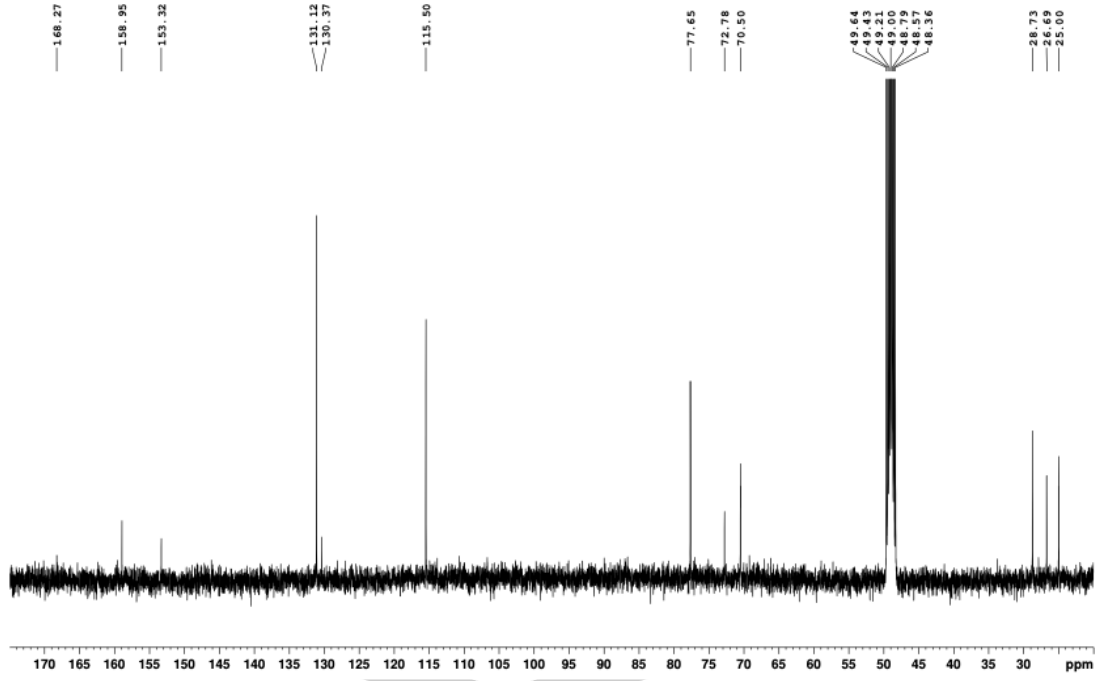

Figure A48. ^{13}C NMR spectrum of **10** (CD_3OD, 100 MHz).

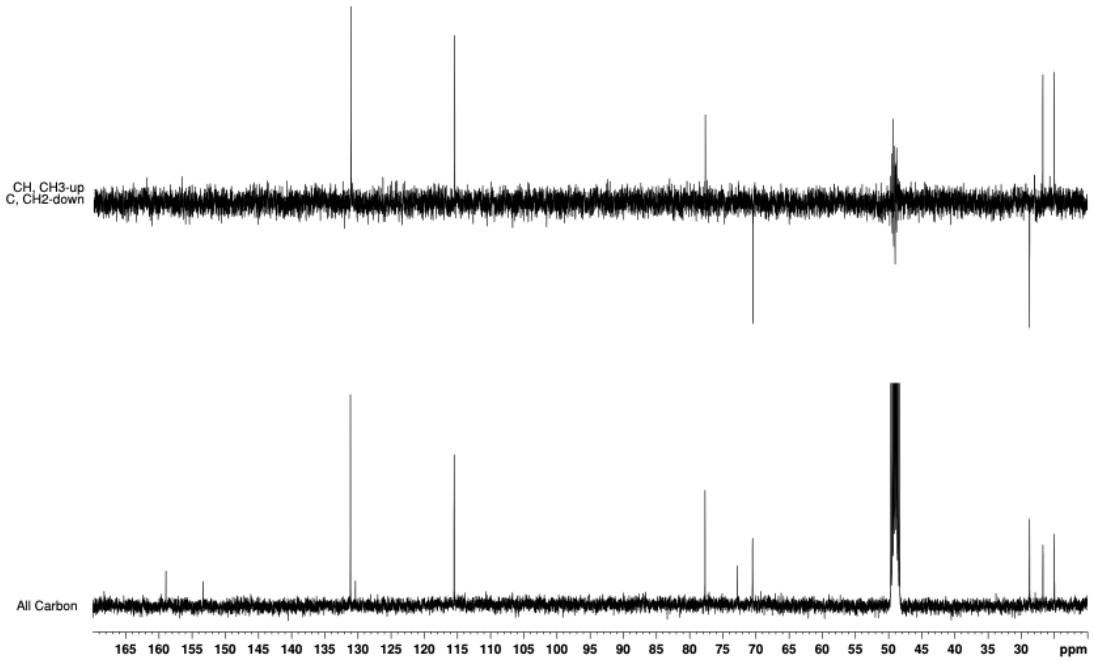

Figure A49. DEPT-135 spectrum of **10** (CD_3OD, 100 MHz).

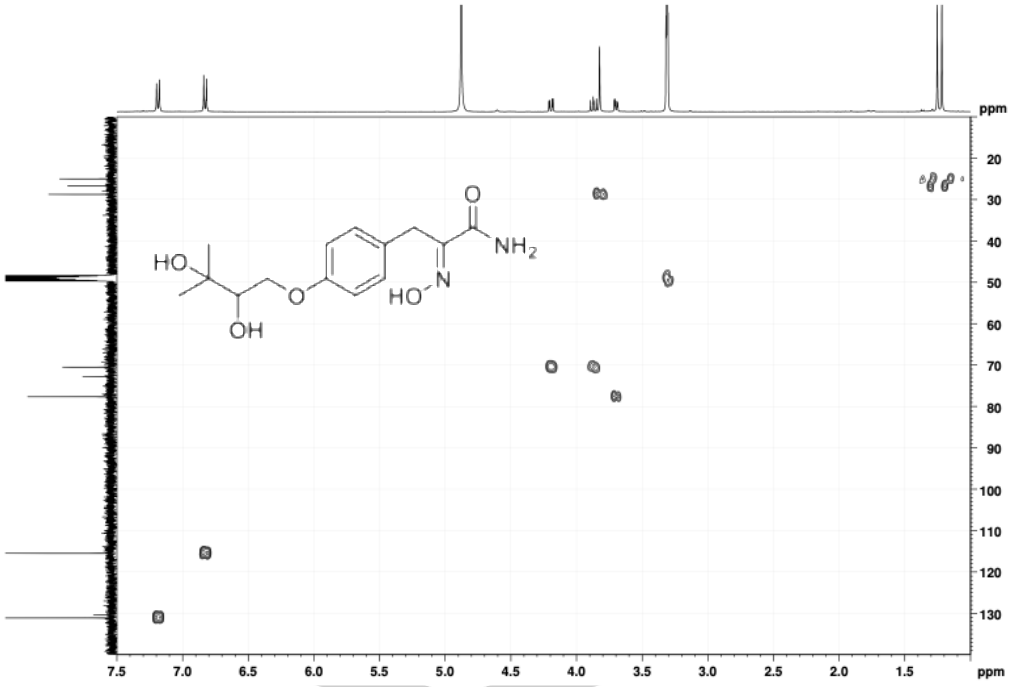

Figure A50. HSQC spectrum of **10** (CD_3OD, 400 MHz).

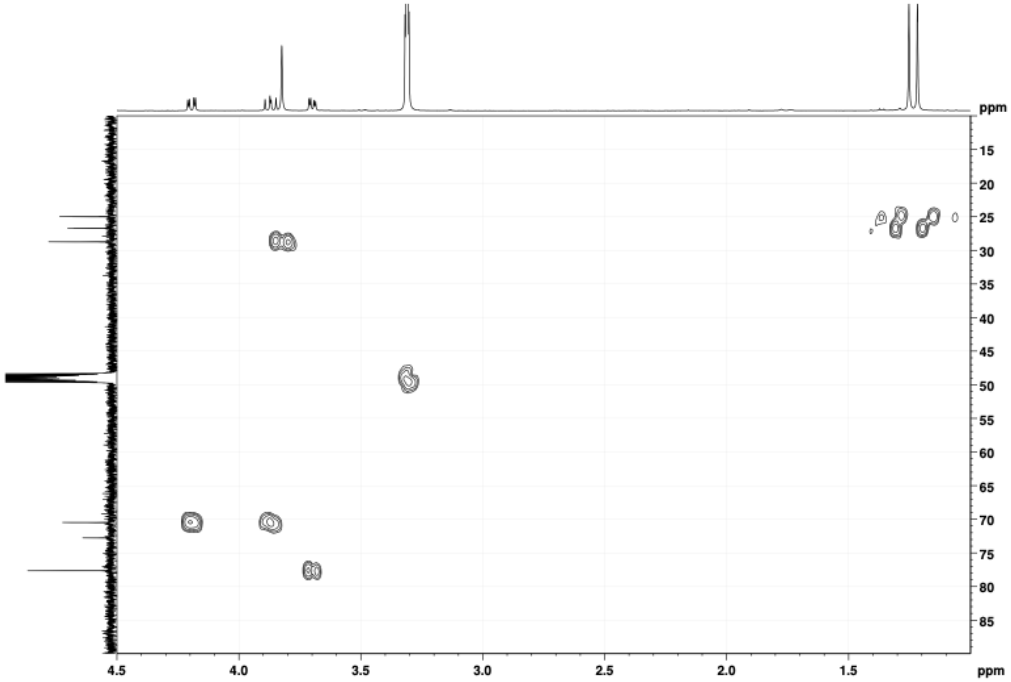

Figure A51. HSQC (expansion-1) spectrum of **10** (CD_3OD, 400 MHz).

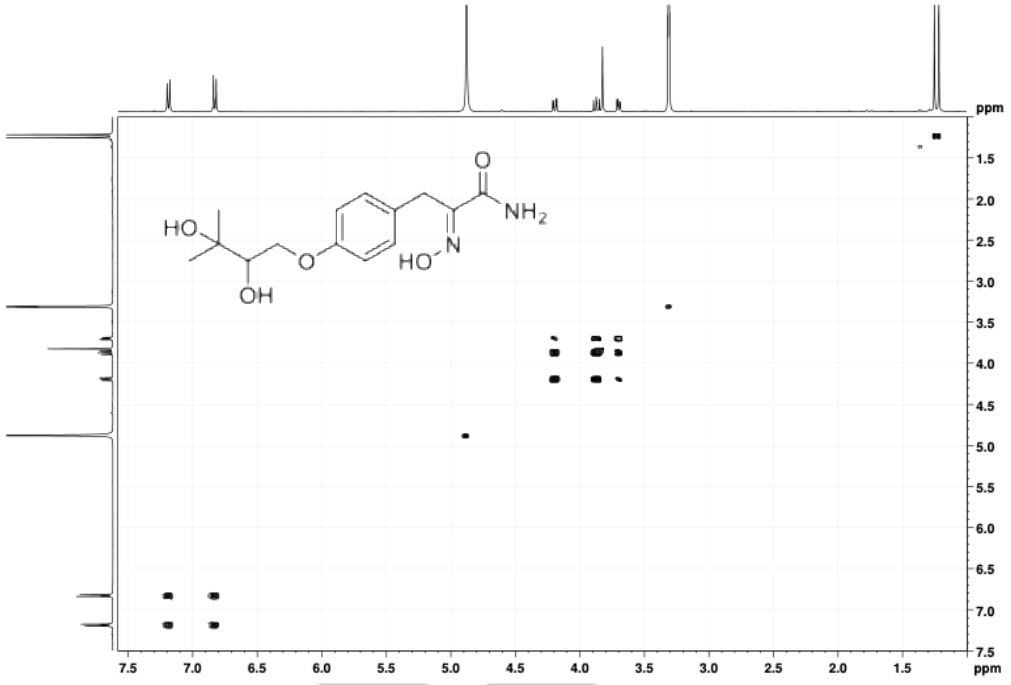

Figure A52. COSY spectrum of **10** (CD_3OD, 400 MHz).

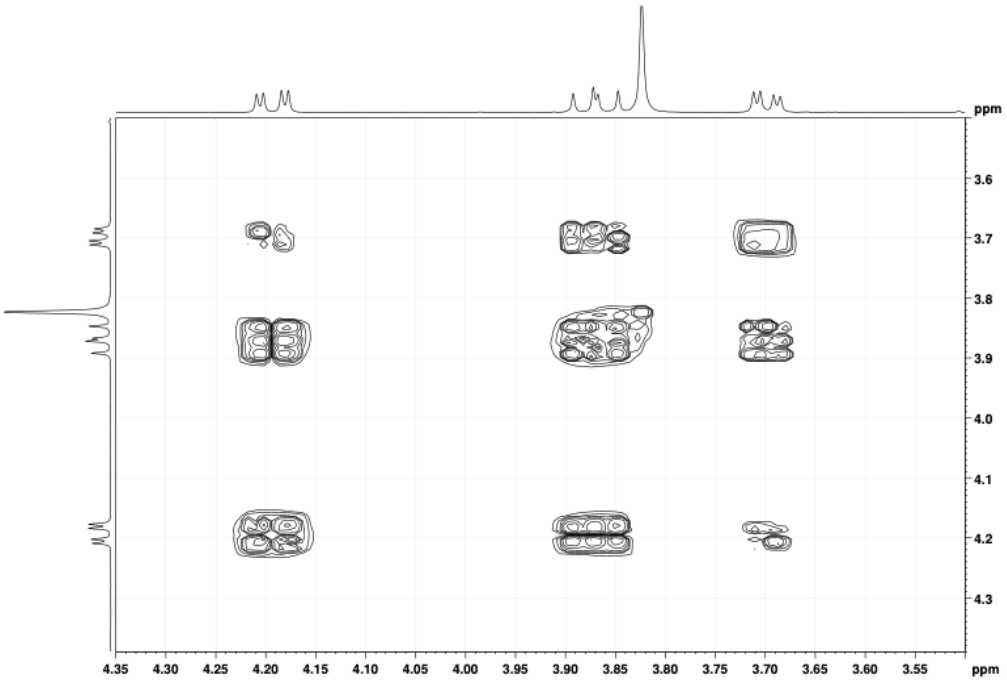

Figure A53. COSY (expansion-1) spectrum of **10** (CD_3OD, 400 MHz).

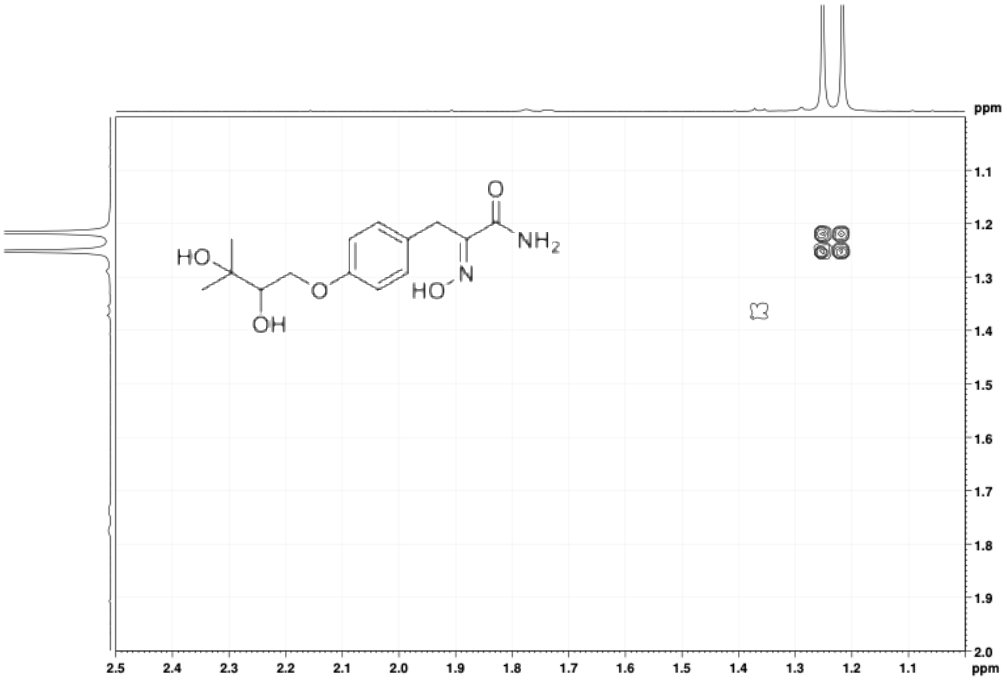

Figure A54. COSY (expansion-2) spectrum of **10** (CD_3OD, 400 MHz).

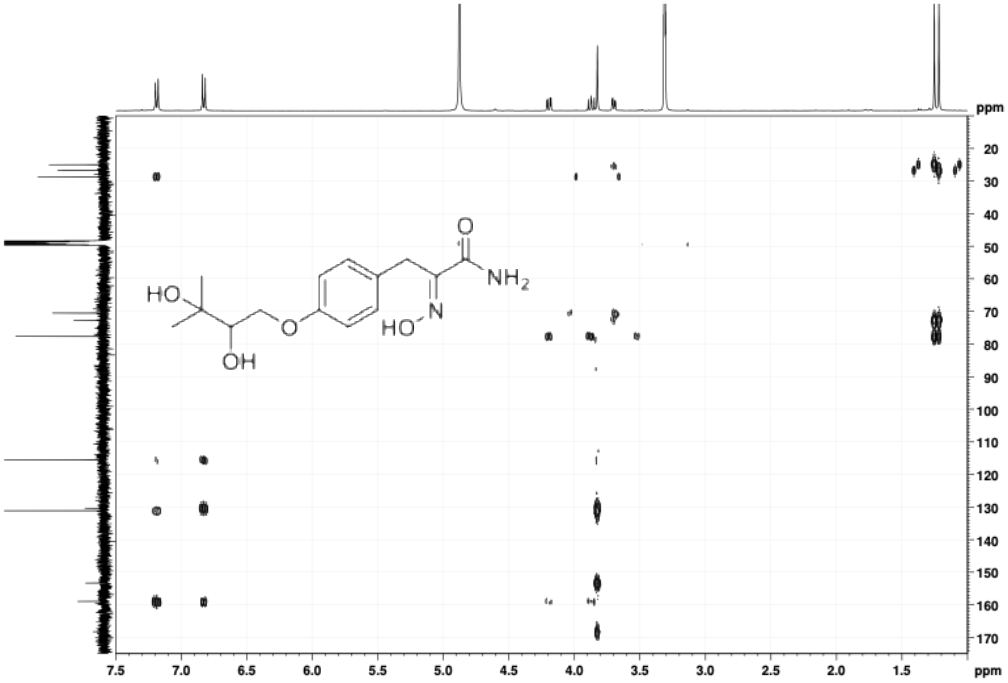

Figure A55. HMBC spectrum of **10** (CD_3OD, 400 MHz).

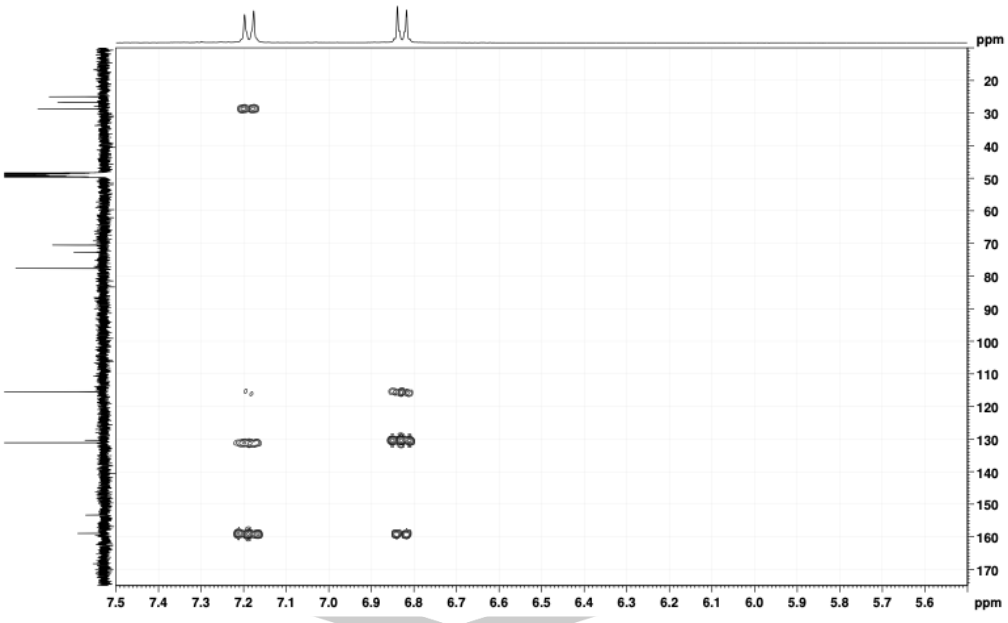

Figure A56. HMBC (expansion-1) spectrum of **10** (CD_3OD, 400 MHz).

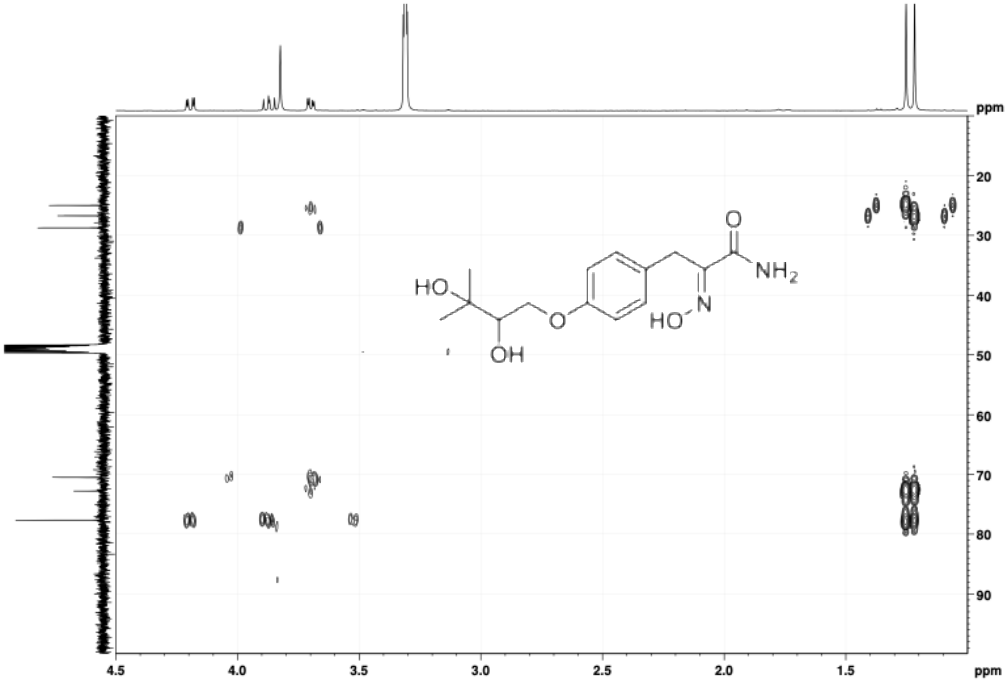

Figure A57. HMBC (expansion-2) spectrum of **10** (CD_3OD, 400 MHz).

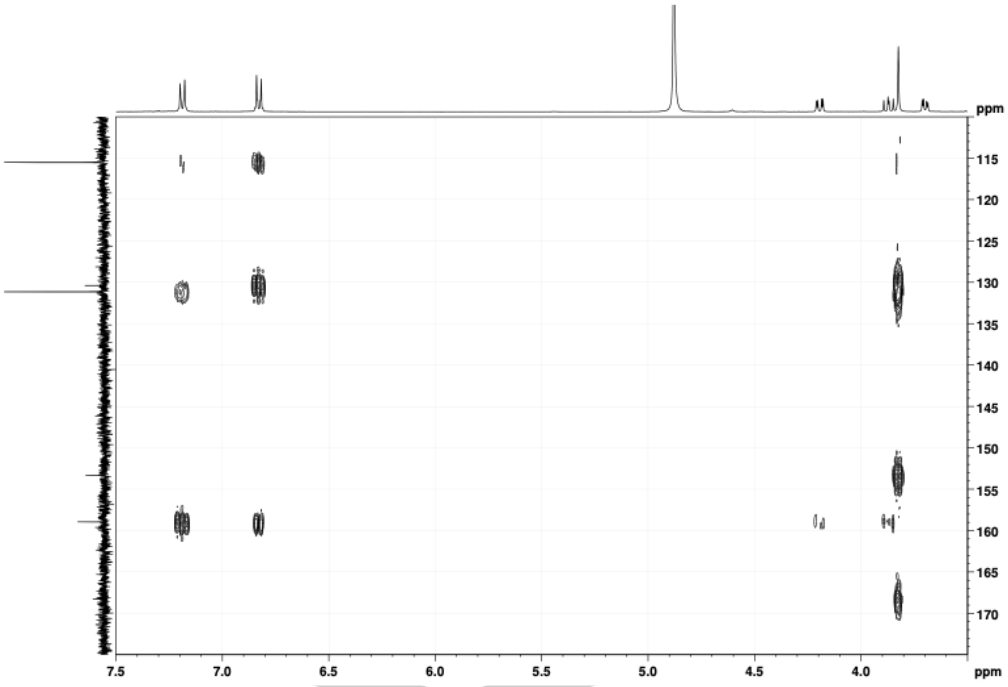

Figure A58. HMBC (expansion-3) spectrum of **10** (CD_3OD, 400 MHz).

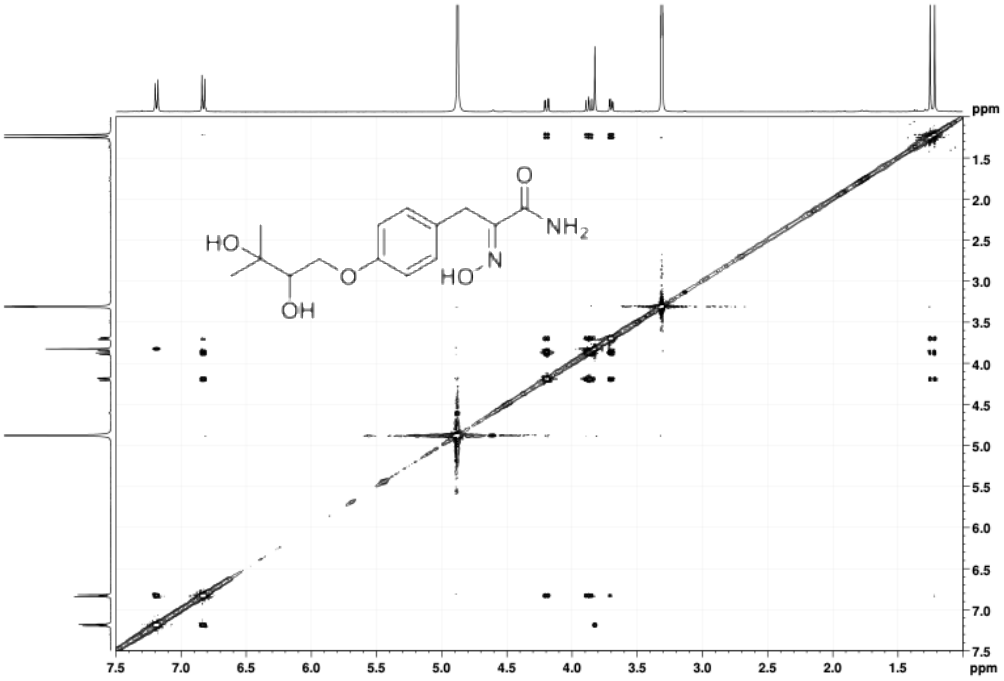

Figure A59. NOESY spectrum of **10** (CD_3OD, 400 MHz).

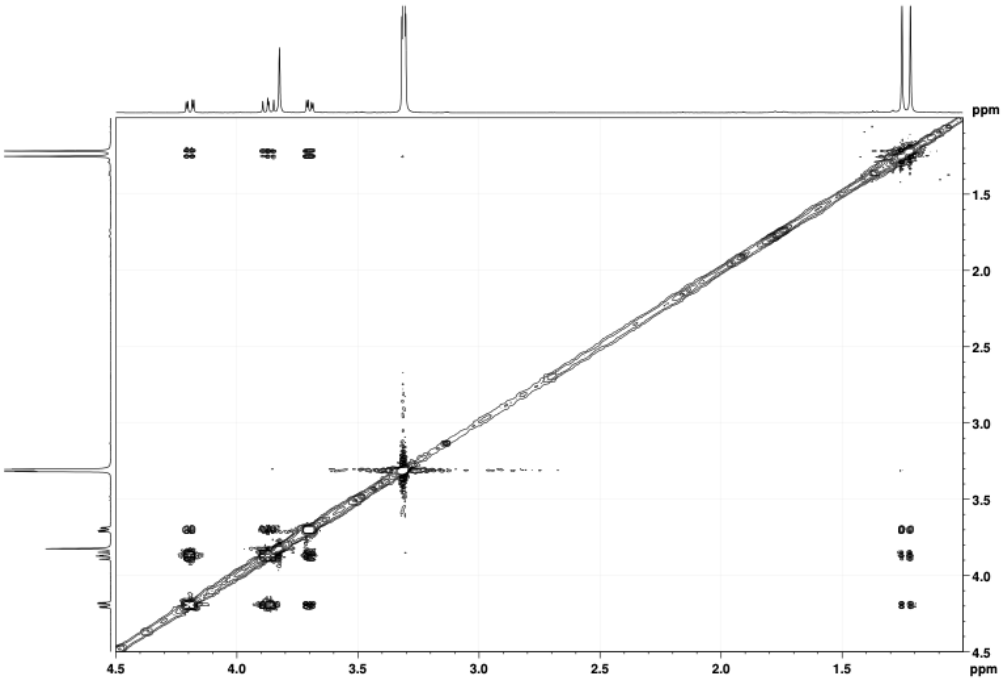

Figure A60. NOESY (expansion-1) spectrum of **10** (CD_3OD, 400 MHz).

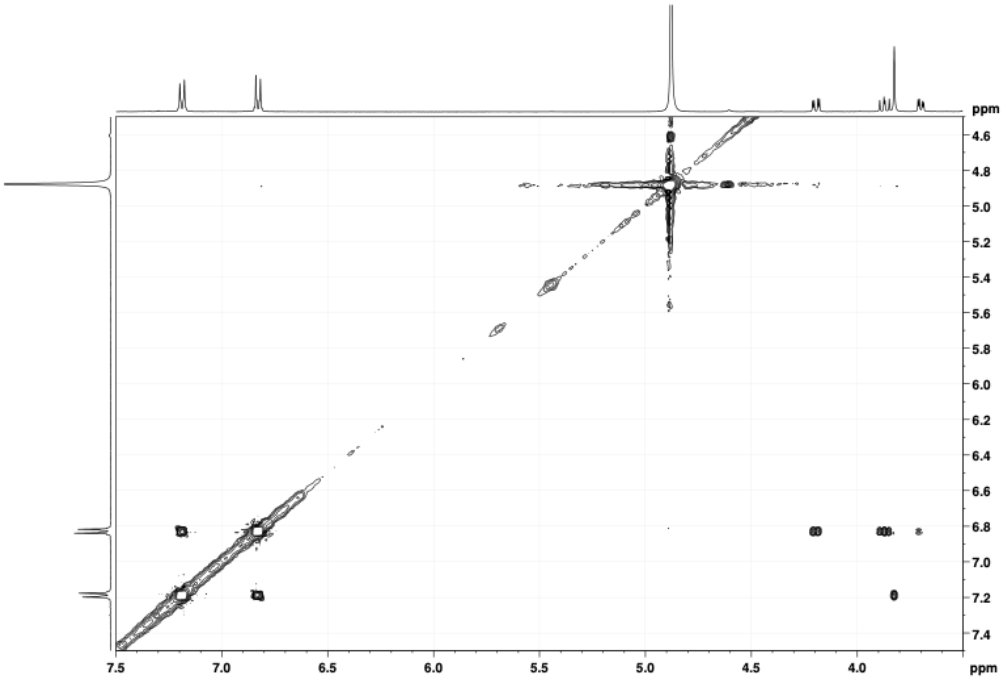

Figure A61. NOESY (expansion-2) spectrum of **10** (CD_3OD, 400 MHz).

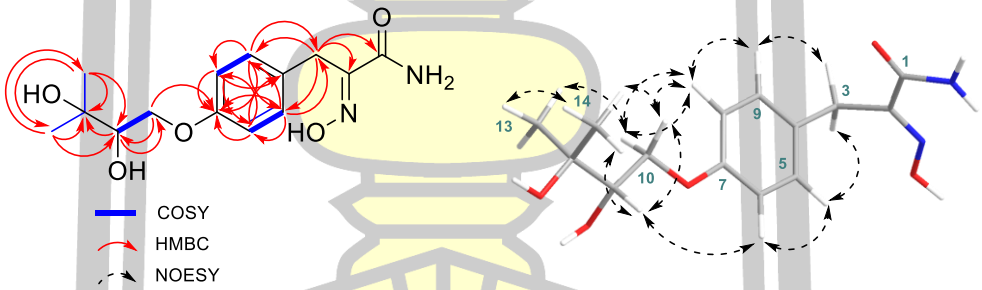

Figure A62. COSY, HMBC, and NOESY correlations of **10** (CD_3OD).

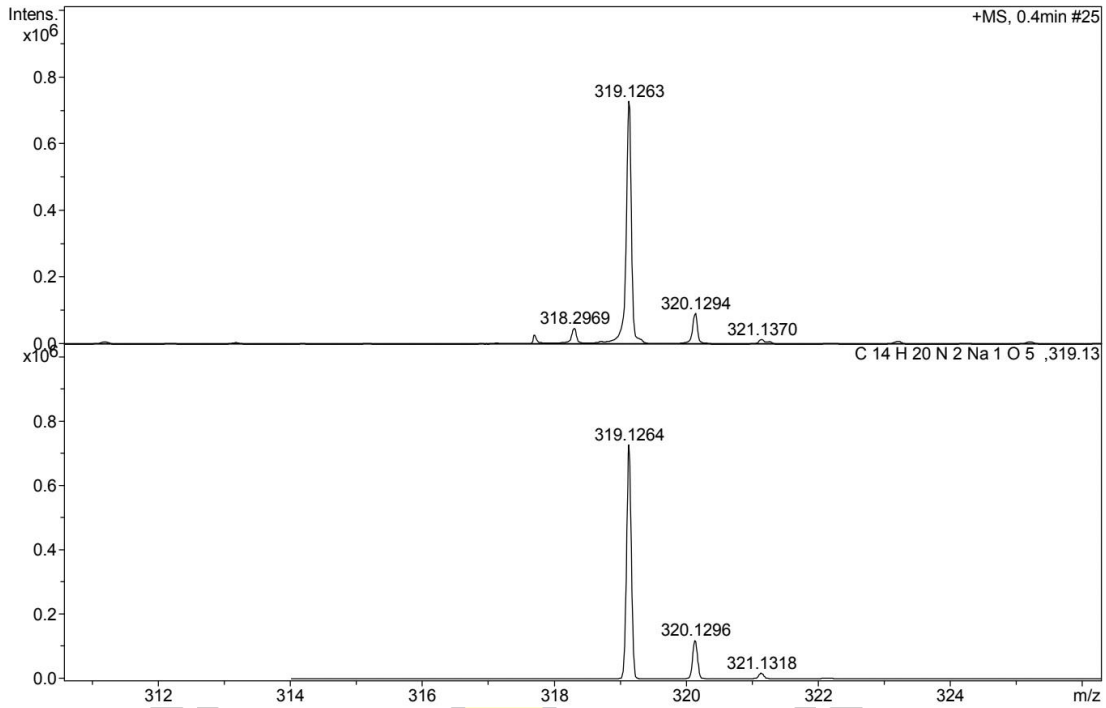

Figure A63. HRESIMS of **10** (positive ion mode).

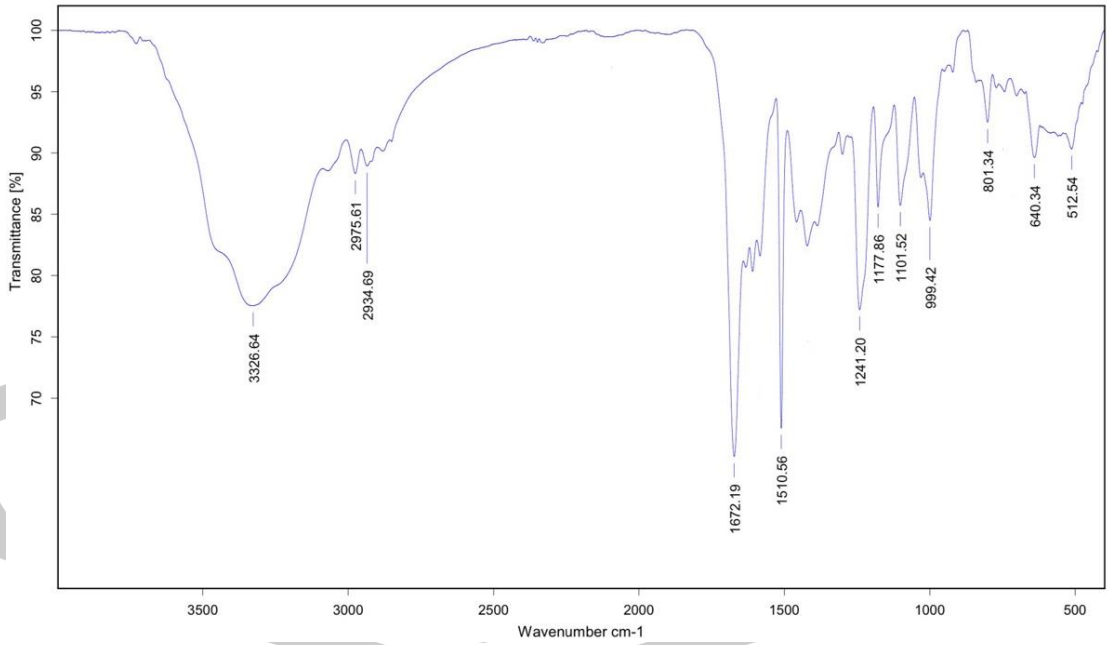

Figure A64. FTIR spectrum of **10**.

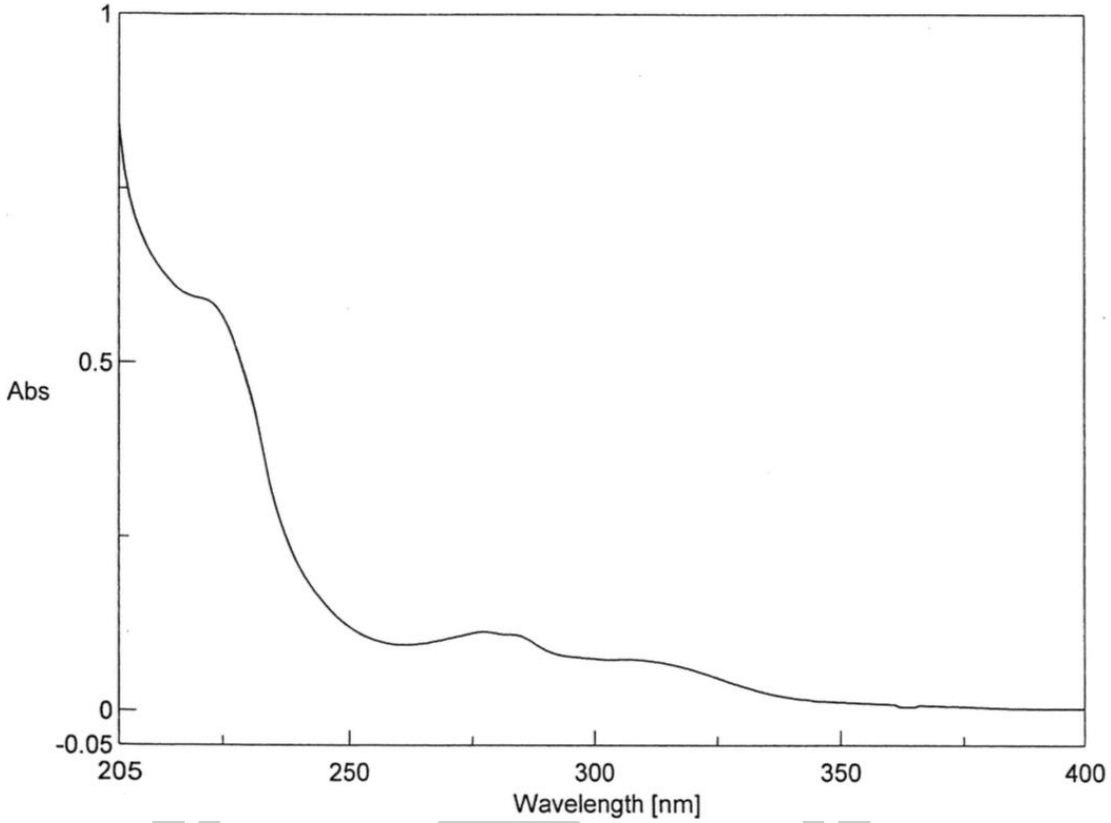

Figure A65. UV spectrum of **10**.

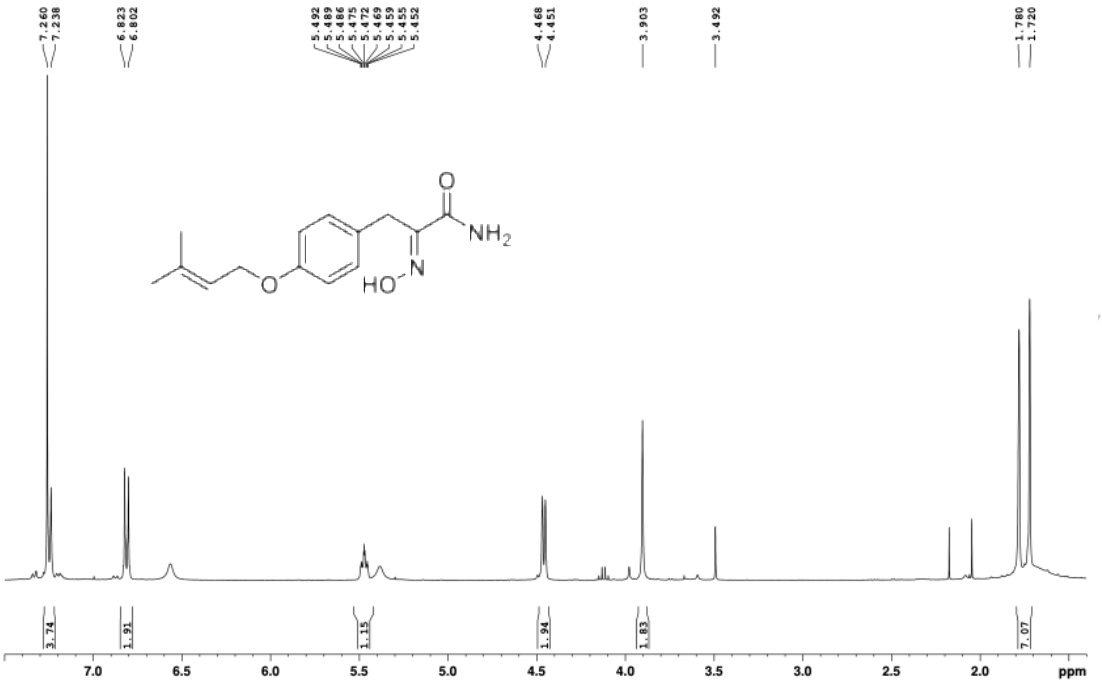

Figure A66. ^{1}H NMR spectrum of **3** ($CDCl_3$, 400 MHz).

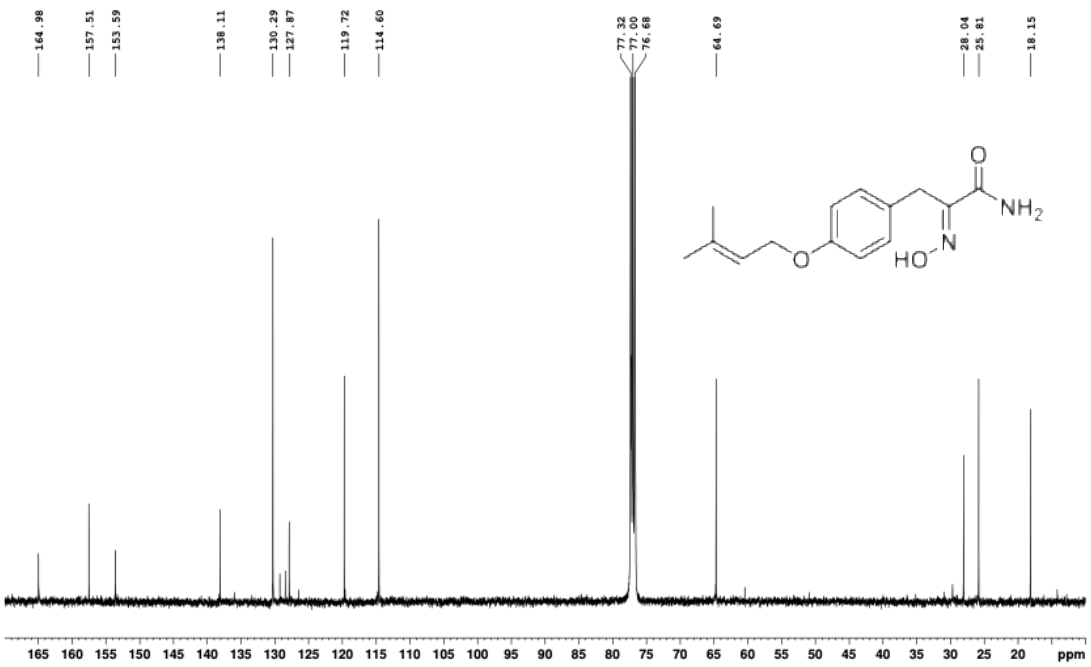

Figure A67. ^{13}C NMR spectrum of **3** ($CDCl_3$, 100 MHz).

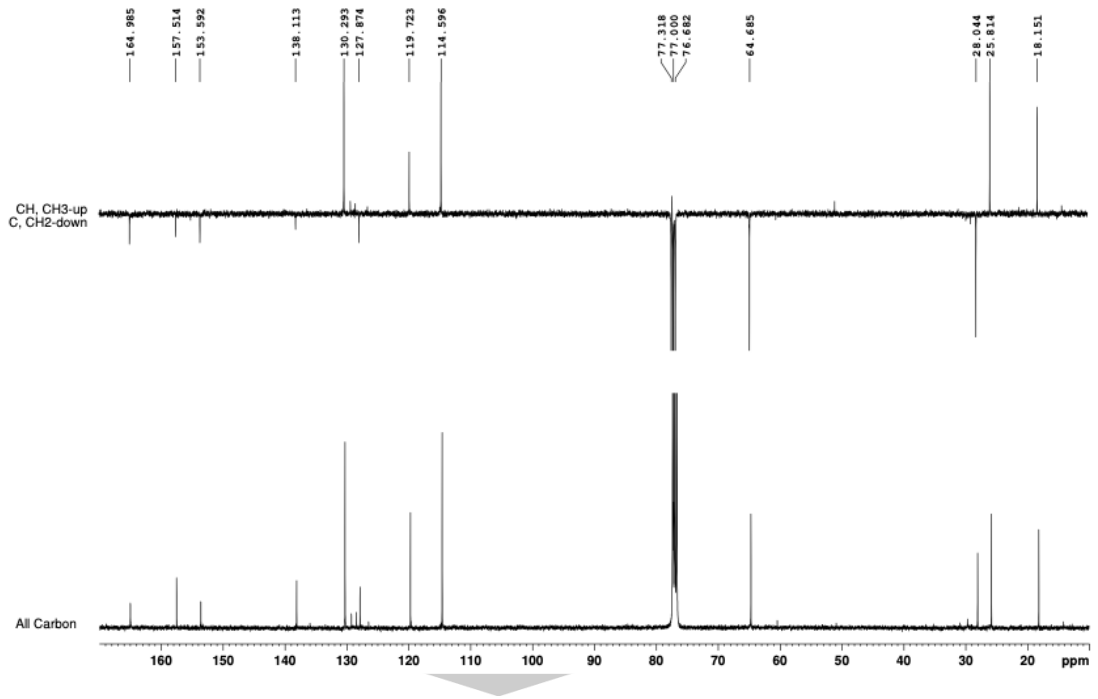

Figure A68. DEPT-135 spectrum of **3** ($CDCl_3$, 100 MHz).

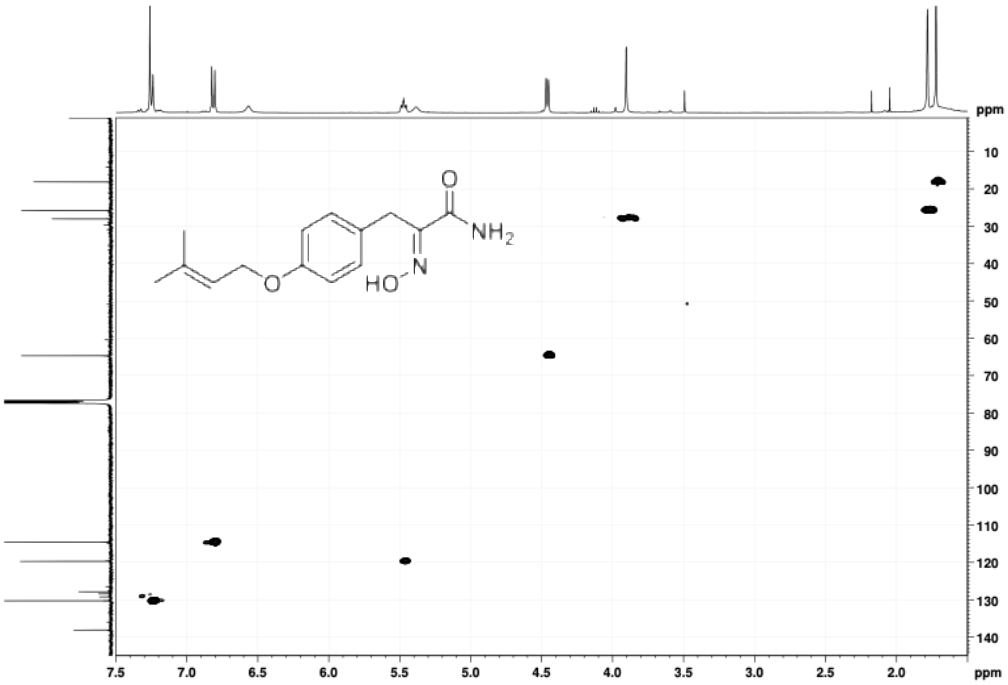

Figure A69. HSQC spectrum of **3** ($CDCl_3$, 400 MHz).

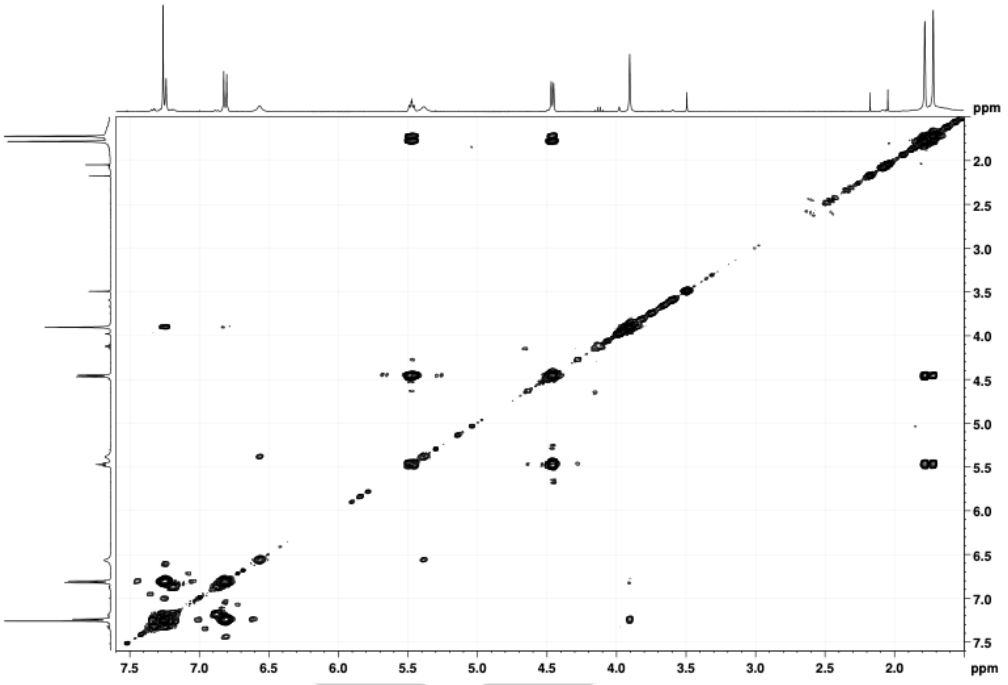

Figure A70. COSY spectrum of **3** ($CDCl_3$, 400 MHz).

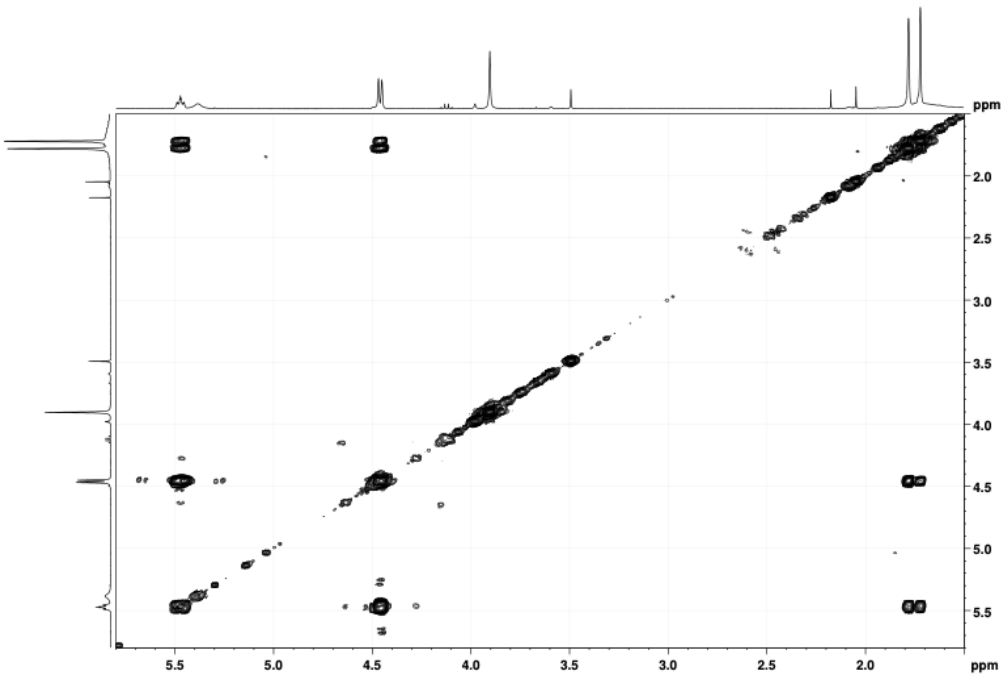

Figure A71. COSY (expansion-1) spectrum of **3** ($CDCl_3$, 400 MHz).

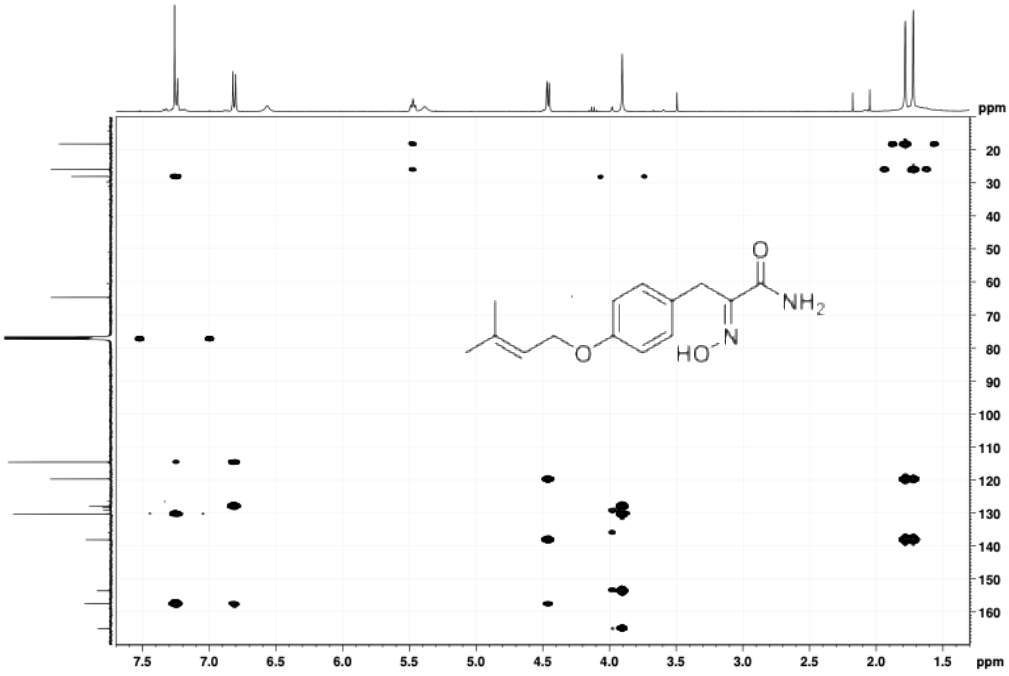

Figure A72. HMBC spectrum of **3** ($CDCl_3$, 400 MHz).

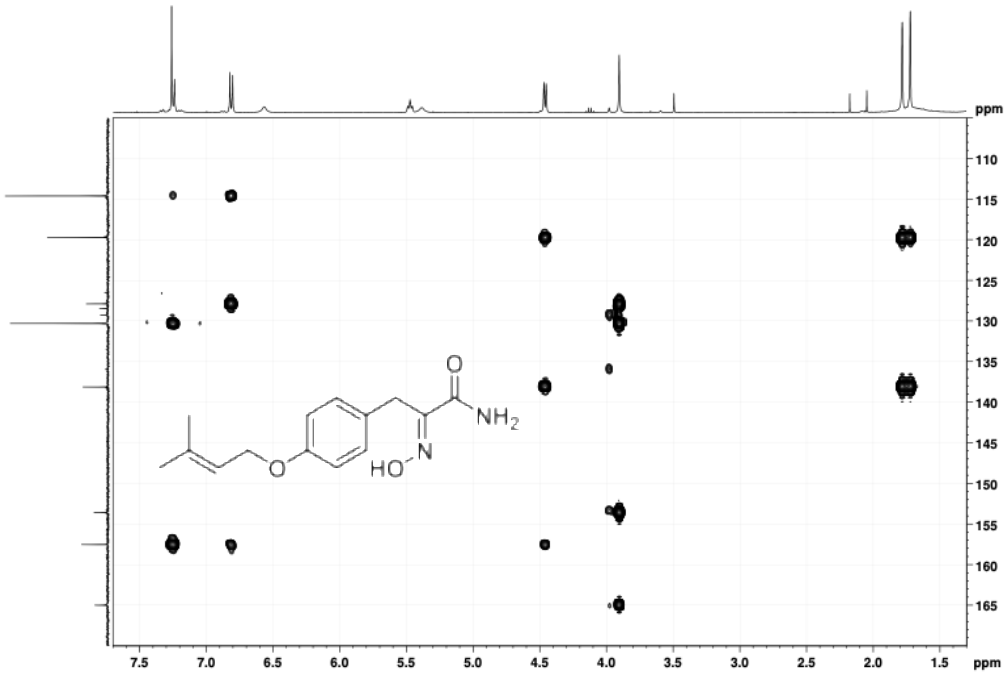

Figure A73. HMBC (expansion-1) spectrum of **3** ($CDCl_3$, 400 MHz).

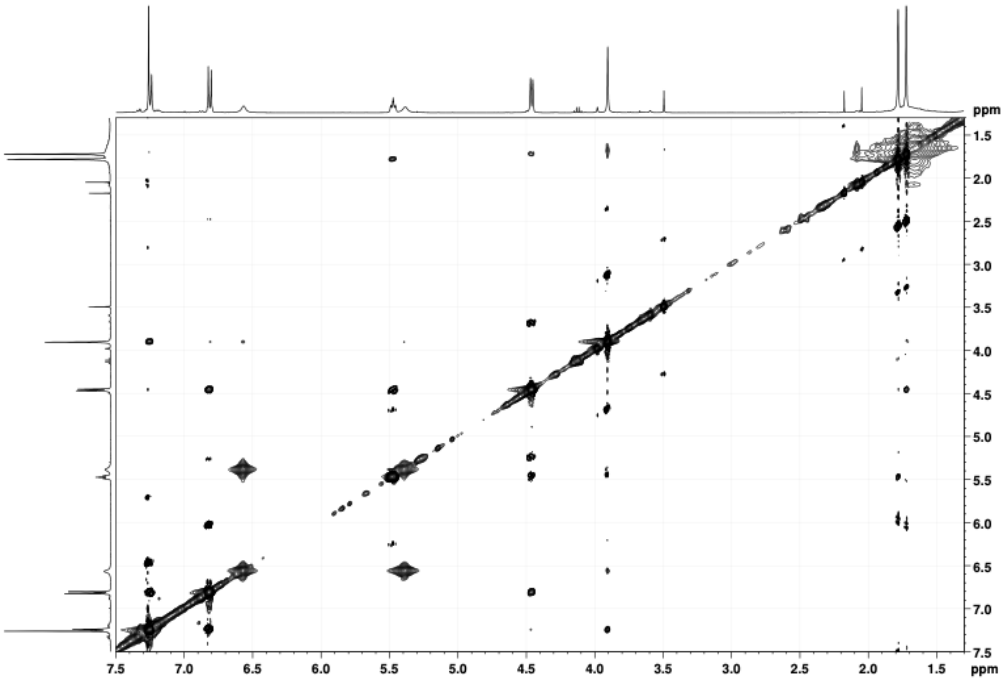

Figure A74. NOESY spectrum of **3** ($CDCl_3$, 400 MHz).

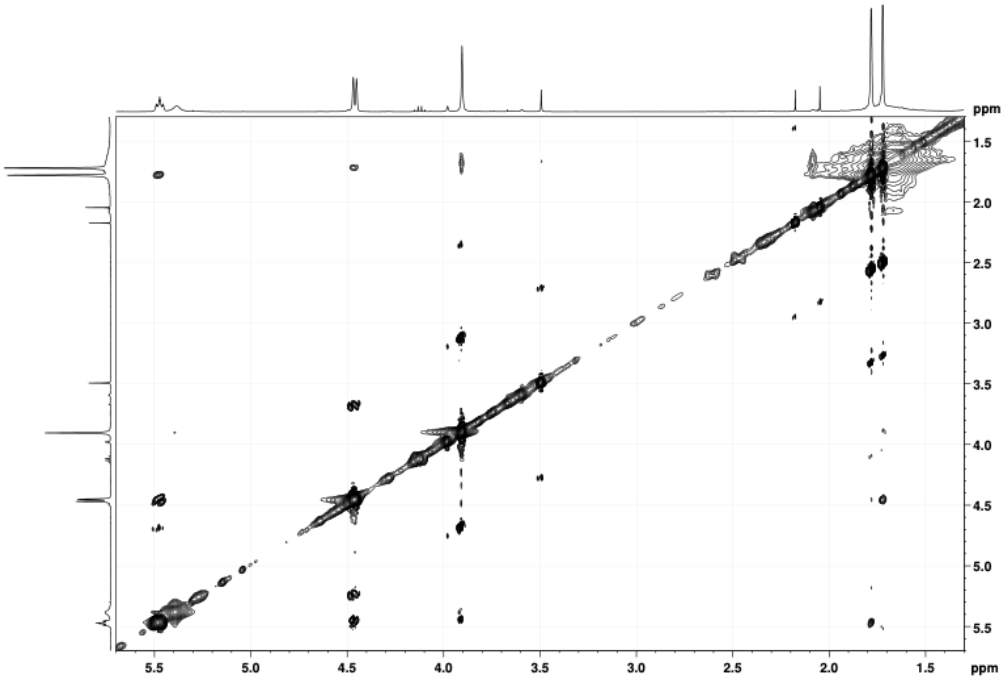

Figure A75. NOESY (expansion-1) spectrum of **3** ($CDCl_3$, 400 MHz).

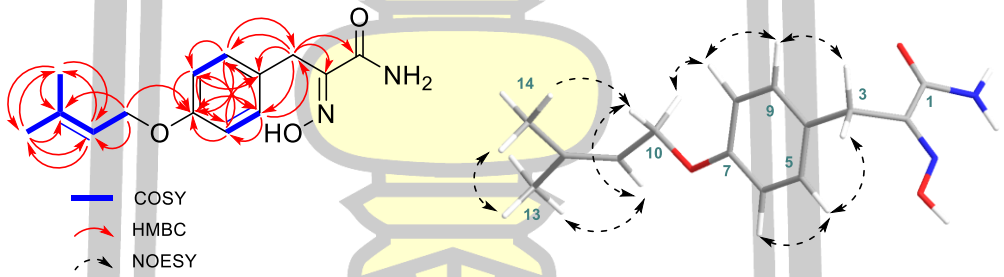

Figure A76. COSY, HMBC, and NOESY correlations of **3** ($CDCl_3$).

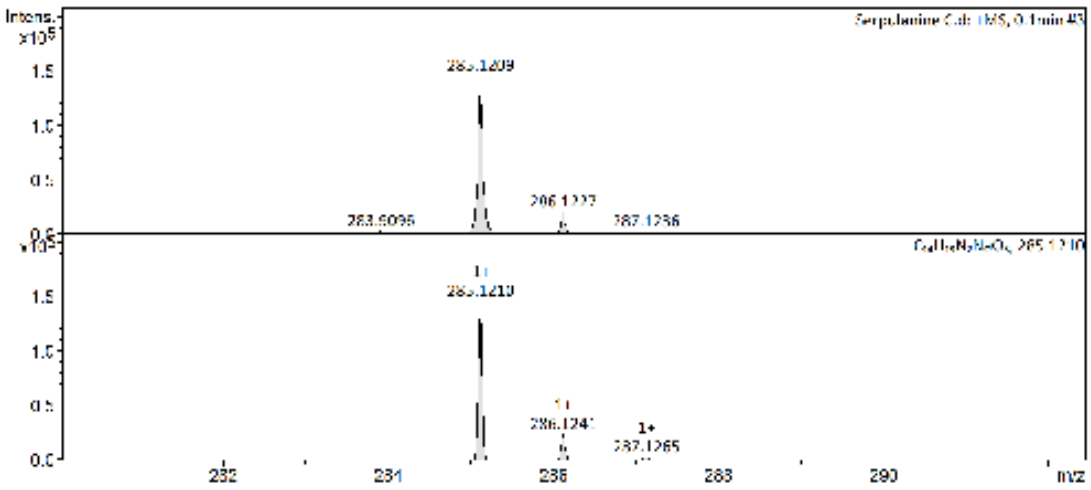

Figure A77. HRESIMS of **3** (positive ion mode).

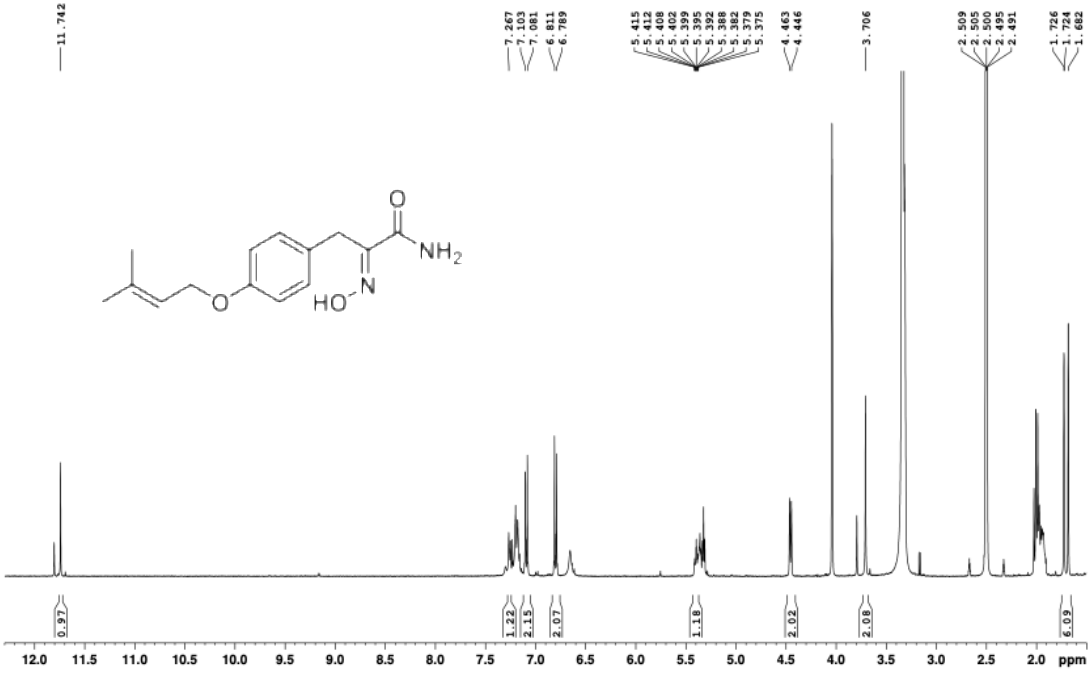

Figure A78. ^{1}H NMR spectrum of **3** (DMSO-d_6, 400 MHz).

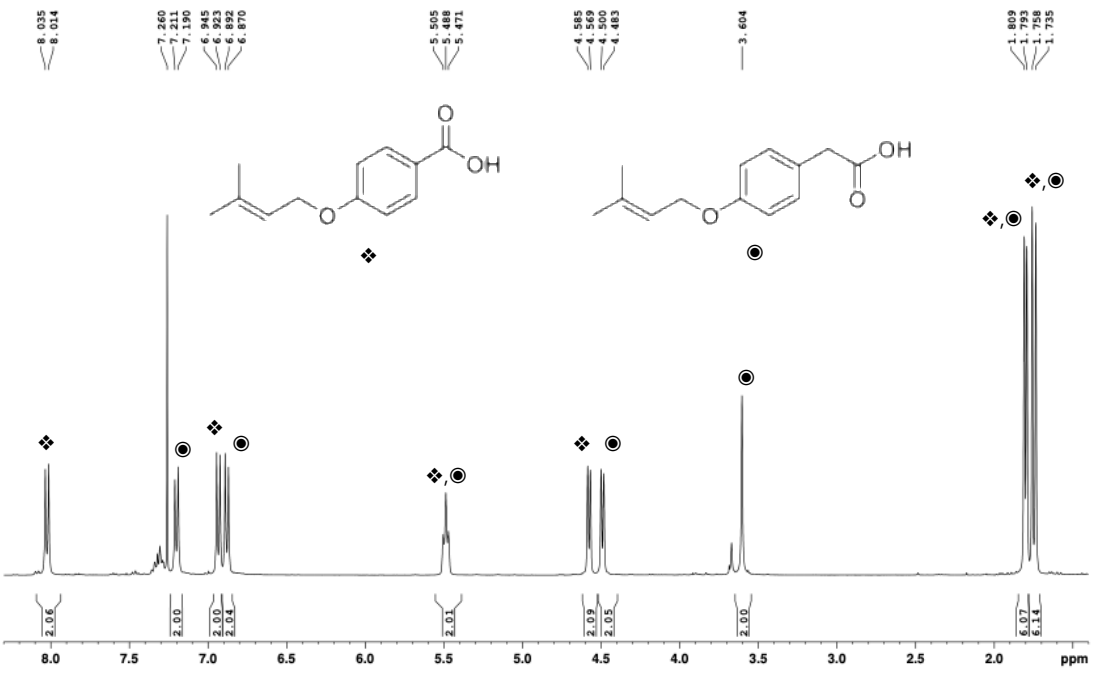

Figure A79. ^{1}H NMR spectrum of **11** and **12** ($CDCl_3$, 400 MHz).

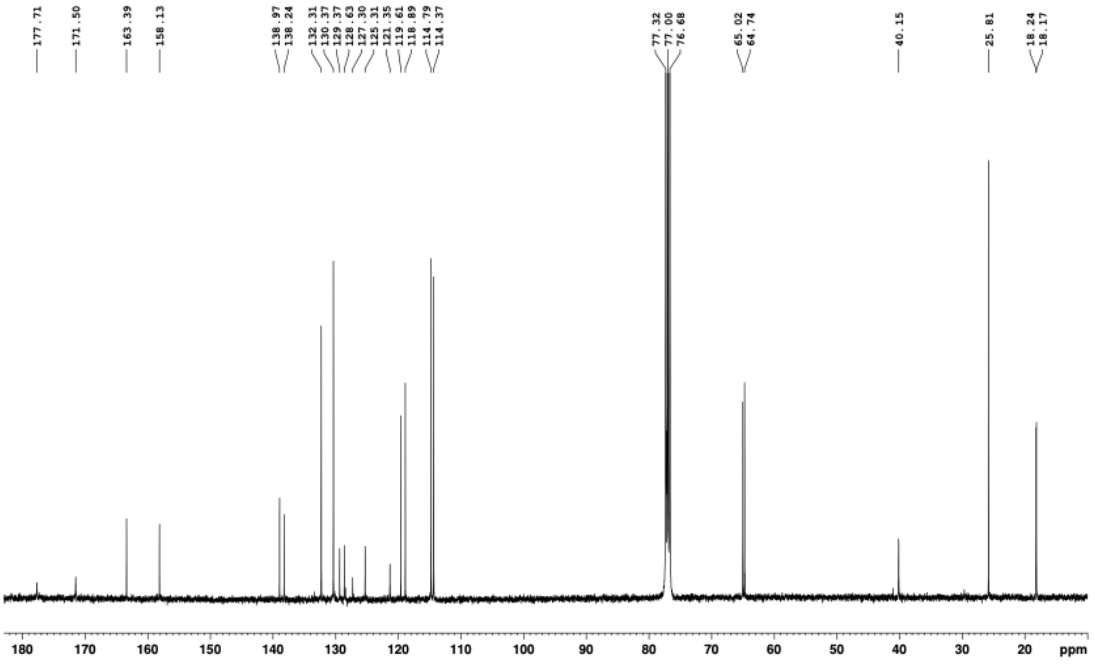

Figure A80. ^{13}C NMR spectrum of **11** and **12** ($CDCl_3$, 100 MHz).

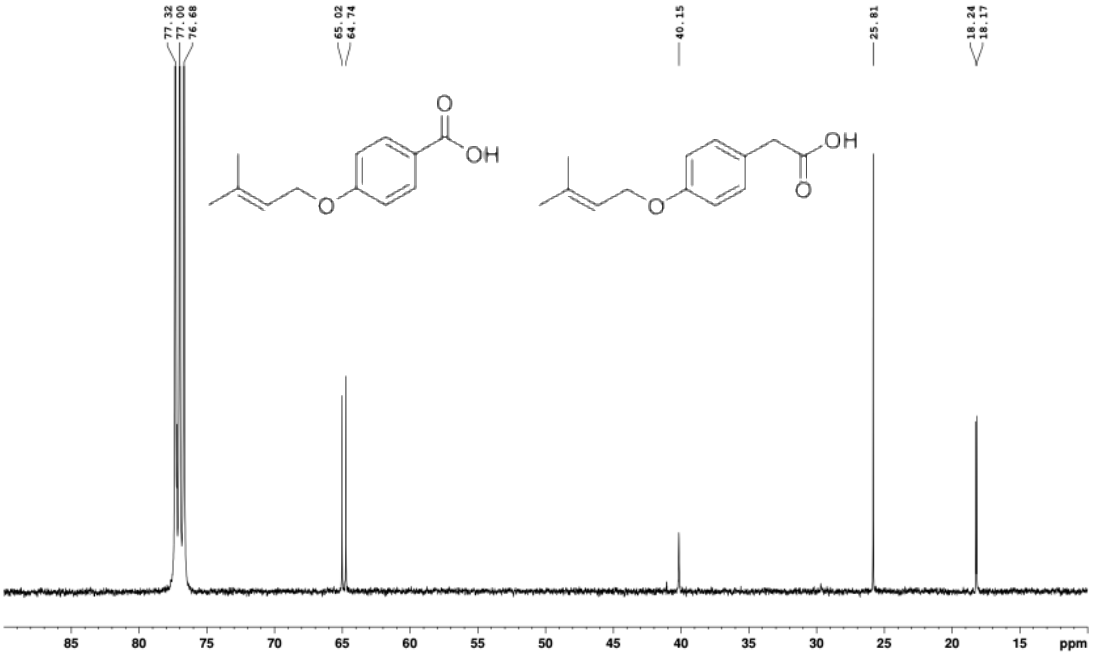

Figure A81. ^{13}C NMR (expansion-1) spectrum of **11** and **12** ($CDCl_3$, 100 MHz).

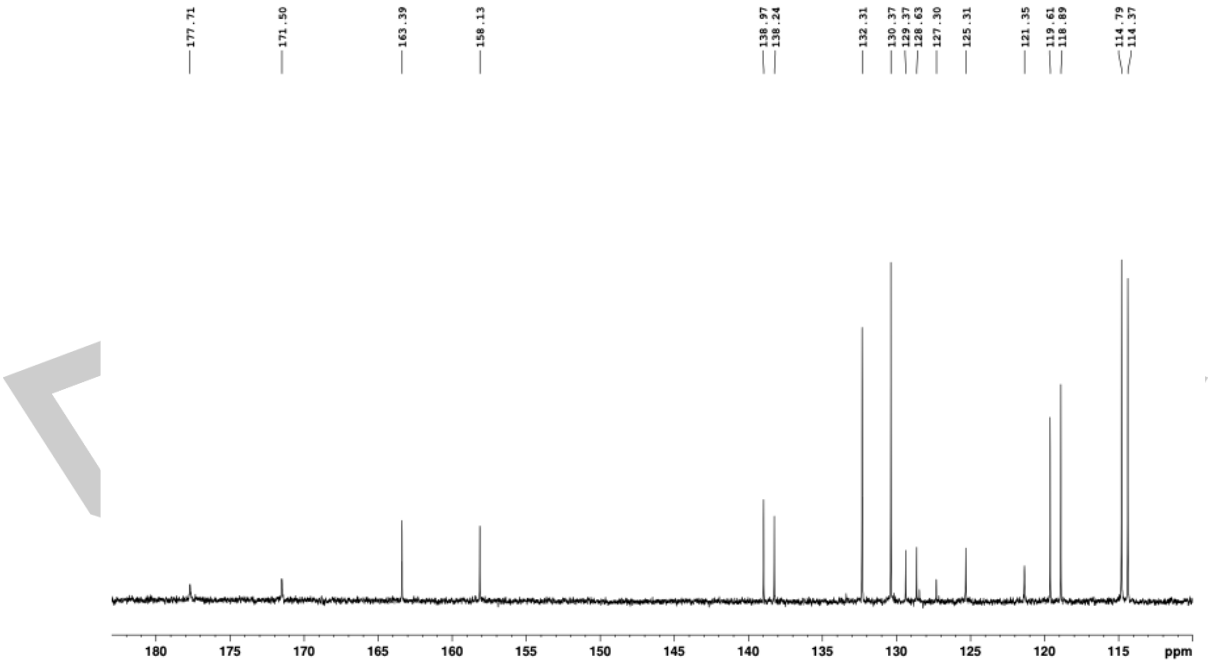

Figure A82. ^{13}C NMR (expansion-2) spectrum of **11** and **12** ($CDCl_3$, 100 MHz).

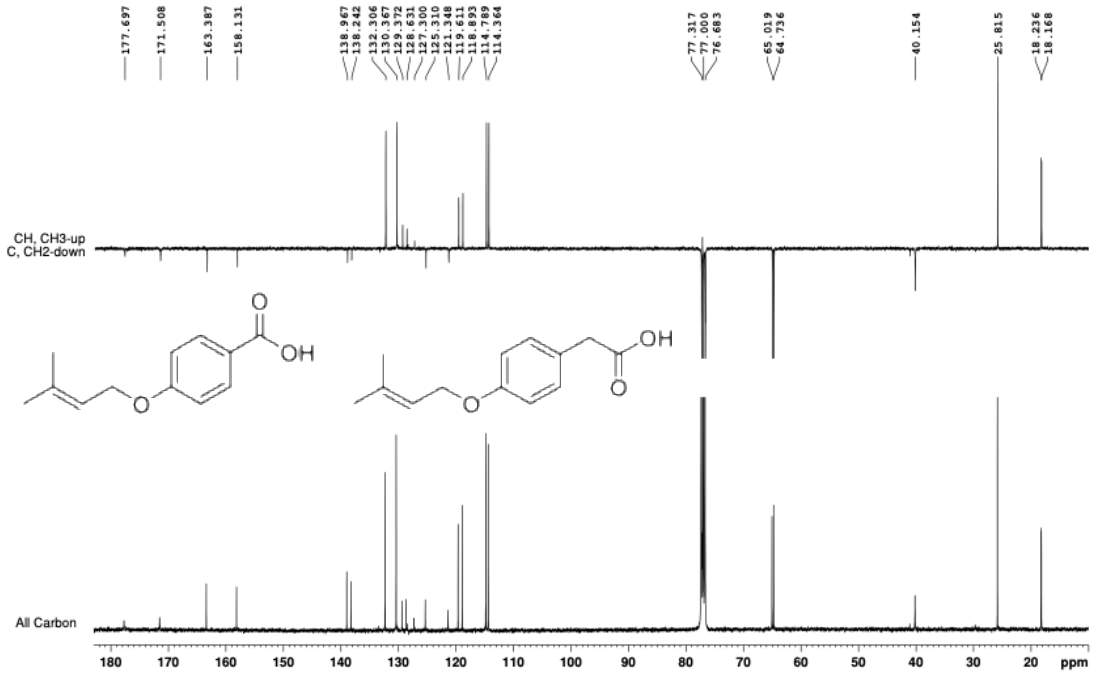

Figure A83. DEPT-135 spectrum of **11** and **12** ($CDCl_3$, 100 MHz).

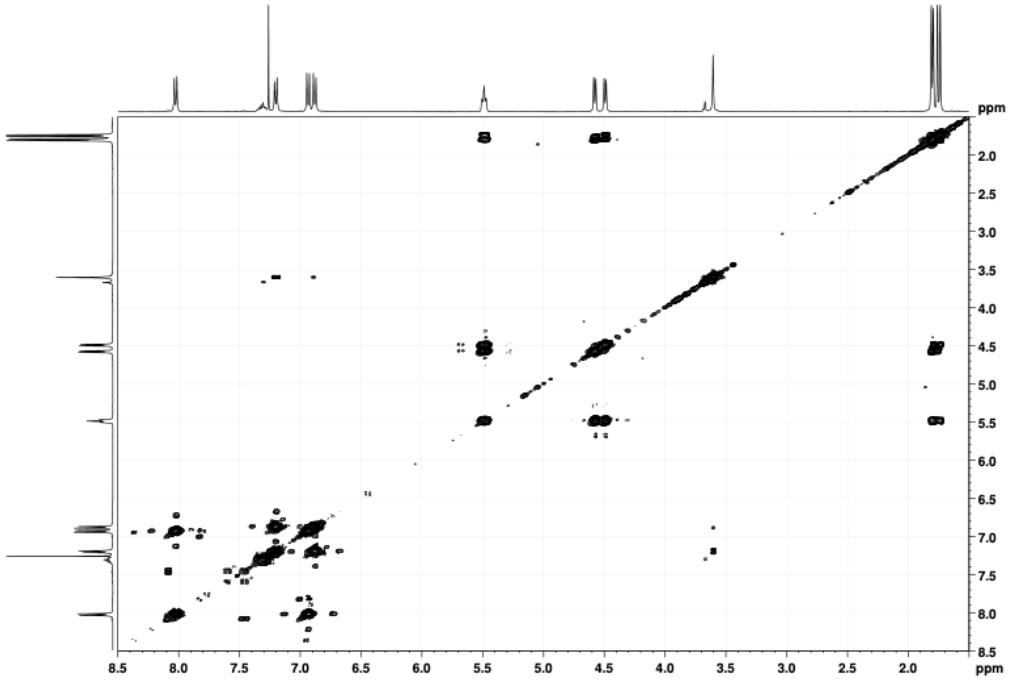

Figure A84. COSY spectrum of **11** and **12** ($CDCl_3$, 400 MHz).

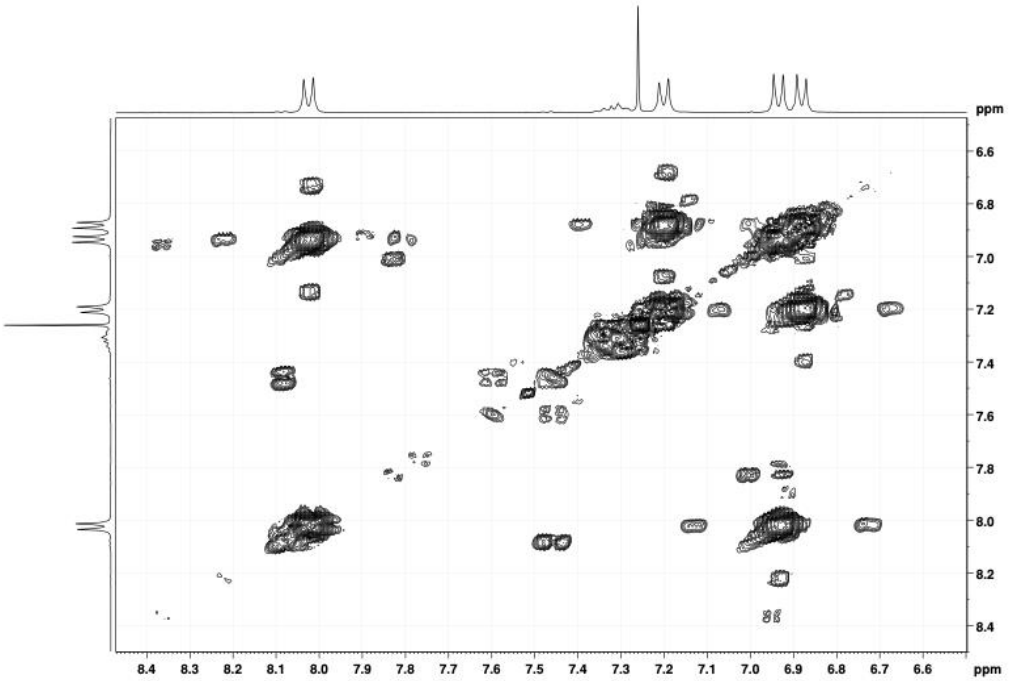

Figure A85. COSY (expansion-1) spectrum of **11** and **12** ($CDCl_3$, 400 MHz).

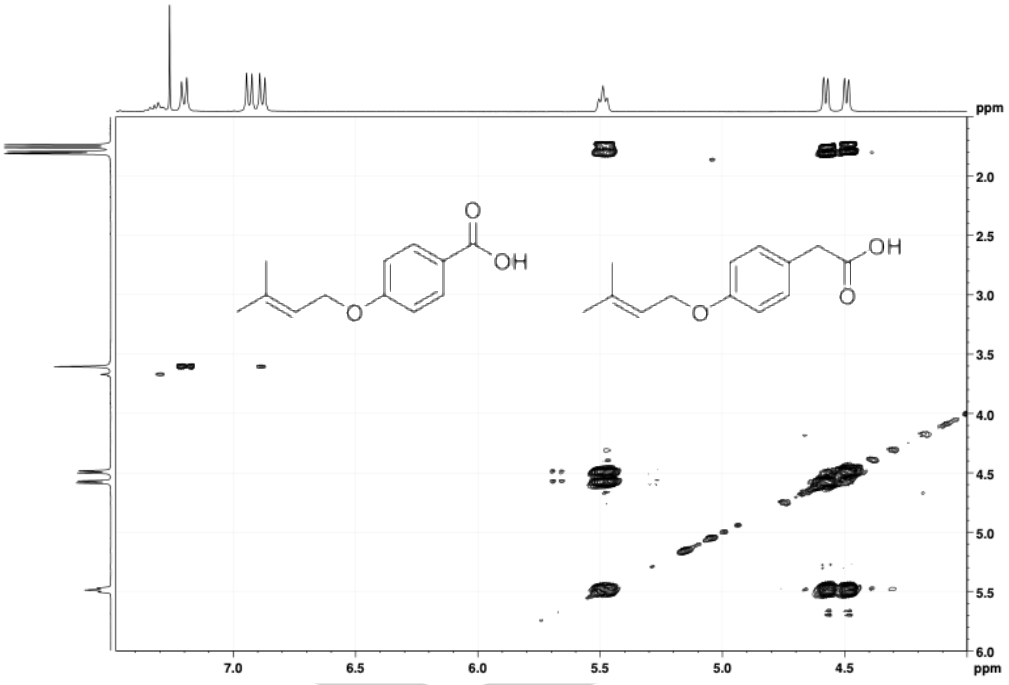

Figure A86. COSY (expansion-2) spectrum of **11** and **12** ($CDCl_3$, 400 MHz).

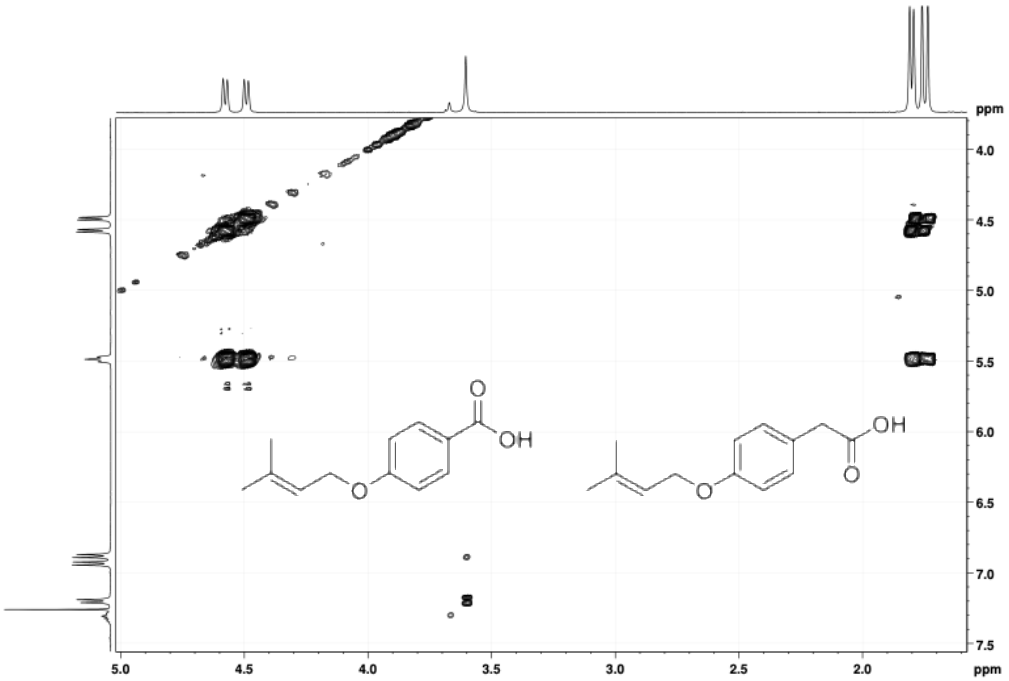

Figure A87. COSY (expansion-3) spectrum of **11** and **12** ($CDCl_3$, 400 MHz).

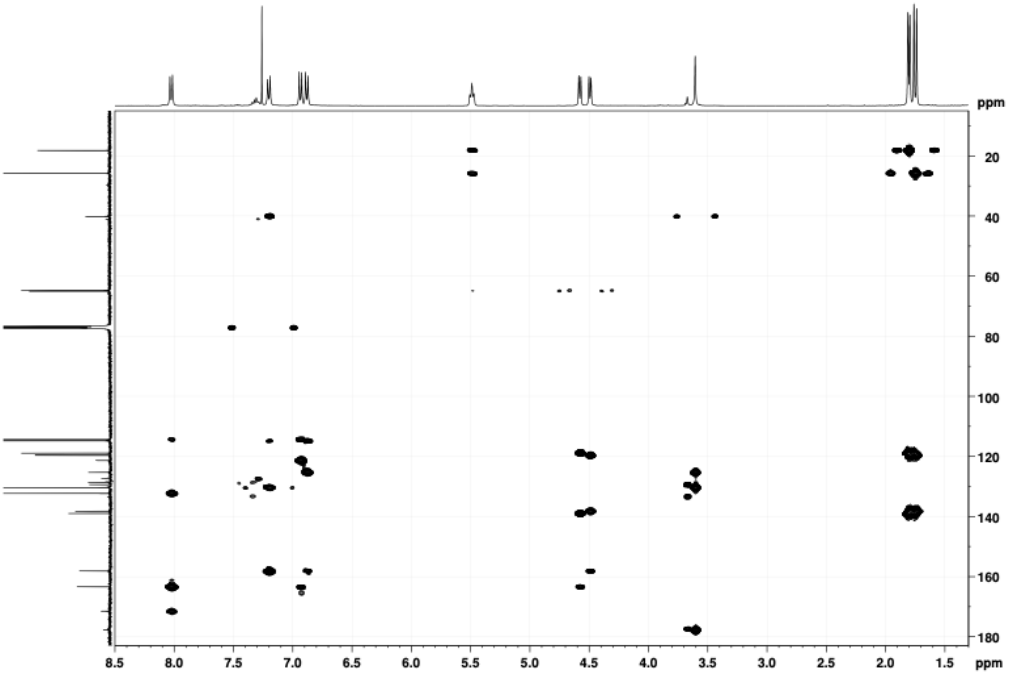

Figure A88. HMBC spectrum of **11** and **12** ($CDCl_3$, 400 MHz).

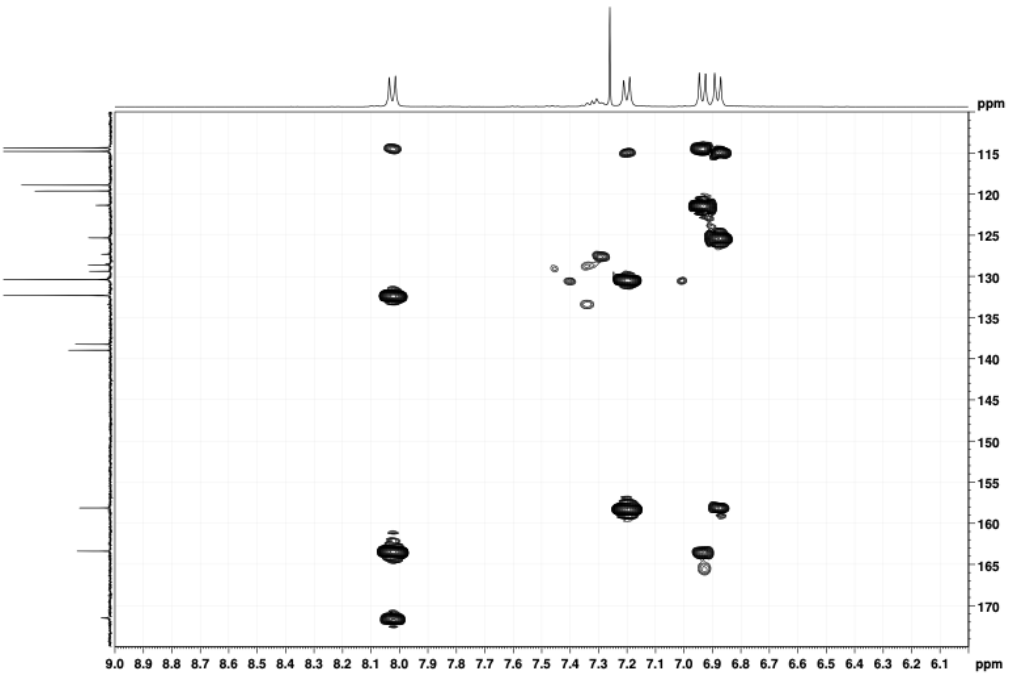

Figure A89. HMBC (expansion-1) spectrum of **11** and **12** ($CDCl_3$, 400 MHz).

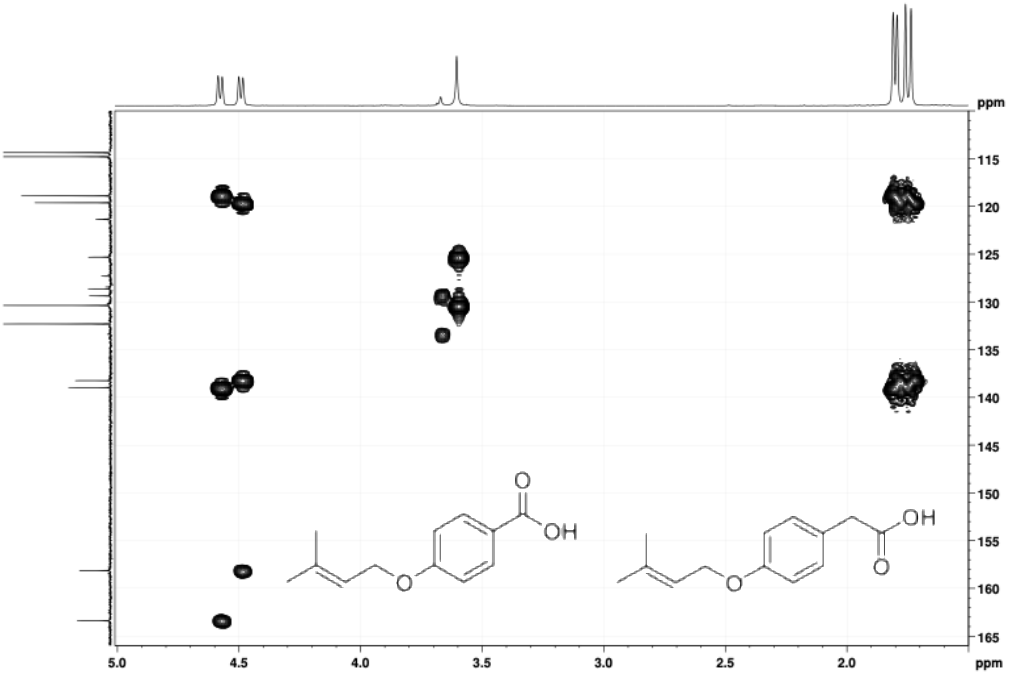

Figure A90. HMBC (expansion-2) spectrum of **11** and **12** ($CDCl_3$, 400 MHz).

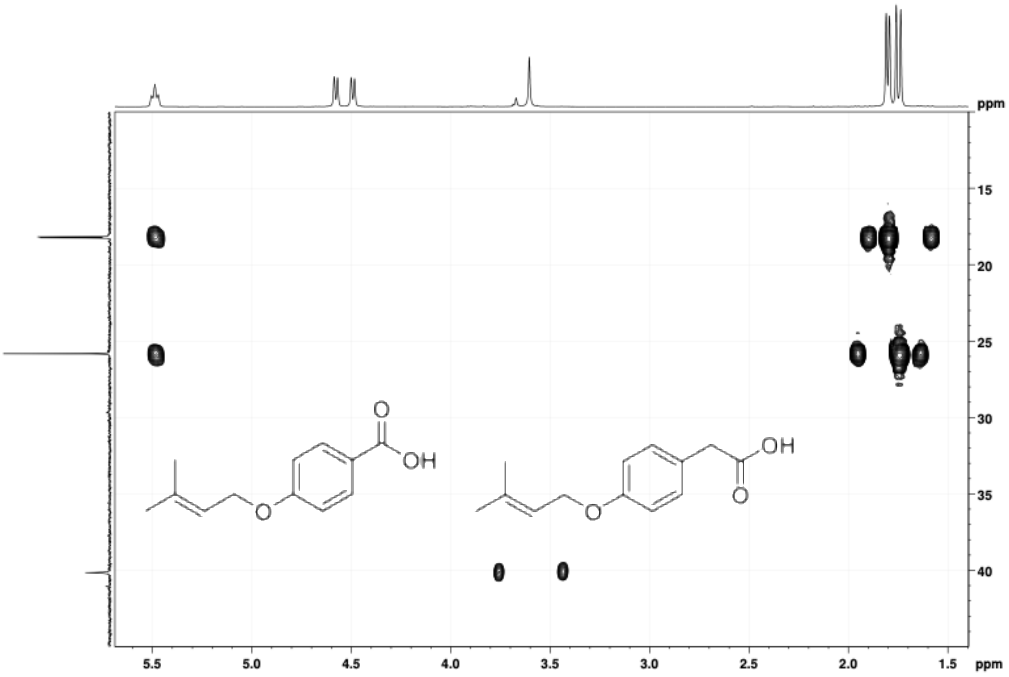

Figure A91. HMBC (expansion-3) spectrum of **11** and **12** ($CDCl_3$, 400 MHz).

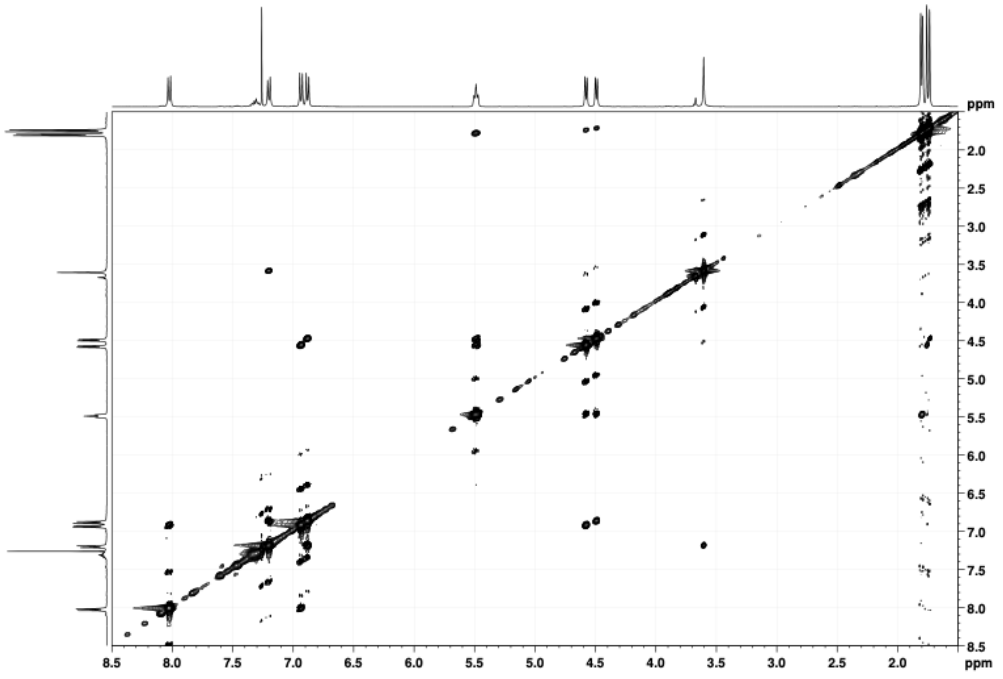

Figure A92. NOESY spectrum of **11** and **12** ($CDCl_3$, 400 MHz).

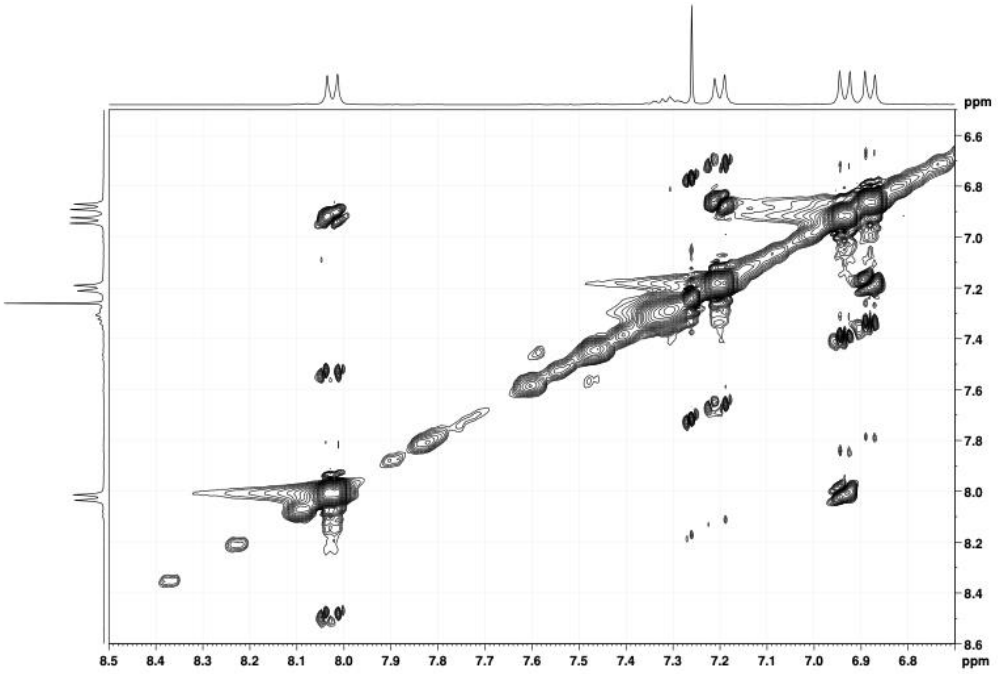

Figure A93. NOESY (expansion-1) spectrum of **11** and **12** ($CDCl_3$, 400 MHz).

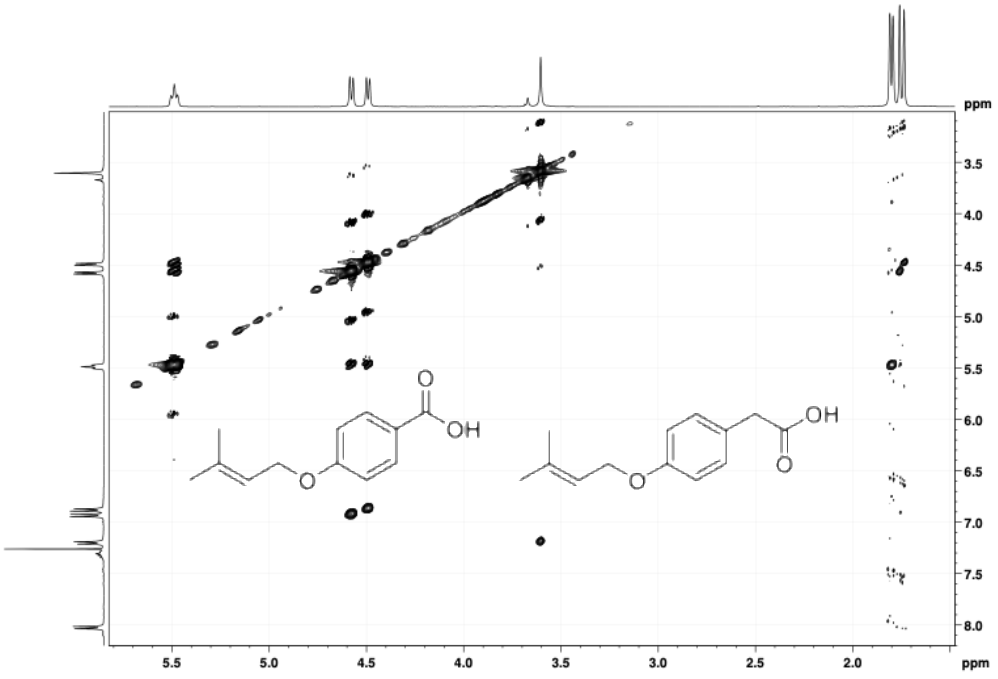

Figure A94. NOESY (expansion-2) spectrum of **11** and **12** ($CDCl_3$, 400 MHz).

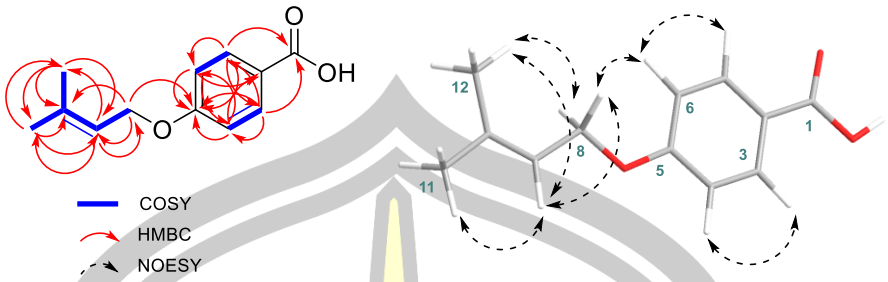

Figure A95. COSY, HMBC, and NOESY correlations of **11** (in $CDCl_3$)

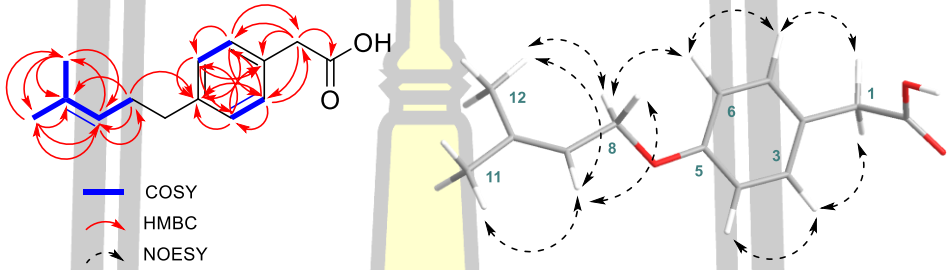

Figure A96. COSY, HMBC, and NOESY correlations of **12** (in $CDCl_3$)

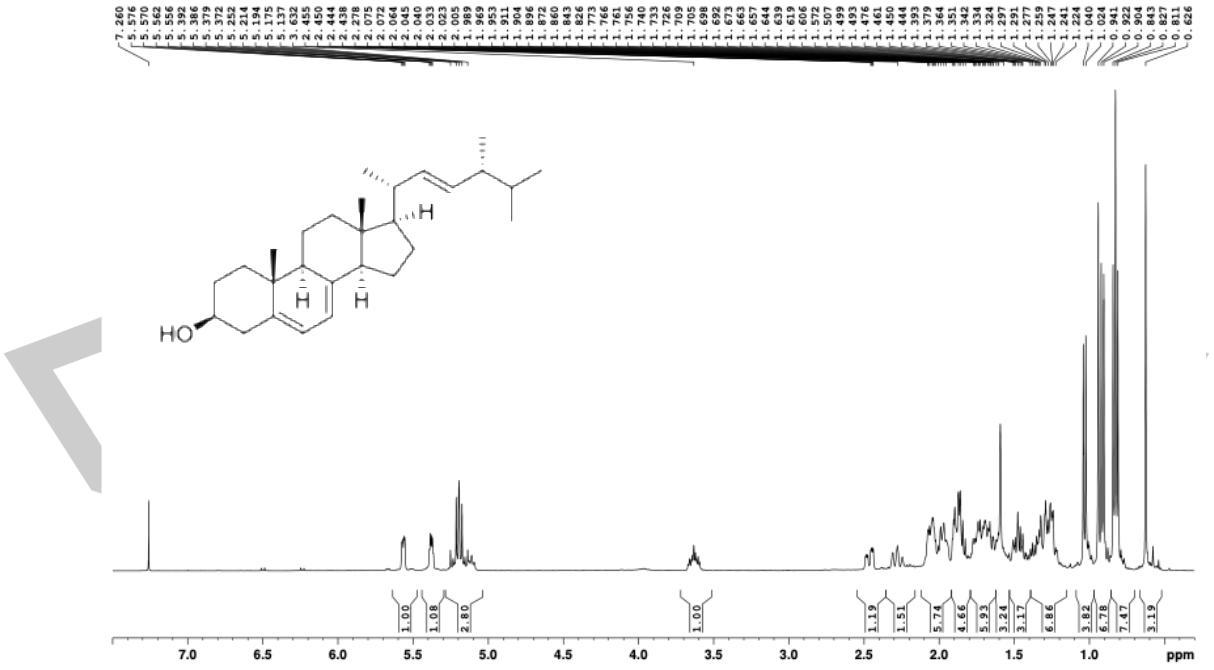

Figure A97. ^1H NMR spectrum of **13** ($CDCl_3$, 400 MHz).

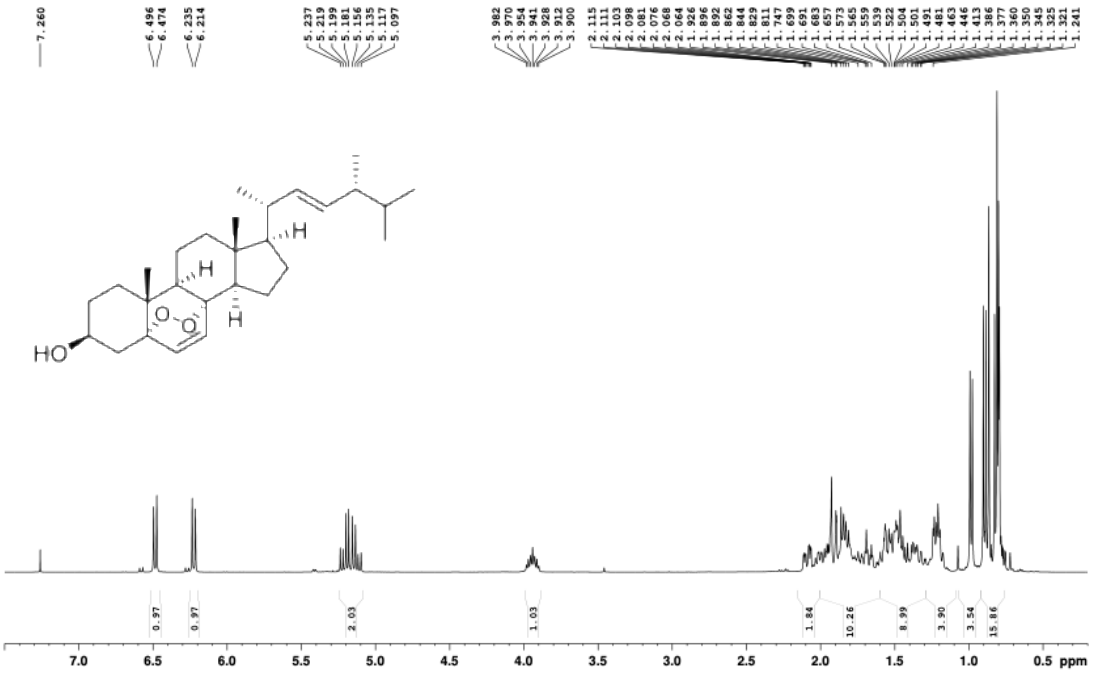

Figure A98. ^{1}H NMR spectrum of **14** ($CDCl_3$, 400 MHz).

BIOGRAPHY

NAME	Chiraphat Takpho
DATE OF BIRTH	2 July 2000
PLACE OF BIRTH	Nakhon Phanom
ADDRESS	17/1 Kham Pok, Tha Champa, Tha Uthen, Nakhon Phanom, Thailand 48120
EDUCATION	2018 Senior High School, Piyamaharachalai School 2022 Bachelor of Science (B.Sc.) in Chemistry, Mahasarakham University
Research output	1) Srisit, S.; Bunloed, C.; Soma, W.; Panchompoo, J.; Takpho, C.; Rattarom, R.; Sangdee, A.; Seephonkai, P. The isolation of 5-hydroxymethylfuran metabolites from the broth extract of Fomitopsis meliae (Agaricomycetes). International Journal of Medicinal Mushrooms. 2024; 26(12): 21–30. 2) Takpho, C.; Panchompoo, J.; Singmahan, K.; Rattarom, R.; Naksuwankul, K.; Sangdee, K.; Sangdee, A.; Isaka, M.; Seephonkai, P. Tyrosine oxime derivatives from the natural fruiting bodies of basidiomycete Serpula dendrocalami. Natural Product Research. 2024; https://doi.org/10.1080/14786419.2024.2438267.